RECLAMATION

Managing Water in the West

Historical and Future Irrigation Water Requirements for Select Reclamation Project Areas

Western United States

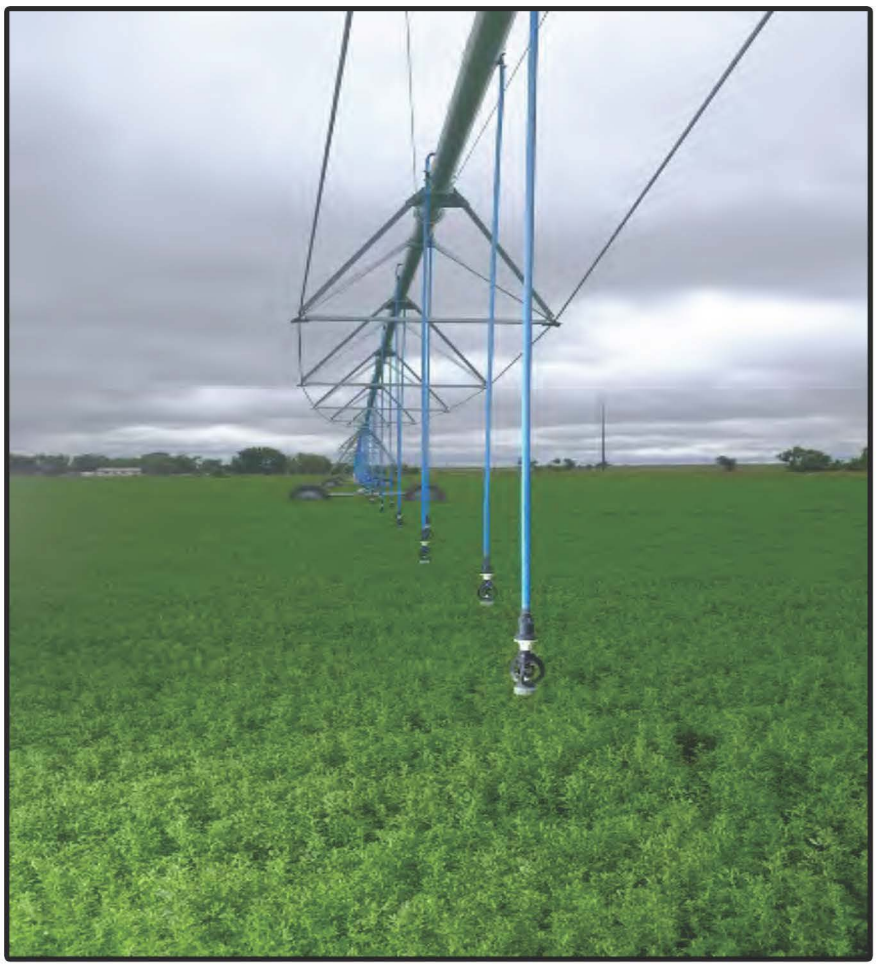

U.S. Department of the Interior
Bureau of Reclamation

December 2016

Mission Statements

The U.S. Department of the Interior protects America's natural resources and heritage, honors our cultures and tribal communities, and supplies the energy to power our future.

The mission of the Bureau of Reclamation is to manage, develop, and protect water and related resources in an environmentally and economically sound manner in the interest of the American public.

Historical and Future Irrigation Water Requirements for Select Reclamation Project Areas

Western United States

Justin L. Huntington[1,2]
Charles G. Morton[3]
Daniel McEvoy[4,2]
Matthew Bromley[1]
Katherine Hedgewisch[5]
Richard Allen[6]
Subhrendu Gangopadhyay[7]

Prepared by

[1]Division of Hydrologic Sciences, Desert Research Institute
[2]Western Regional Climate Center, Desert Research Institute
[3]Division of Earth and Ecosystem Sciences, Desert Research Institute
[4]Division of Atmospheric Sciences, Desert Research Institute
[5]University of Idaho, Geography Department
[6]University of Idaho, College of Agricultural and Life Sciences
[7]Bureau of Reclamation, Denver, Colorado

Prepared for
Bureau of Reclamation

U.S. Department of the Interior
Bureau of Reclamation

December 2016

ABSTRACT

Evapotranspiration (ET) is the second largest component of hydrologic systems and water balances, following precipitation, and is the driving component for net irrigation water requirements (NIWR) of agricultural crops. It is the application of irrigation water that sustains many western populations and economies, and drives the observable process of ET. Quantifying ET for specific crops and regions is required for design of irrigation systems, basin water balance estimates, irrigation water management, and for the review and litigation of water right applications and disputes; all of which are increasingly becoming a greater priority. The goal of this report is to summarize enhancements and applications of irrigation demands estimation methods related to WaterSMART Basin Study and West Wide Climate Risk Assessment (WWCRA) activities directed under the SECURE Water Act by providing scientifically sound historical and future estimates of reference evapotranspiration, crop ET, and NIWR that are produced using accepted and practiced state-of-the-art procedures, and that can be used as building blocks for follow-on enhancements and studies. One of the limitations outlined in a recent WWCRA study was the need to calculate future irrigation demands for tens to hundreds of climate projections using the time evolving, or transient method, which at the time was not practical given the diversity of crops and agricultural practices across the major Reclamation river basins, and enormous computational and data handling requirements. However, with the development of open source open platform crop ET and automated batch pre- and post-processing scripts, such transient crop ET and NIWR simulations can be made.

The primary objective of this study was to develop, enhance, and apply open source open platform crop ET software (ET Demands) that estimates historical and future reference ET, crop ET, and NIWR, using widely accepted approaches for five study areas comprised of Altus, OK (W.C. Austin Project), Arkansas River basin, CO (Fryingpan-Arkansas Project), Central UT (Central Utah Project), San Angelo, TX (San Angelo Project), and the Truckee, Carson, Walker, Lower Humboldt (TCWLH) basins NV-CA (including the Newlands Project). Overall, this work is intended to help meet the needs of Reclamation for developing and applying ET software that can be used for estimating crop ET and NIWR for historical climate, as well as for multiple future climate scenarios, while accounting for the potential effects of increased atmospheric CO_2 on reduced transpiration. Baseline and future estimates of ET Demand model components for each study area are summarized through illustration and discussion of spatial and time series plots of precipitation, temperature, reference ET, crop ET, and NIWR estimates. Results indicate that precipitation projections are highly variable and basin dependent, with the ensemble medians showing both slight increases and decreases within most basins, temperature shows a persistent increasing trend from the baseline level, and reference ET is projected to increase in all basins. Crop ET is projected to increase in all basins, especially areas where perennial crops are grown, and with smaller increases in areas where annual crops are grown. Because the NIWR incorporates growing season and non-growing season soil moisture gains and losses from precipitation, bare soil evaporation, and crop ET, projections of NIWR largely reflect changes in crop ET and projected precipitation. Comparisons between TCWLH baseline and future projections of crop ET and NIWR from this study are generally lower than from a previous WWCRA study using different climate projection information. Lower estimates of crop ET and NIWR are primarily due to lower reference ET when compared to WWCRA estimates of reference ET.

CONTENTS

LIST OF FIGURES

LIST OF ACRONYMS

ASCE	American Society of Civil Engineers
ASCE-PM	American Society of Civil Engineers Penman-Monteith
BCSD	Bias-Correction Spatial Disaggregation
CAT	Climate Analysis Tools
CDL	USDA Cropland Data Layer
CGDD	Cumulative Growing Degree Days
CMIP3	Coupled Model Intercomparison Project3
CMIP5	Coupled Model Intercomparison Project5
COOP	Cooperative Observer Network
D_{Percp}	Deep Percolation of any Precipitation Below the Maximum Root Zone
ET	Evapotranspiration
ET_0	Reference ET
ET_c	Crop Evapotranspiration
FAO	Food and Agriculture Organization of the United Nations
GHG	Greenhouse Gas
HUC8	Hydrologic Unit Code of 8 digits
IPCC	Intergovernmental Panel on Climate Change
K_c	Crop Coefficient
K_{cb}	Basal Crop Coefficient
K_e	Coefficient Representing Bare Soil Evaporation
K_s	Stress Coefficient
LAI	Leaf Area Index
LCRAS	Lower Colorado River Accounting System
MACA	Multivariate Adapted Constructed Analogs
METDATA	University of Idaho Gridded Surface Meteorological Data
Metnode	Point Location Representative of Agricultural Location
NIWR	Net Irrigation Water Requirement
NWS	National Weather Service
PPM	Parts Per Million
PRISM	Parameter Regression on Independent Slopes Model
P_{rz}	Precipitation Residing in Root Zone
RCP	Representative Concentration Pathways
STATSGO	NRCS State Soil Geographic Dataset
T_{30}	30-day Moving Average Air Temperature
TCWLH	Truckee, Carson, Walker, and Lower Humboldt Basins
USDA-NASS	U.S. Department of Agriculture- National Agricultural Statistics Service
USDA-NRCS	U.S. Department of Agriculture- Natural Resources Conservation Service
WCRP	World Climate Research Programme
WWCRA	West Wide Climate Risk Assessment

INTRODUCTION

Evapotranspiration (ET) is the second largest component of hydrologic systems and water balances, following precipitation, and is the driving component for net irrigation water requirements (NIWR) of agricultural crops. It is the application of irrigation water that sustains many western populations and economies, and drives the observable process of ET. Quantifying ET for specific crops and regions is required for design of irrigation systems, basin water balance estimates, irrigation water management, and for the review and litigation of water right applications and disputes; all of which are increasingly becoming a greater priority.

NIWR under future climates is largely unknown, however, it is essential for long-term water resources planning in the Western United States. The Bureau of Reclamation (Reclamation) is responsible for managing water resources that sustain irrigation projects in 17 western states, and has been directed to address climate change in long-term water resources planning and management (Section 9504 of the SECURE Water Act). The SECURE Water Act section 9503 authorizes Reclamation to assess climate change risk for water and environmental resources in "major Reclamation river basins." Providing a scientifically sound and widely accepted basis for estimating historical and future irrigation water demands is necessary for addressing this directive. The goal of this report is to summarize enhancements and applications of irrigation demands estimation methods related to WaterSMART Basin Study and West Wide Climate Risk Assessment (WWCRA) activities directed under the SECURE Water Act by providing scientifically sound historical and future estimates of reference evapotranspiration, crop ET, and NIWR that are produced using accepted and practiced state-of-the-art procedures, and that can be used as building blocks for follow-on enhancements and studies. This work was funded through the WaterSMART Climate Analysis Tools (CAT) grant program.

PREVIOUS WORK

This work closely follows recent work of Huntington et al. (2015) for estimating crop ET and the NIWR as part of the West Wide Climate Risk Assessment (WWCRA) using the ET Demands software package. One of the limitations outlined in Huntington et al. (2015) was the need to calculate future irrigation demands for tens to hundreds of climate projections using the time evolving, or transient method, which at the time was not practical given the diversity of crops and agricultural practices across the major Reclamation river basins, and enormous computational and data handling requirements. However, with the development of the Python version of the ET Demands model, and automated batch pre- and post-processing scripts in this work, such transient crop ET and NIWR simulations can be made.

While full crop simulation and growth models have many research advantages and are largely physically based, irrigation water demand methodology developed by the

American Society of Civil Engineers (ASCE) and the Food and Agriculture Organization of the United Nations (FAO), which the ET Demands model is built on, is well suited for robust application under historical and future climate at the regional scale. This methodology also has wide spread acceptance among the ASCE and international agricultural engineering community, and is currently being used in Arizona, California, Colorado, Idaho, Kansas, Nebraska, Nevada, New Mexico, and by Reclamation for the Lower Colorado River Accounting System (LCRAS) and ET Toolbox models (Jensen, 1998; Brower, 2008). The University of Idaho, Nevada Division of Water Resources, and Desert Research Institute have recently modified and enhanced the ASCE and FAO-56 reference ET and dual crop coefficient approach, and have made state wide applications of the modified model, named here as the ET Demands Model (Allen 1998; Allen et al., 2005a; Allen and Robison, 2009; Huntington and Allen, 2010). Results from ET Demands applications are being used by the State of Idaho and State of Nevada for water rights transfers and supporting modeling and water budget studies.[1] The primary factors in selecting ET Demands for this study included the following:

- Model heritage traced to the widely accepted FAO-56 reference ET and dual crop coefficient approach
- Wide spread general application across major Western United States river basins
- Flexibility for simulating future irrigation water demands by considering non-growing season soil moisture accumulation and variable growing season lengths
- Application in the WWCRA study.

OBJECTIVES

The primary objective of this study was to develop, enhance, and apply open source open platform crop ET software (ET Demands) that estimates historical and future reference evapotranspiration, crop ET, and NIWR, using widely accepted approaches for five study areas comprised of Altus, OK (W.C. Austin Project), Arkansas River basin, CO (Fryingpan-Arkansas Project), Central UT (Central Utah Project), San Angelo, TX (San Angelo Project), and the Truckee, Carson, Walker, Lower Humboldt (TCWLH) basins NV-CA (including the Newlands Project) (Figures 1-5). Overall, this work is intended to help meet the needs of Reclamation for developing and applying ET software that can be used for estimating crop ET and NIWR for historical climate, as well as for multiple future climate scenarios. Four of

[1] ET Demands Model background and state applications described at "ET Idaho" http://www.kimberly.uidaho.edu/ETIdaho/online.php and at "ET Nevada" http://water.nv.gov/mapping/et/et_general.cfm documented in Allen and Robison, 2009, and Huntington and Allen, 2010, respectively.

the five study areas include lands served by Reclamation projects that were not included in the previous work discussed above. The combined results provide a comprehensive set of estimates for future crop irrigation demands under similar climate change scenarios for all lands served by Reclamation projects. In addition, since this work and the previous work included the Truckee/Carson Basins, results are compared with consideration of transient climate and atmospheric carbon dioxide (CO_2) effects employed in this work.

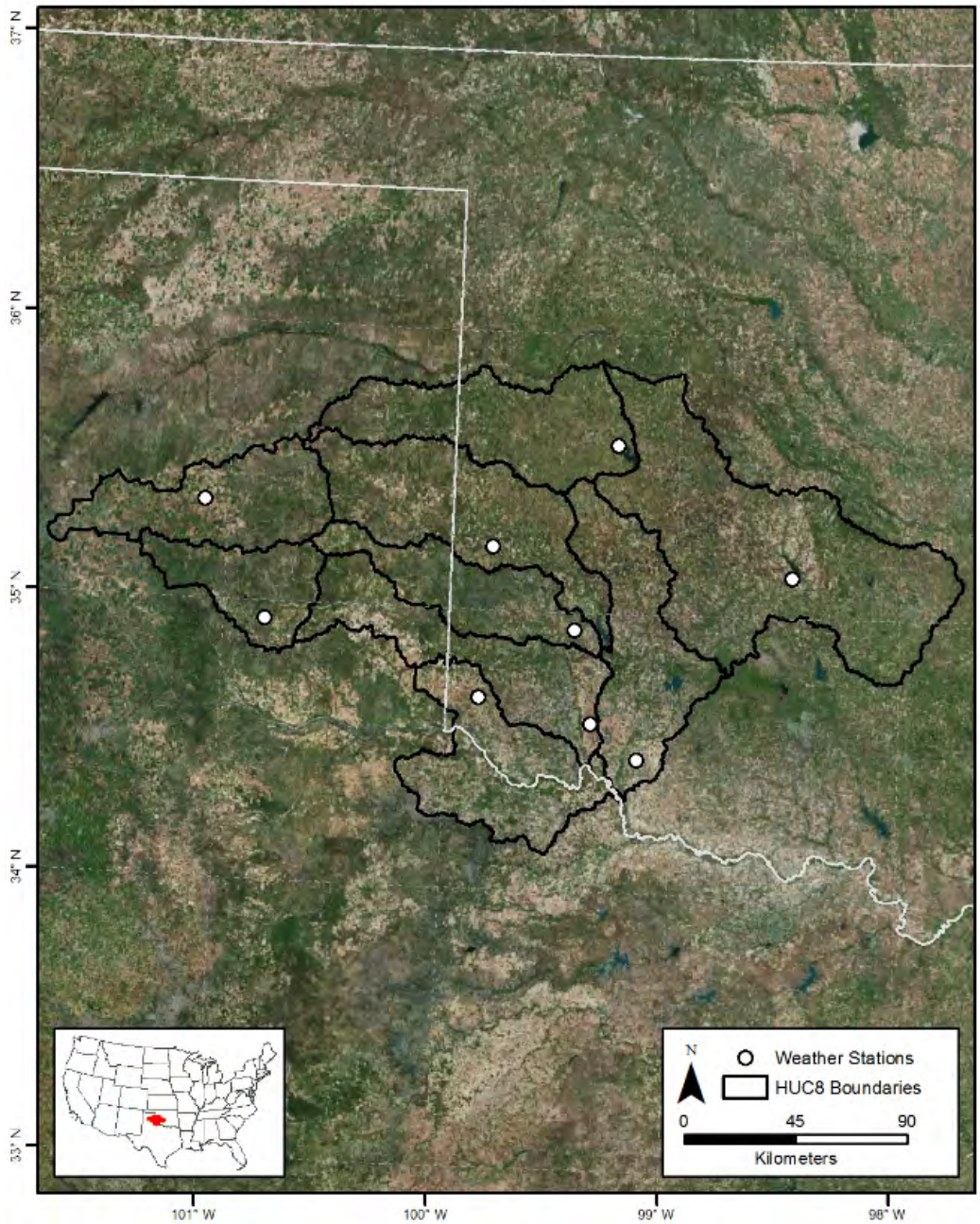

Figure 1 - Altus, Oklahoma HUC8 areas, and Metnode weather stations used to represent agricultural climate conditions within each HUC8.

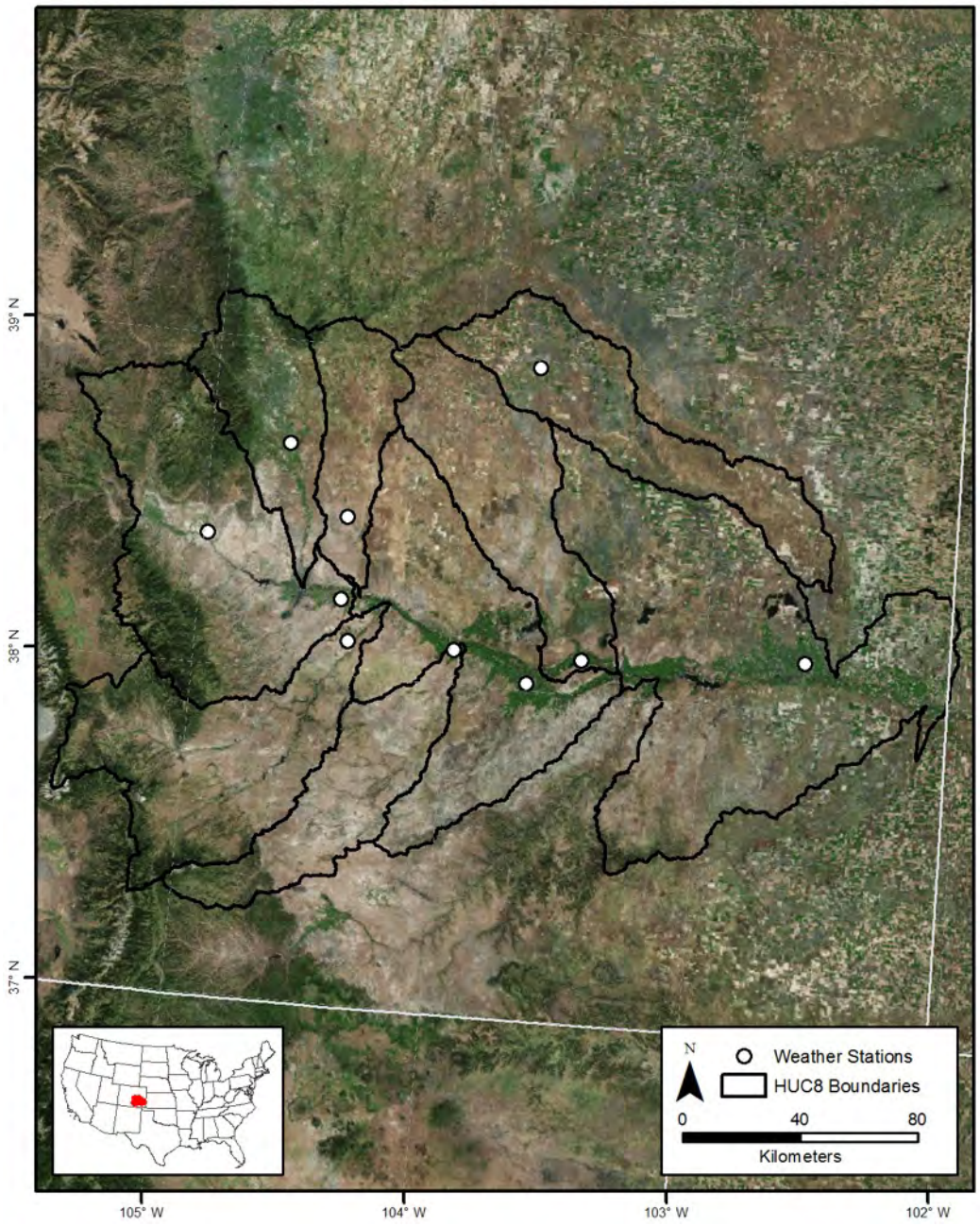

Figure 2 - Arkansas, Colorado HUC8 areas, and Metnode weather stations used to represent agricultural climate conditions within each HUC8.

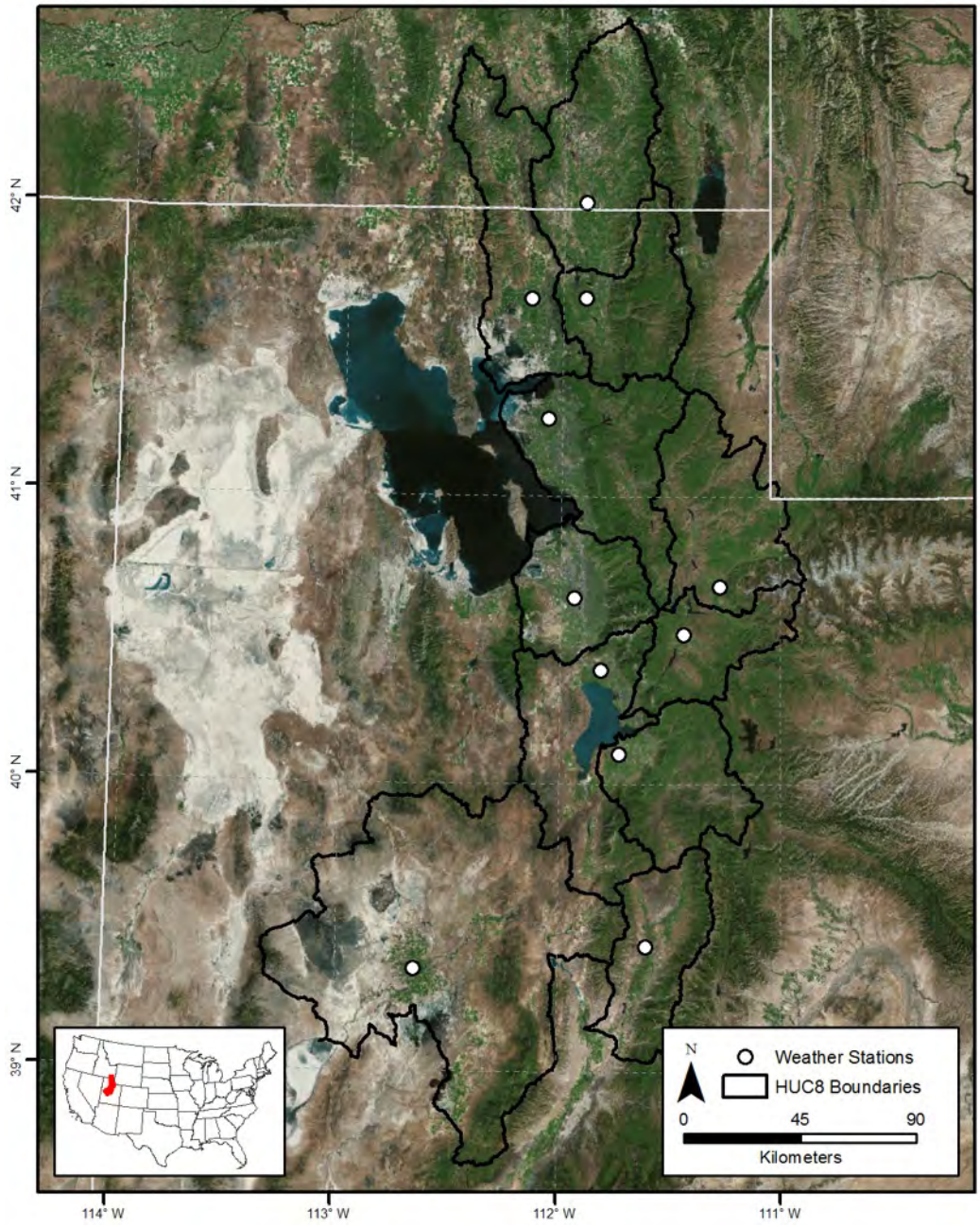

Figure 3 - Central, Utah HUC8 areas, and Metnode weather stations used to represent agricultural climate conditions within each HUC8.

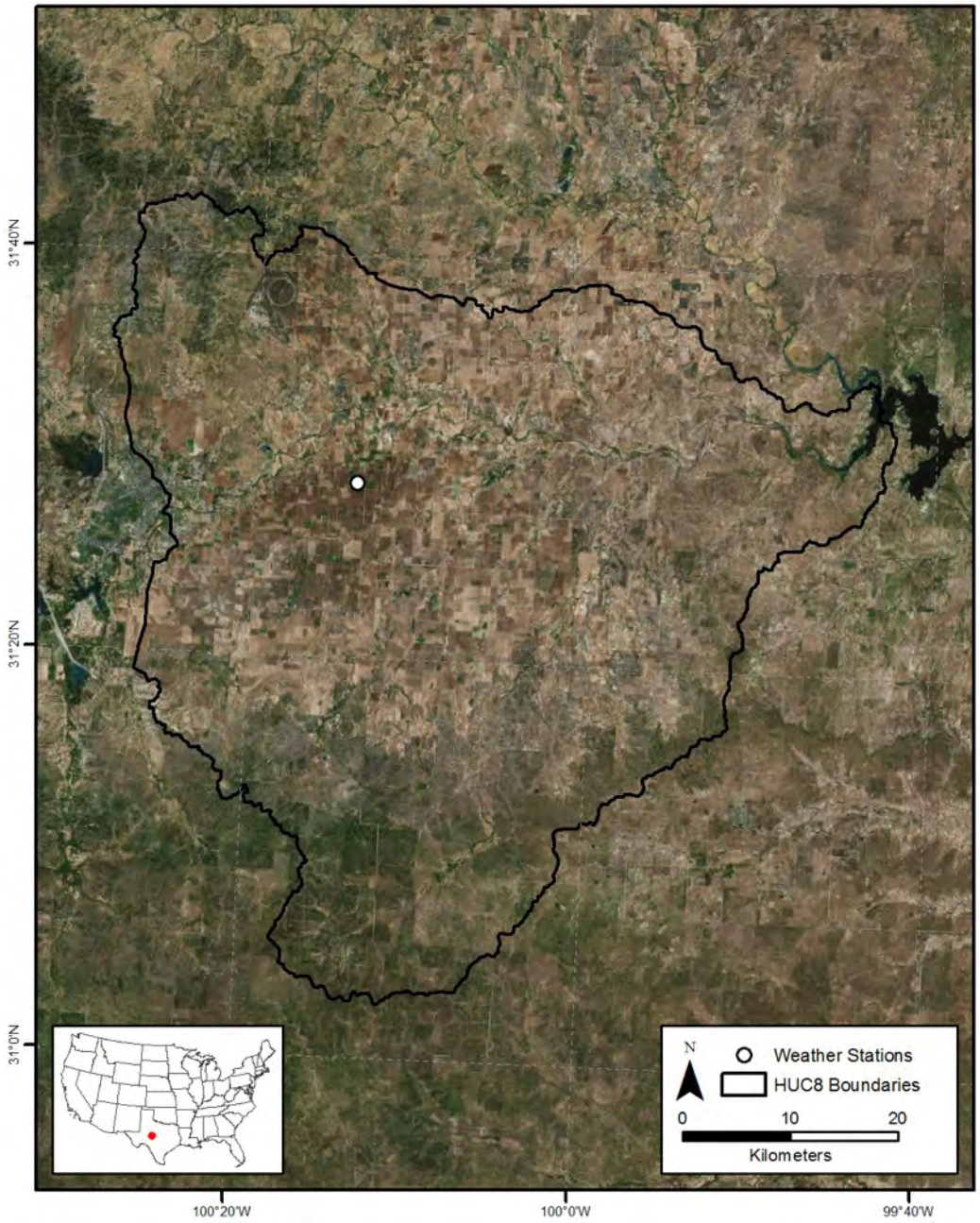

Figure 4 - San Angelo, Texas HUC8 subbasin, and Metnode weather stations used to represent agricultural climate conditions within each HUC8.

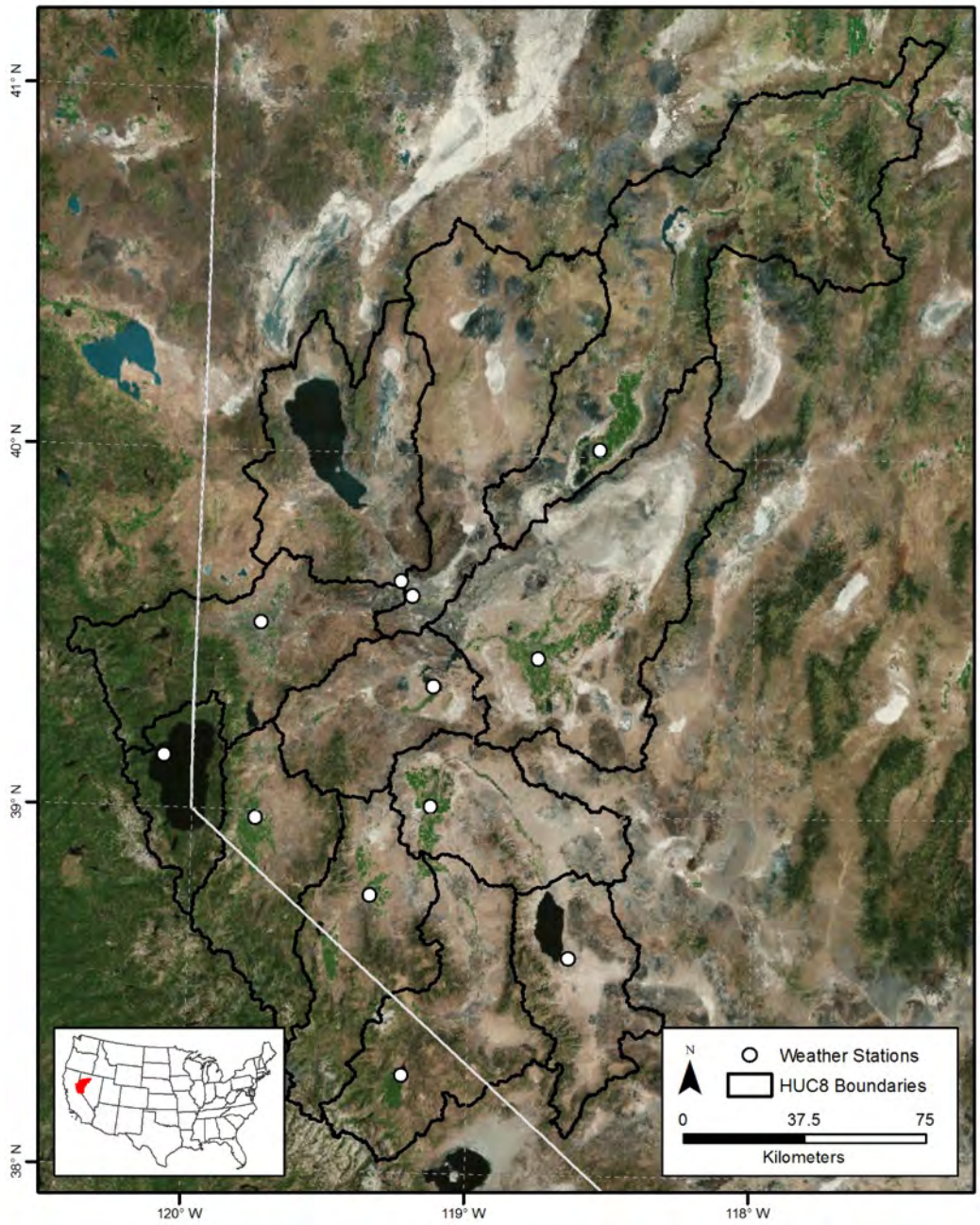

Figure 5 - Truckee, Carson, Walker, and Lower Humboldt (TCWLH) HUC8 areas, and Metnode weather stations used to represent agricultural climate conditions within each HUC8.

APPROACH

This study implements the Python version of the ET Demands model applied in the WWCRA study summarized by Huntington et al. (2015), and develops annual crop ET and NIWR estimates for multiple agriculturally representative locations within each study area basin, and for historical and future climate. The analysis involves developing crop ET and NIWR estimates associated with World Climate Research Programme Coupled Model

Intercomparison Project5 (WCRP CMIP5) climate projections that have been bias-corrected and spatially downscaled to 4 km spatial resolution using the Multivariate Adapted Constructed Analogs (MACA) approach (Abatzoglou and Brown, 2012). Changes to components of reference ET (i.e. air temperature, solar radiation, humidity, and wind speed), reference ET, and crop area weighted annual crop ET and NIWR rates are analyzed for 40 time-evolving, or transient, climate change projections, and results are summarized by 5^{th}, 25^{th}, 50^{th}, 75^{th}, and 95^{th} percentiles at three future periods: 2020s (years 2006-2039), 2050s (years 2040– 2069), and 2080s (2070-2099) with 1950–2005 as the baseline period. Time series, change maps, and tables of ET Demand variables and results are presented for different percentiles and future time periods.

METHODS

The following sections outline general details of climate data, the ET Demands methodology, application for historical and future climate, and summary of results. Readers are encouraged to refer to the WWCRA study by Huntington et al (2015) and the above-mentioned references for more detailed explanation about the ET Demands model and approach.

Reference ET

The ET Demands model is based on the common reference ET-crop coefficient approach, in which the reference ET (ET_0), representing climatic demand for water and based on physical relationships, is multiplied by a crop coefficient (K_c) to estimate the crop ET (ET_c) of a vegetated area. ET_0 refers to ET from a reference surface that is actively growing, not limited by soil moisture, and is at full cover and peak height. There are many methods available for estimating ET_0 and while many of these methods are simple temperature-based techniques, others are more data intensive, physically based models such as the Penman-Monteith (PM) method. Estimates of ET_0 vary widely among the methods, and until the last decade there was considerable debate as to the more correct and appropriate method. The professional and scientific communities now generally recognize the FAO-56 (Allen et al. 1998) and ASCE-EWRI (2005) (American Society of Civil Engineers - Environmental & Water Resources Institute) standardized PM method (ASCE-PM) as the most appropriate and recommended ET_0 method for computing crop ET and NIWR. These endorsements were a primary consideration and the reason that the method was incorporated into the ET Demands model.

Comprehensive measurements of solar radiation, air humidity, and wind speed are often subject to limited availability, but are required for the ASCE-PM method and other physically based ET_0 methods. Difficulty in acquiring the input data necessary for physically based ET_0 methods has, in the past, led to the use of simpler and limited temperature-based methods to assess historical and future crop ET. Future climate projections have traditionally been limited to temperature and precipitation. However, in recent years new gridded climate

datasets for historical and future time periods have included all the variables needed for computing the ASCE-PM equation (i.e. air temperature, solar radiation, humidity, and wind speed). These new gridded observation and future climate datasets were used and applied in the ET Demands model, and further described below.

Climate Data

Historical climate datasets were acquired from gridded observations derived from University of Idaho's METDATA, which is provided at 4 km spatial resolution, daily time step, and includes daily maximum and minimum air temperature, solar radiation, humidity, and wind speed (Abatzoglou, 2011). METDATA is a hybrid dataset of the North American Data Assimilation System (NLDAS) (Mitchell, 2004) and the Parameter Regression on Independent Slopes Model (PRISM) (Daly, 2008). Point locations, termed Metnodes, that are representative of agricultural locations within each study area HUC8 (Hydrologic Unit Code of 8 digits) subbasin were identified based on high resolution imagery and USDA cropland data layer (CDL) information, and were used to extract time series of historical climate and future climate projections at each location (Figures 1-5). Metnode location information for each basin are listed in Appendices (see appendix directory structure information in last section of report).

ET Demands model was run for each Metnode using historical climate data from METDATA from 1979-2015 to compute the ASCE-PM based ET_0, and was compared to weather station based calculated ET_0. Weather station variables of solar radiation, temperature, humidity, and wind speed were all visually and manually quality assured and controlled according to method outlined by Allen (1996) and ASCE-EWRI (2005). The comparison of METDATA derived ET_0 to agricultural weather station based ET_0 was done to evaluate potential biases in METDATA derived reference ET_0. Because NLDAS and PRISM datasets, which are the primary datasets behind METDATA, do not explicitly account for the evaporative cooling effect from agriculture, METDATA derived ET_0 is typically biased high (Abatzoglou, 2011). To remove these biases, ET_0 was computed using data from 18 agricultural weather stations (average of five per basin), and the ratio of station measured ET_0 to station coincident METDATA estimated ET_0 was computed at mean monthly time steps, and multiplied by METDATA and future projections of daily ET_0 time series (which use METDATA as the training dataset as described in the following section) for respective months. Mean monthly ET_0 corrections effectively removed high bias of historical and future projections of ET_0 providing a more representative evaporative demand estimate reflective of irrigated agriculture.

Transient climate impacts methods involve translating time series climate projections into time series projections of weather inputs for impacts modeling (e.g., for hydrology, irrigation demands, open-water evaporation, etc.). There have been numerous applications of this approach for hydrology impacts assessment (e.g., Wood et al. 2004; Payne et al. 2004; Christensen et al. 2004; Van Rheenen et al. 2004; Christensen and Lettenmaier 2007; Maurer

2007; Reclamation 2011). This approach often involves having to reconcile time resolutions when translating from climate projections to weather input projections (e.g., for Reclamation 2011, monthly Bias Corrected Spatially Disaggregated climate projections had to be time-disaggregated to the daily timestep of hydrology analysis). The majority of downscaling methods and widely available downscaled climate projections are not ideal for estimating evaporative demand due to the lack of downscaled humidity, solar radiation, and wind speed fields, and monthly time steps. In this work, the Multivariate Adaptive Constructed Analogs (MACA) dataset (Abatzoglou and Brown, 2012) is used which relies on adapted constructed analogs of multiple variables, in this case daily maximum and minimum air temperature, solar radiation, humidity, and wind speed – all the variables needed to computed reference ET at daily time steps using the physically based ASCE Standardized Penman-Monteith equation (ASCE, 2005). The MACA approach includes bias correction by mapping daily General Circulation Model (GCM) data to aggregated gridded observations (Maurer et al., 2010), epoch adjustment for no analogs under future climate scenarios (Hidalgo et al. 2008), constructed analogs by finding predictor patterns using gridded observation data, and bias correction using quantile mapping to METDATA, which is the gridded observation training dataset (Abatzoglou, 2011). For more information on the MACA approach, refer to Abatzoglou and Brown (2012) and MACA development steps at http://maca.northwestknowledge.net/MACAmethod.php.

The full suite of MACA data used in this report was acquired from the University of Idaho's MACA project page at http://maca.northwestknowledge.net/. The full suite of MACA data includes climate projections from 20 different models (http://maca.northwestknowledge.net/GCMs.php) that participated in CMIP5 (i.e. only 20 CMIP5 models archived daily outputs). MACA data includes GCM outputs from the historical CMIP5 experiment for the years 1950-2005 and GCM outputs from 2 future experiments for Representative Concentration Pathways (RCPs) of 4.5 and 8.5 for 2006-2100. RCP 4.5 refers to the experiment where an additional radiative forcing of 4.5 W/m^2 is simulated by 2100 compared to preindustrial conditions, which is a future scenario of moderate climate action and controlled greenhouse emissions. RCP 8.5, refers to the experiment where an additional radiative forcing of 8.5 W/m2 is simulated by 2100, and represents a future with no climate action and increased greenhouse emissions. In total, 40 MACA transient projections were obtained for each representative agricultural station location, and each transient projection was treated as an individual ET Demands model run to simulate reference ET, crop ET, and the NIWR for each crop. MACA variables and ET Demands output using MACA data were summarized for baseline (1950-2005) and future time periods (i.e. 2020s (years 2006-2039), 2050s (years 2040– 2069), and 2080s (2070-2099)).

ET Demands Model Overview

At the core of the ET Demands model is the FAO-56 dual crop coefficient model (Allen et al., 1998), which was run for historical and future climate periods. ASCE-PM-based grass reference ET_0 was computed for baseline and projected climate data sets at each Metnode using historical and projected climate variables of daily maximum and minimum air temperature, solar radiation, humidity, and wind speed. Actual ET for a range of crop types was estimated at each Metnode using the FAO-56 dual crop coefficient approach having the form:

$$ET_c = (K_s K_{cb} + K_e) ET_0$$

where ET_0 is ASCE-PM grass reference ET, K_{cb} is the basal crop coefficient, and K_e is a coefficient representing evaporation from the soil surface. K_{cb} and K_e are dimensionless and range from 0 to 1.4 when used with ASCE-PM grass reference ET. Daily K_{cb} values over a season, commonly referred to as the crop coefficient curve, represent impacts of changes in vegetation phenology on crop ET, which can vary from year to year depending on the start, duration, and termination of the growing season, all of which are dependent on temperature conditions during spring, summer, and fall periods. The stress coefficient (K_s) ranges from 0 to 1, where 1 equates to no water stress, which is generally the case for fully irrigated crops during the irrigation season as opposed to rain fed crops or native vegetation, which commonly experience some soil water-induced stress. A daily soil water balance for the simulated effective root zone is required to calculate K_s and is computed in ET Demands. K_s is generally 1 when computing ET_c and NIWR for irrigated crops, but can become less than 1 during winter when precipitation is low. ET Demands estimates of K_s during winter, for dormant covers of mulch and grass, can go below 1 since there is no irrigation specified for dormant periods. A second daily soil water balance for the upper 0.1 m of soil is used in ET Demands to estimate K_e. The upper 0.1 m zone is assumed to be the only layer supplying water for direct evaporation from the soil surface.

The NIWR is estimated as the ET_c minus precipitation residing in the root zone, P_{rz}. Precipitation residing in the root zone is the amount of gross reported precipitation that infiltrates into the soil and that remains in the root zone for consumption by evaporation or transpiration. Although P_{rz} includes precipitation that is later evaporated and possibly not transpired by the crop, ETc includes evaporation of precipitation, therefore ETc minus P_{rz} represents the net irrigation water requirement, and not ET_c minus the P_{rz} portion that is effective toward transpiration only. P_{rz} is computed as P – Runoff – D_{Percp} where P is gross reported precipitation. Runoff is estimated surface runoff, and D_{Percp} is deep percolation of any precipitation below the maximum root zone for the crop or land-use condition. For more information on details of the ET Demands model see Huntington et al. (2015)

Soils Data

Soil attributes needed for ET Demands parameterization were obtained from the NRCS State Soil Geographic (STATSGO) database (USDA-NRCS 1991). STATSGO is a spatial soils GIS database and contains attributes of the physical character of soils needed to estimate soil water holding and infiltration parameters in the ET Demands model's dual soil and root zone water balance and runoff modules. STATSGO attributes of available water capacity, and sand, silt, and clay fractions were used to estimate the spatial distribution of total evaporable water and readily evaporable water used in the surface soil layer water balance, and total available water and readily available water were used in the root zone water balance. These parameters affect the estimation of irrigation scheduling, evaporation losses from soil, deep percolation from root zones, antecedent soil moisture condition, and runoff from precipitation. Gridded soil attributes for available water capacity and sand, silt, and clay fractions were averaged over 60-inch (150-cm) depths and were then intersected with irrigated crop land areas, and spatially averaged within each HUC8.

Crop Coefficients

For this work, basal crop coefficient (K_{cb}) curves from Allen and Robison (2009) and applied in Huntington et al. (2015) were adopted for the application of ET Demands. The Allen-Robison curves are largely traceable to lysimeter-based K_{cb} curves of Wright (1982, 2001) and are based on the taller alfalfa reference ET (ET_r). The three methods define the advancement of the K_{cb} curve based on (1) normalized cumulative growing-degree-days from planting or greenup to effective full cover, with this ratio extended until termination of the cropping period; (2) percent time from planting to effective full cover, with this ratio extended until termination; and (3) percent time from planting to effective full cover and then number of days after full cover to termination. These K_{cb} development approaches allow for time interpolation and shape of crop-specific K_{cb} curves to be a function of cumulative growing degree days (CGDD) and temperature dependent planting or greenup estimates such as 30 day moving average air temperature (T_{30}) rather than specified and constant calendar dates. CGDD has previously been used for defining planting and greenup times, crop coefficient development, scaling of development periods, and transferring K_{cb} curves among regions in a wide range of studies (Sammis et al. 1985; Slack et al. 1996; Howell et al. 1997; Snyder et al. 1999; Wright 2001; deTar 2004; Marek et al. 2006; Allen and Robison 2009). Calibration of crop stage parameters that determine planting, greenup, effective full cover, and harvest stages of K_{cb} curves was accomplished by running the ET Demands model using historical METDATA climate time series at each Metnode, and determining optimal values for T_{30}, time, and CGDD to effective full cover or termination / harvest for each crop to fit observed planting, greenup, and development dates. Optimal values were concluded when simulated crop stages compared well with documented dates in each basin and sub-basin. Values for T_{30}, time, and CGDDEFF or TERM (i.e. the specified crop-dependent value for CGDD from the time of planting or greenup to the attainment of effective full cover and

termination) were initially adopted from Huntington et al. (2015) and modified accordingly during the calibration process for each basin and crop. Documented crop stage dates for respective areas were derived from published data, as well as from verbal and written communications (USDA, 2010; Huntington and Allen, 2010; Hill et al., 2011). Simulated greenup, planting, and cutting and harvest dates were assumed to represent average conditions, recognizing the large variations in actual populations of cutting, harvest, and termination dates that occur due to differing farming practices and rotations of cuttings. Calibration results suggest that historical mean annual greenup, planting, cutting, and harvest can be relatively well simulated considering the large spatial variation in air temperature within each basin and sub-basin. Simulated crop stages were typically within ~ ±20 days of the documented stages for each crop and basin.

Because planting and harvest dates for annual crops are temperature dependent, and are simulated using the T_{30} and the GDD approach, shifts in planting, development, and harvest dates for future time periods occur in simulations, especially towards the 2080 time period. Projections of changes in future farming practices for annual crops, such as potential earlier plantings and more rapid development and harvest, are uncertain under warming climatic conditions. These potential changes will likely be highly dependent on future crop cultivars, water availability, and economics. For these reasons, simulation of thermally based annual crop K_{cb} curves for future time periods were based on detrending future temperature time series to simulate planting, crop development, and harvest dates in accord with the T_{30} and GDD approaches as previously described. For each MACA time series of maximum and minimum temperature, the temperature trend was removed using the detrend function in Matlab, which is a least-squares fitting function.

Planting, development, and harvests for perennial crops were assumed to be subject to actual temperature projections, which results in earlier greenup, later killing frost, and longer growing length. It is important to once again note the assumption of adequate irrigation water supplies to fulfill crop water needs when estimating ET demands and NIWR, especially with regard to growing-season length impacts on total crop water consumption. This analysis assumes that as climate warms, given that there are no constraints on crop cycles due to water scarcity, ET_c rates will increase, plant phenologies may shift, and the growing season could expand or stay the same depending on crop type. For more information on crop coefficents used in the ET Demands model see Huntington et al. (2015).

The impact of increased CO_2 on crop transpiration, water use efficiency, and yield is of particular interest and is probably one of the largest uncertainties in future crop ET and K_{cb} curve magnitudes. Several studies have described how elevated CO_2 concentrations may reduce stomatal aperture, transpiration, and crop production processes (Rosenberg 1981; Kimball and Idso 1983; Manabe and Wetherald 1987; Kruijt et al. 2008; Islam et al. 2012). However, estimating CO_2-induced changes on irrigation demands remains an extremely difficult task because of plant dependency, adaptation, unknown non-linear near-surface

boundary-layer feedbacks from reduced transpiration and resulting increased leaf temperatures and vapor pressure deficits, uncertainties of increased leaf area index, stomatal and aerodynamic resistances, and plant-dependent stomatal sensitivities (i.e., C3 versus C4 plants). Allen et al. (1991) simulated CO_2 induced climate changes on NIWR for the Great Plains States (Texas, Oklahoma, Kansas, and Nebraska), and suggested that uncertainties in potential leaf area index (LAI) under future CO_2 and in stomatal resistance increases studied under laboratory conditions were too large to give conclusive results, recommending further research on interactions between elevated leaf temperature and CO_2 concentrations and plant mechanisms be conducted in open, agricultural environments. Since then, there have been numerous open chamber and open field environment CO_2 – stomatal conductance sensitivity studies. Kruijt et al. (2008) recently summarized over 30 of these studies and developed general CO_2 – stomatal conductance sensitivity functions for grouped C3 and C4 plant species. Still, there is a large gap in research on the sensitivity of stomatal conductance and thus ET to increased CO_2 for many western crops to be analyzed in this work. As a means to describe the potential effect of rising CO_2 on ET_c sensitivity functions developed by Kruijt et al. (2008) were applied within the ET Demands model for future climate projections. However, it is understood that there are other uncertainties associated with open agricultural environment sensitivities of stomatal conductance, transpiration, and leaf area index to increased CO_2, and unknown land surface energy balance feedbacks from increased leaf temperatures and vapor pressure deficits.

Impacts of CO_2 on ET_c considered following methods outlined by Kruijt et al. (2008). These methods include applying CO_2-dependent, crop-specific coefficients based on three factors relating to stomatal conductance, boundary-layer properties, and the transpiration fraction of ET_c. Specifically, the basal crop coefficient, K_{cb}, under current conditions, representing the transpiration portion of ET, was adjusted according to

$$K_{cb\_projected} = K_{cb} * c$$

and

$$c = (1 - (S_{gs} * S_T * \Delta CO_2))$$

where c is the CO_2 correction factor, $K_{cb\_projected}$ is the projected basal crop coefficient (dimensionless), K_{cb} is the basal crop coefficient under current conditions (dimensionless), ΔCO_2 is the change in CO_2 concentration (ppm), S_{gs} is the relative sensitivity of crop stomatal conductance to CO_2 (ppm^{-1}) computed as $S_{gs} = (dg_s/g_s)/dCO_2$, and S_T is the relative sensitivity of transpiration (T) to a change in crop stomatal conductance (dimensionless) computed as $S_T = (dT/T)/(dg_s/g_s)$. Sensitivities were derived from previous study summaries and functions given in Kruijt et al. (2008), Jacobs and De Bruin (1992), and Jacobs and De Bruin (1997). Future projections of ET_c were computed using the ET Demands dual crop coefficient approach previously discussed and fully described in Huntington et al. (2015), but

supplementing K_{cb} with $K_{cb\_projected}$ for respective C3 and C4 crop/plant types and RCP projections at daily time steps. Figure 6 illustrates the CO_2 correction factor, c, through time according to different plant species and RCP values. Figure 6 illustrates that c approaches a value of approximately 0.8 by 2100 for C4 RCP 8.5, effectively reducing the K_{cb} value by approximately 20 to 25% during effective full cover periods when the K_{cb} curve is typically at values of 1 to 1.2.

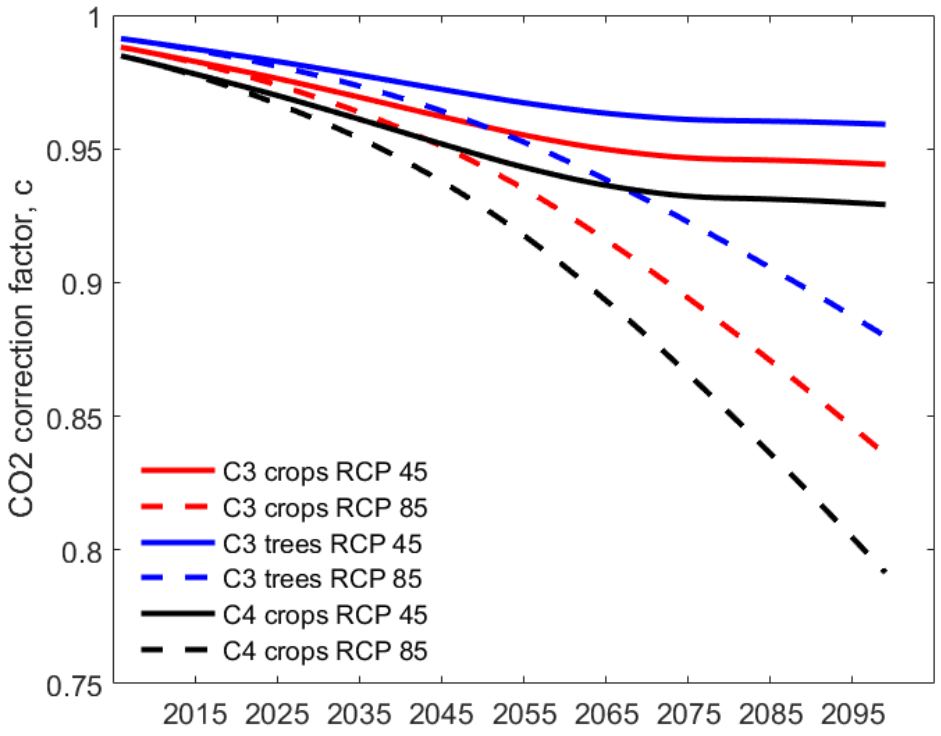

Figure 6 - The CO2 correction factor, c, through time according to different plant species and RCP values. The factor c was applied at daily time steps to ET Demands model simulated Kcb values for respective C3 and C4 crop/plant types and RCP projections. Most crops were classified as C3 crops, with the exception of corn, millet, and sugarcane, which were classified as a C4 crops. All orchards were considered to be C3 tree crops.

ET Demands Model Application

The ET Demands model was run with historical METDATA time series representative of observed climate histories from 1979-2015 for K_{cb} curve calibration and ET_0 bias correction purposes (described in the above climate and crop coefficient sections). The ET Demands model was then run with 40 individual MACA climate projection time series from 1950-2100 to derive and illustrate baseline (1950-2005) and projected (2006-2100) estimates of annual average temperature, solar radiation, humidity, wind speed, and total precipitation, ET_0, ET_c, and NIWR for Metnode using Python programs that can be found on GitHub at https://goo.gl/iGCfQN. While the ET Demands results from running the model with historical METDATA are not summarized in this report, the digital files are available (see Appendix directories). The Python programs simulate for each ET_0, growing-

season and non-growing-season soil and root zone water balance components (K_{cb}, K_s, K_e), irrigations, and ET_c and NIWR, all at daily time-steps (Figure 7). ET_0 was computed at each Metnode, which contain all relevant information for respective HUC8 areas (termed ET cells), such as soil information, crop type, and crop acreage, and are used by the ET Demands model to compute daily ET_c and NIWR rates for each ET cell (i.e. HUC8 area). Daily ET_c and NIWR rates and volumes for each ET cell were computed using unique irrigated crop types and associated areas derived from CDL data for 2010 (USDA-NASS 2010a). Crop area weighted annual ET_c and NIWR rates ($ET_c - P_e$) for each ET cell (i.e. HUC8 area) were computed as the total annual ET_c and NIWR volume for all crops divided by the total crop acreage. Crop area weighted annual time series and change maps of ETc and NIWR and associated variables for historical and future time periods are presented in the results section.

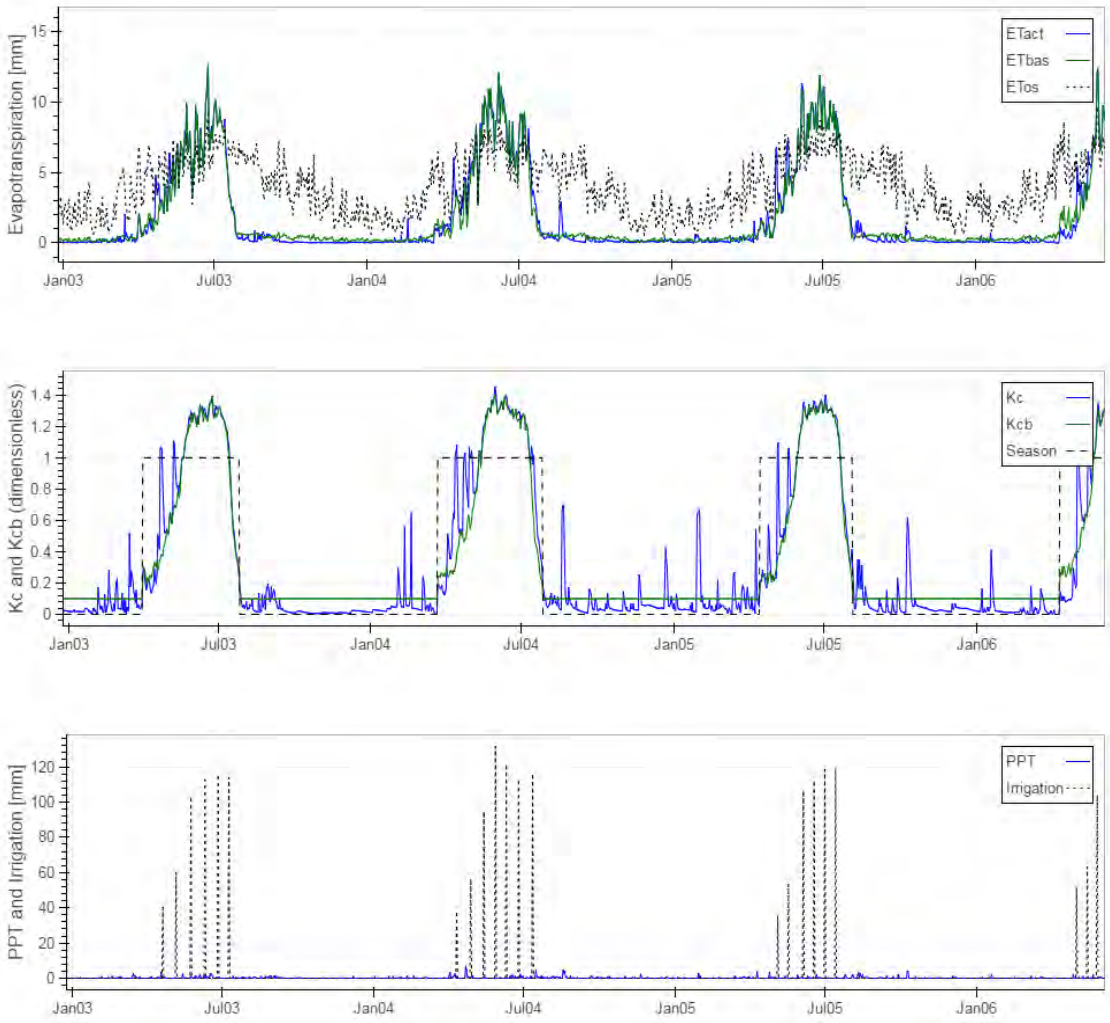

Figure 7- ET Demands model simulation of METDATA derived ET0 (labeled ETos), Spring Grain ETc (ETact) and basal ET (ETbas), basal crop coefficient curve (Kcb), total crop coefficient curve (Kc), simulated irrigations, estimated METDATA precipitation for ET cell 11020002, located in the Arkansas basin, representative of Penrose and Canon City irrigated areas, Colorado. The simulated Kc curve, irrigations, and estimated precipitation are shown to illustrate the development of the Kc curve, and response of the Kc curve and ETact due to wetting events from precipitation and simulated irrigation events.

RESULTS

This section presents an overview of baseline and future estimates of ET Demand model components for each study area. Results include spatial and time series plots of baseline and change from baseline conditions for precipitation, temperature, reference evapotranspiration (ET_0), crop evapotranspiration (ET_c), and net irrigation water requirement (NIWR). A summary of the results and figures is presented for each basin. For the TCWLH basins, results from this study are compared to results from a previous Reclamation climate change study (Huntington et al., 2015) in which ET_c and NIWR was estimated using CMIP3 and BCSD hybrid-delta ensemble climate data, and where solar radiation, humidity, and wind speed were estimated (based on empirical relationships) for computing ET_0 rather than using CMIP5 MACA required variables directly for computing ET_0.

The first set of plots for each basin results summary includes spatial plots of baseline (1950–2005) average median precipitation, temperature, solar radiation, humidity, wind speed, ET_0, and crop area weighted ET_c and NIWR. All spatial plots are presented at the HUC8 level, even though the simulations are point-based (i.e., Metnodes) (i.e. Metnode results are assigned to respective HUCs). The second set of plots include spatial plots of projected changes from the baseline for average median precipitation, temperature, solar radiation, humidity, wind speed, ET_0, and crop area weighted ET_c and NIWR for 5^{th}, 25^{th}, 50^{th}, 75^{th}, and 95^{th} percentiles at three future periods: 2020s (years 2006-2039), 2050s (years 2040– 2069), and 2080s (2070-2099), with 1950–2005 as the baseline period. Transient time series anomaly plots of annual precipitation, temperature, solar radiation, humidity, wind speed, ET_0, and crop area weighted ET_c and NIWR are also provided for all HUC8s for each basin in digital appendices. Digital appendices are organized by basin and contain HUC8 (i.e. ET Cell and Metnode) properties, statistics for MACA baseline and future ET Demands simulation results illustrated as spatial plots within the results section, and baseline and future time series plots for all variables and Metnodes. Digital appendices can be found at www.dri.edu/water-use/cat.

Altus Area

Figure 1 illustrates Metnodes that were used to estimate irrigation water demands, as well as HUC8 boundaries used to upscale Metnode estimates in the Altus area. Figure 8 illustrates the spatial distribution of MACA derived baseline (1950–1999) average median precipitation (top left), temperature (top right), solar radiation (bottom left), and specific humidity (bottom right). Figure 9 illustrates the spatial distribution of MACA derived baseline (1950–1999) average median wind speed (top left), ET_0 (top right), ET_c (bottom left), and NIWR (bottom right). Figure 8 illustrates relatively cool to warm average median temperatures from west to east, respectively, while precipitation varies from higher to lower amounts from east to west, respectively. The spatial distribution of average median solar radiation and specific humidity is consistent with the distribution of precipitation – where there is more precipitation solar radiation is reduced and specific humidity is higher.

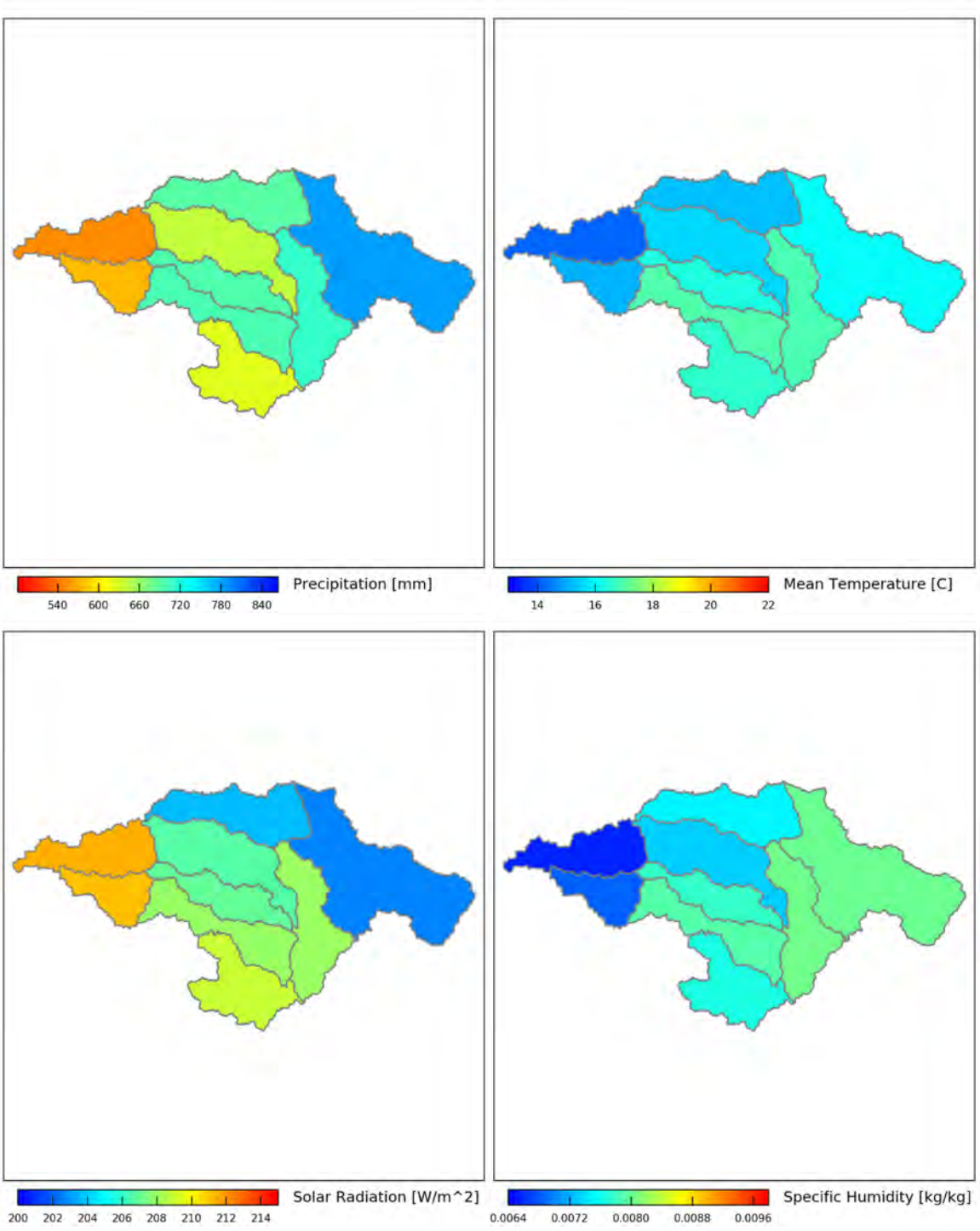

Figure 8 - Altus Area – Spatial distribution of baseline precipitation, temperature, solar radiation, and humidity. Color scales are relative to baseline and future conditions.

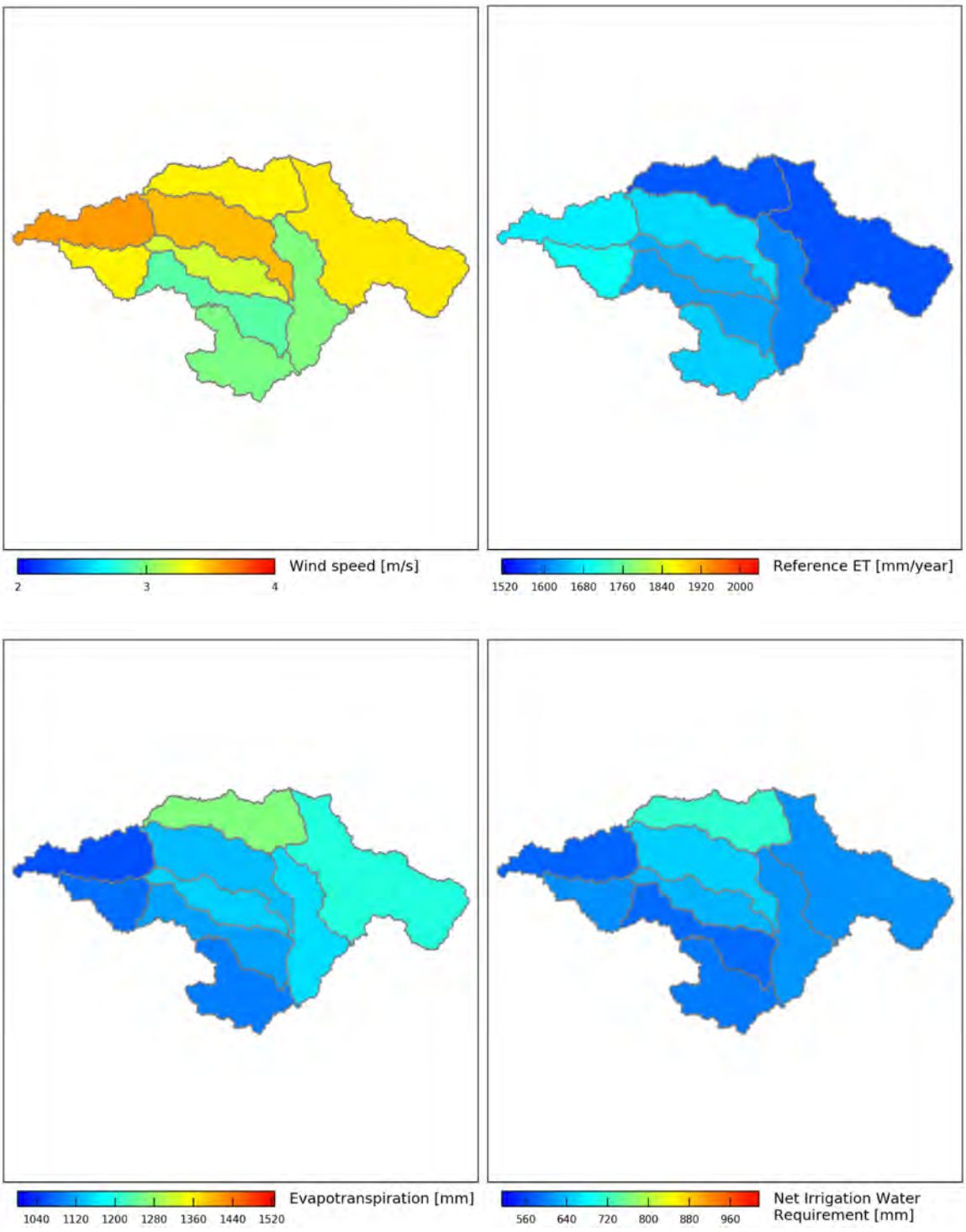

Figure 9 - Altus Area – Spatial distribution of baseline wind speed, reference ET, crop evapotranspiration, and net irrigation water requirement.

Figure 9 illustrates the spatial distribution of average median wind speed, where lower wind speed generally occurs in the southern portion of the basin. Baseline median ET_0, ET_c, NIWR range from around 1600 to 1700, 900 to 1200, and 500 to 640 mm/yr, respectively, with higher rates of ET_c and NIWR occurring in the north eastern and northern portions of the basin, respectively. Notice that while ET_0 is lowest in the eastern portion of the basin, while ET_c is highest in this area. High ET_c in the eastern portion of the basin is due to relatively high precipitation, which reduces the NIWR. Figure 10 shows the spatial distribution of projected precipitation changes for different percentiles and time periods, where it is evident that projected precipitation changes generally increase during the 2020 period, and then decrease in 2050 and 2080 time periods relative to baseline conditions, however, only by ~ -5 to 7 percent. Figure 11 illustrates the spatial distribution of projected temperature change for different scenarios and time periods, which shows spatial uniform warming for all time periods ranging from 0 to 5 ^{o}C. Figures 12 and 13 illustrate solar radiation and specific humidity percent changes, which also show spatial uniform change, with solar radiation increasing by 0 to 2 percent, and specific humidity increasing from 0 to 17 percent. Figure 14 illustrates wind speed percent changes, ranging from -1 to 2 percent. Figure 14 illustrates ET_0 percent change for different percentiles and time periods. Similar to temperature, the projected percent change in ET_0 is generally spatially uniform, and ranges from 0 to 17 percent. Figure 16 illustrates the spatial distribution of projected ET_c percent change, which ranges from 0 to 18 percent. Spatial differences in the distribution of projected percent change in ET_c are largely due to differences in crop type, precipitation, and baseline ET_c rates. The northern portion of the basin is projected to experience the largest percent change for all projected time periods. Perennial forage crops (e.g. alfalfa and grass hay) have larger acreage (relative to the total acreage in each HUC) in the north, and are projected to have earlier greenup, longer harvest periods (i.e., more cuttings), and later killing frosts, leading to longer growing seasons and large percent increases relative to baseline ET_c. The spatial distribution of projected NIWR percent change is shown in Figure 17. The NIWR incorporates growing season and non-growing season soil moisture gains and losses from precipitation, bare soil evaporation, and ET_c, therefore spatial variations in the distribution of NIWR percent change for different time periods and scenarios are a function of respective ET_c (Figures 16) and precipitation (Figure 10) distributions. NIWR percent changes range from 0 to 30 percent, where the northern, western, and northeastern portions of the basin are projected to increase the most. Precipitation in these areas is projected to decrease by 2080, which is partially the cause for increased NIWR change for these areas of the basin. Transient time series anomaly plots of annual precipitation, temperature, solar radiation, humidity, wind speed, ET_0, ET_c, and NIWR are shown in Figure 18 for Metnode 336043 (near Fort Cobb), which illustrates the general increase in all variables relative to the baseline, with the exception of wind speed and precipitation.

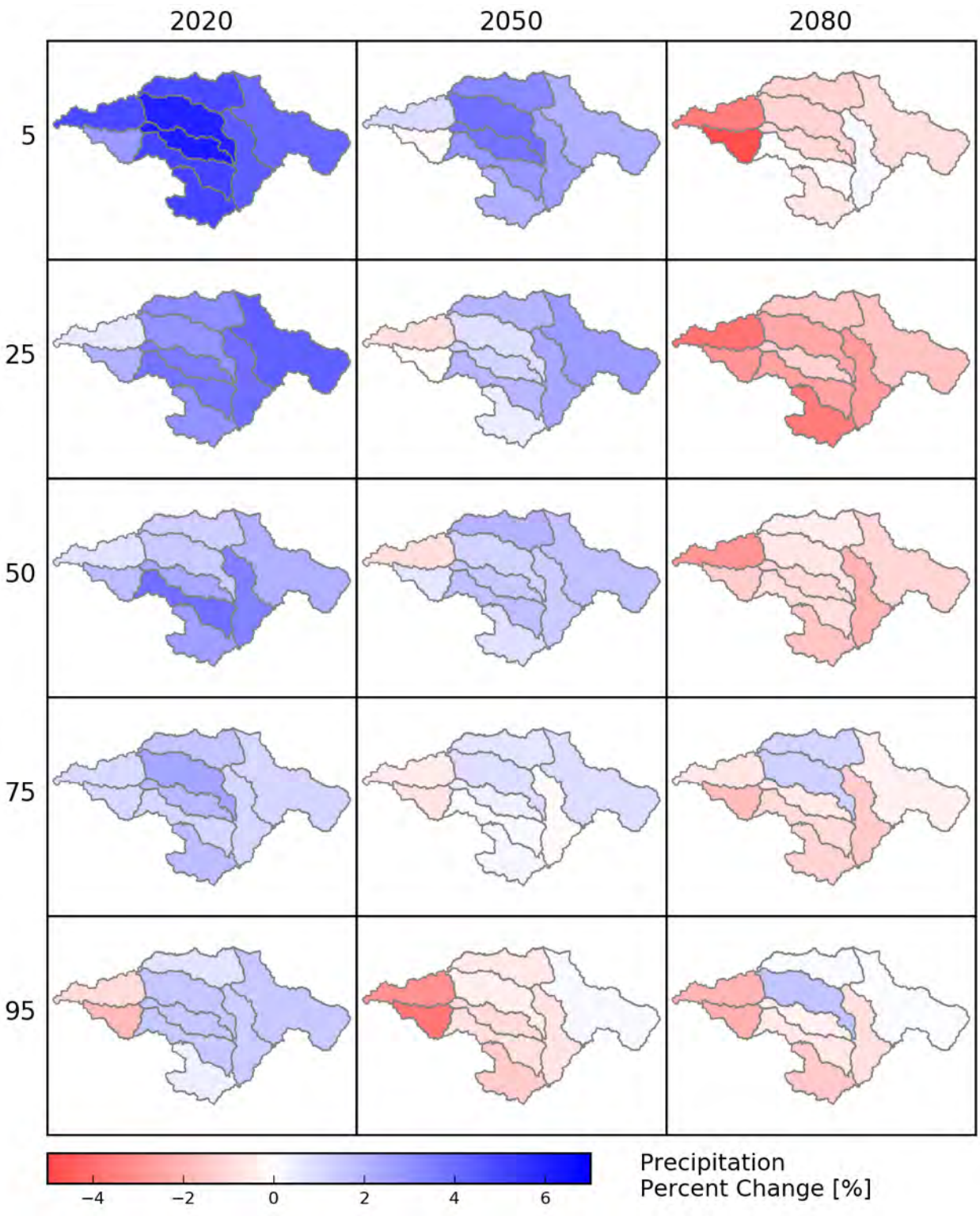

Figure 10- Altus, Oklahoma Area – Spatial distribution of projected precipitation percent change for different percentiles and time periods.

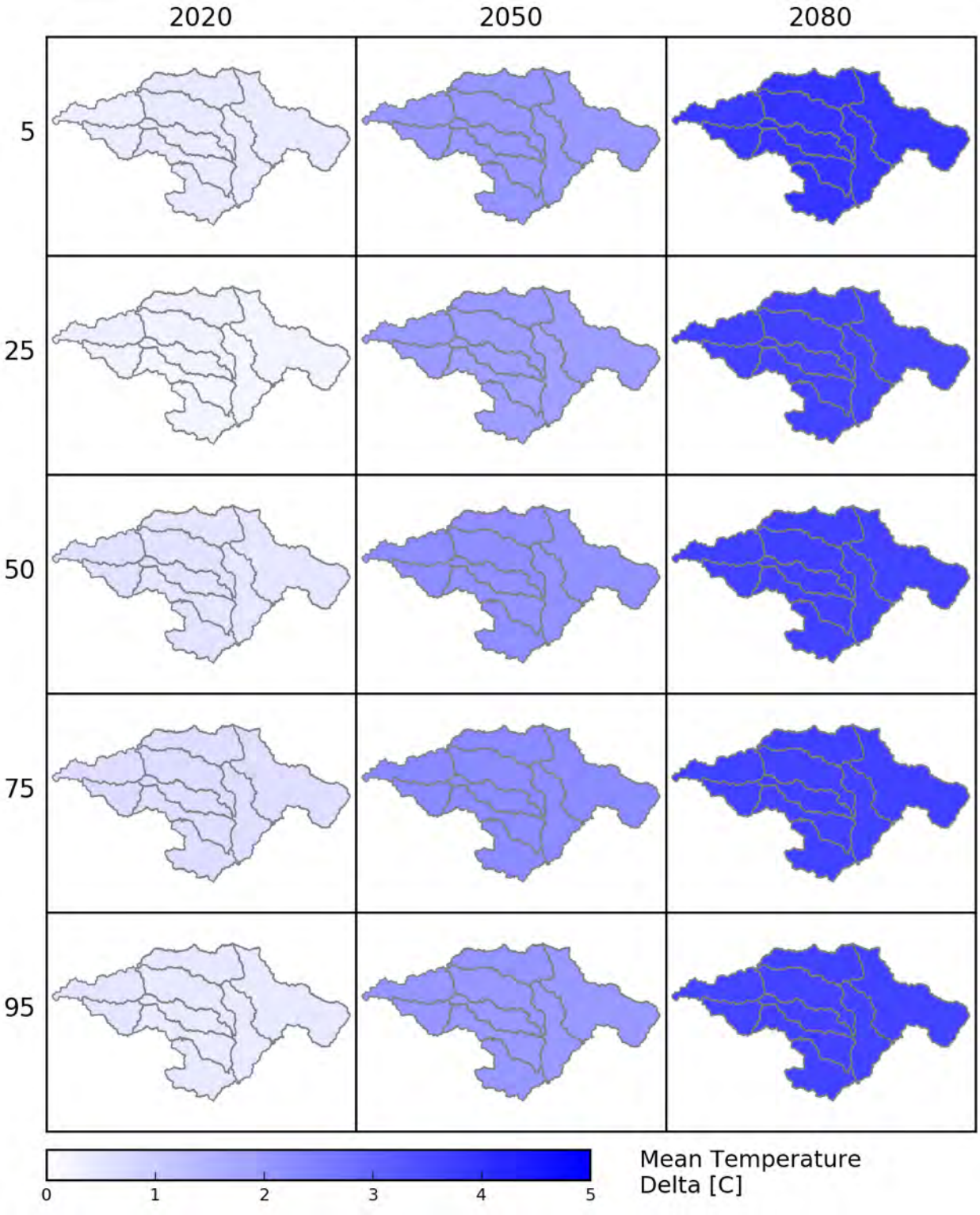

Figure 11 - Altus, Oklahoma Area – Spatial distribution of projected temperature change for different percentiles and time periods.

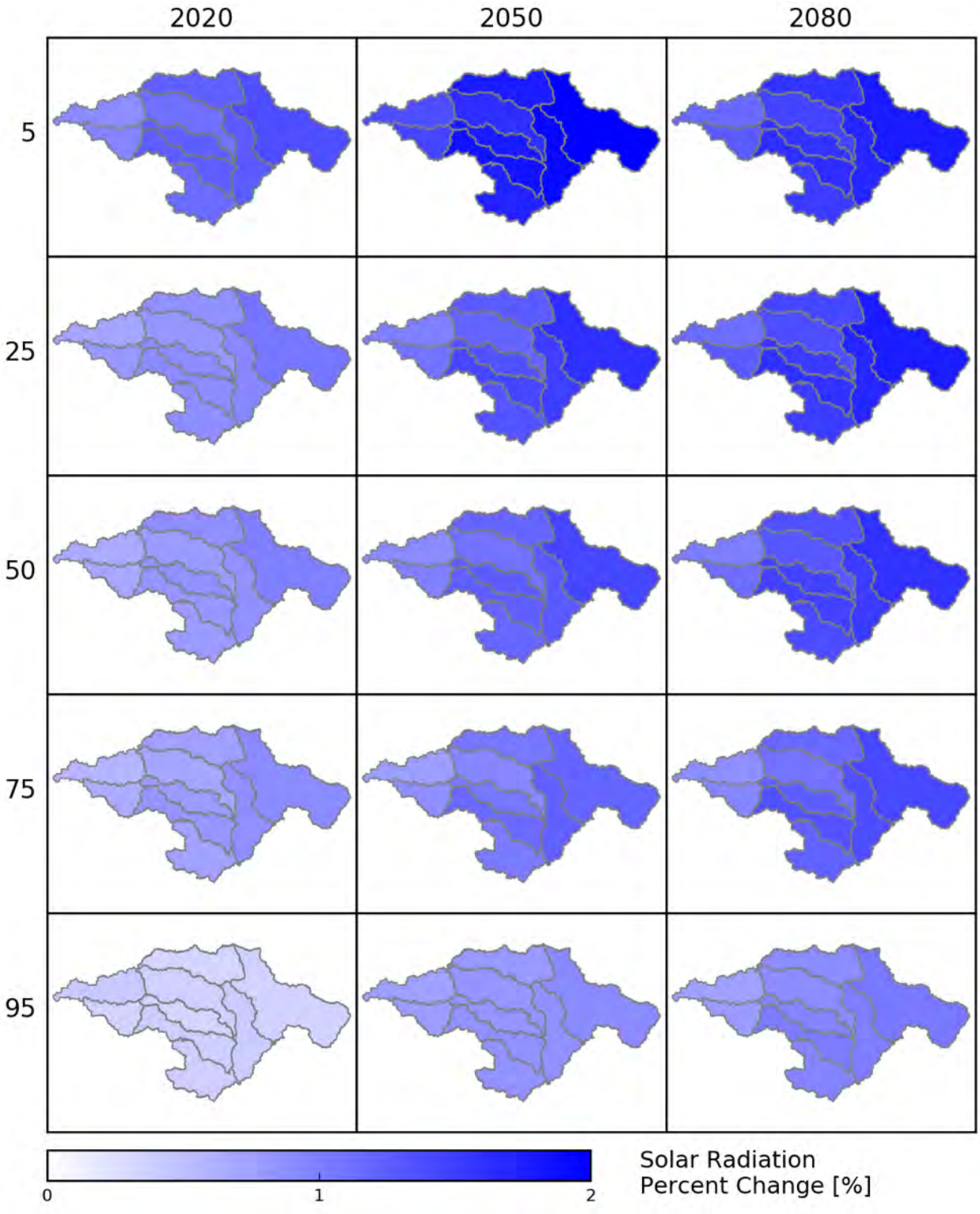

Figure 12 - Altus, Oklahoma Area – Spatial distribution of projected solar radiation percent change for different percentiles and time periods.

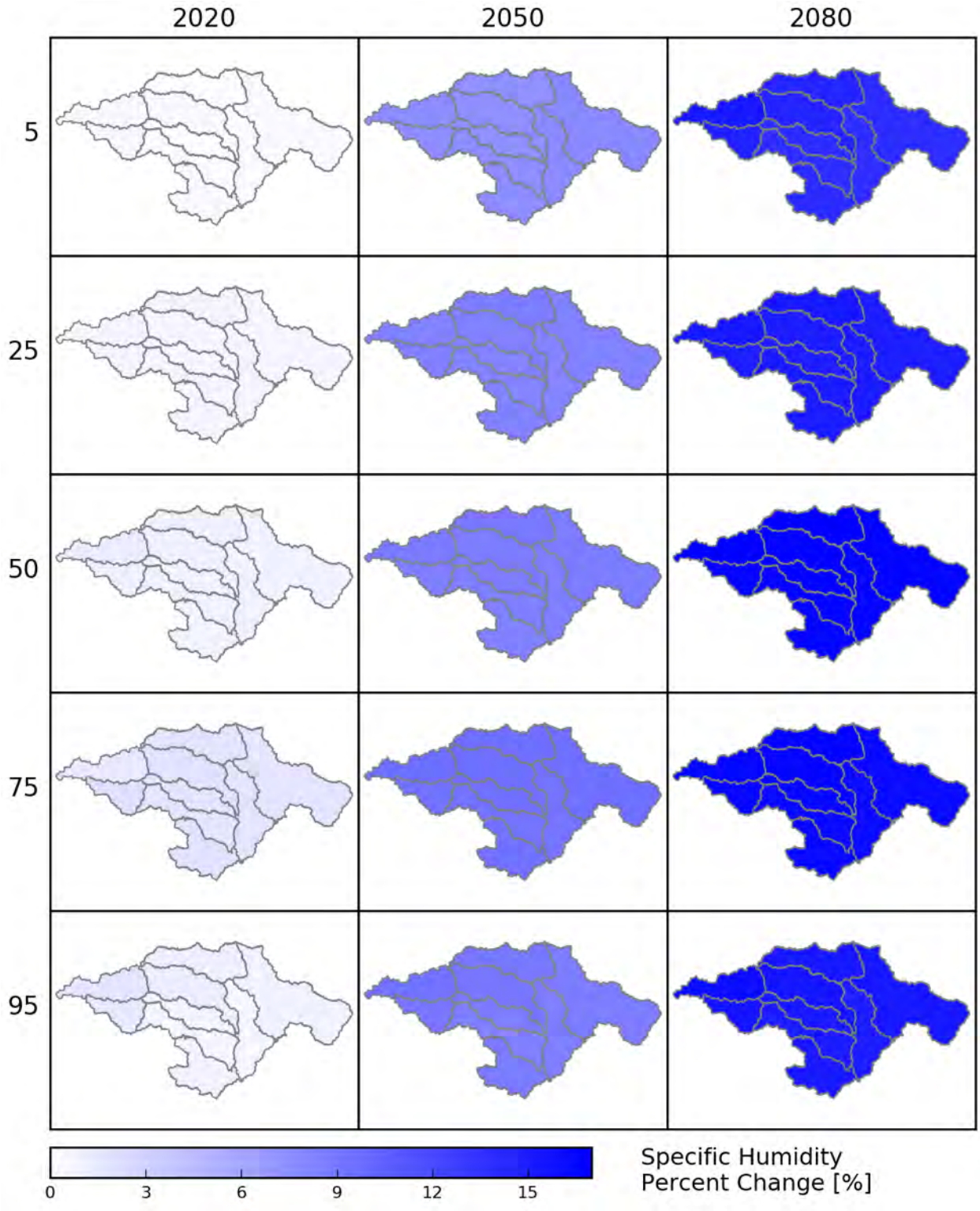

Figure 13 - Altus, Oklahoma Area – Spatial distribution of projected specific humidity percent change for different percentiles and time periods.

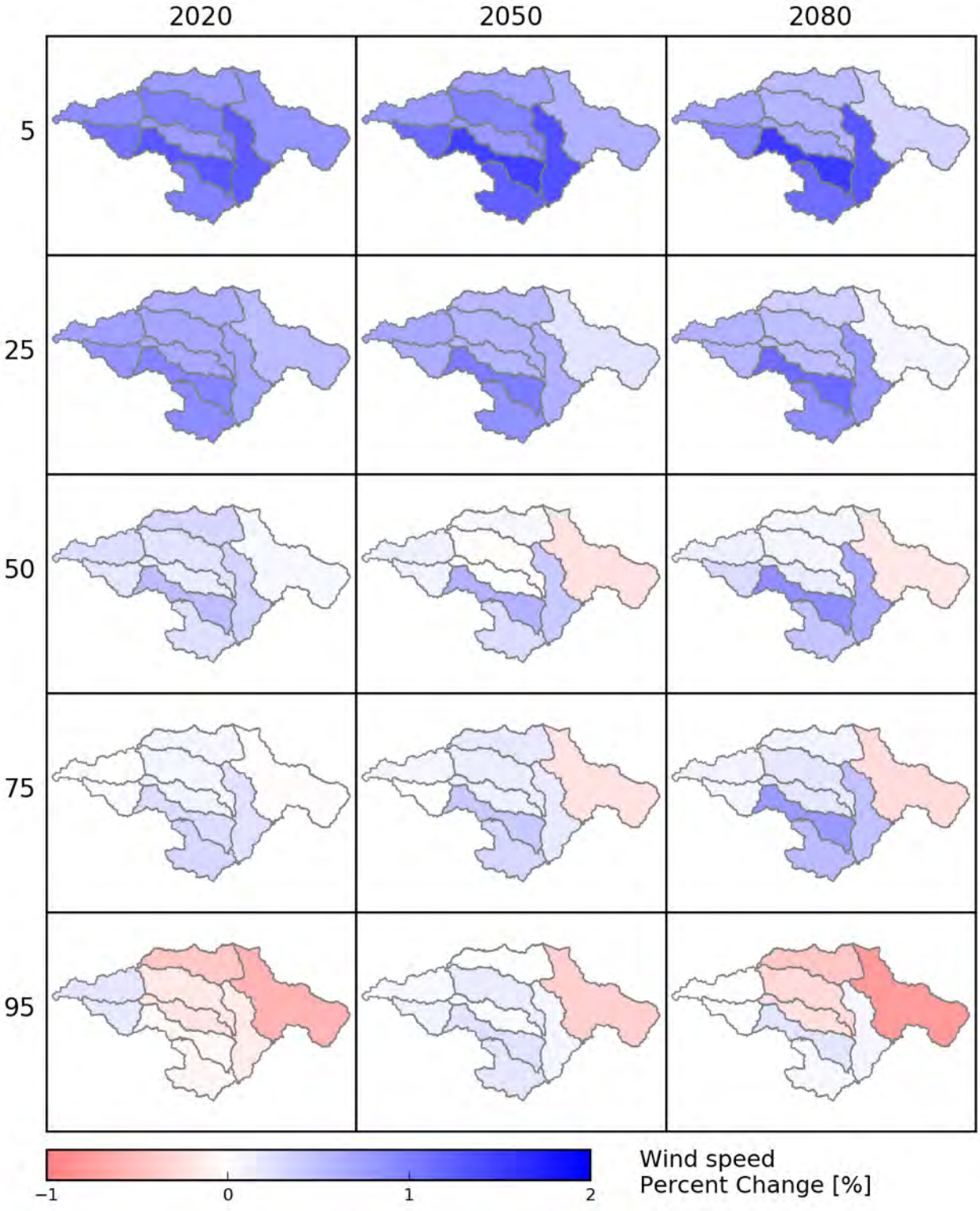

Figure 14 - Altus, Oklahoma Area – Spatial distribution of projected wind speed percent change for different percentiles and time periods.

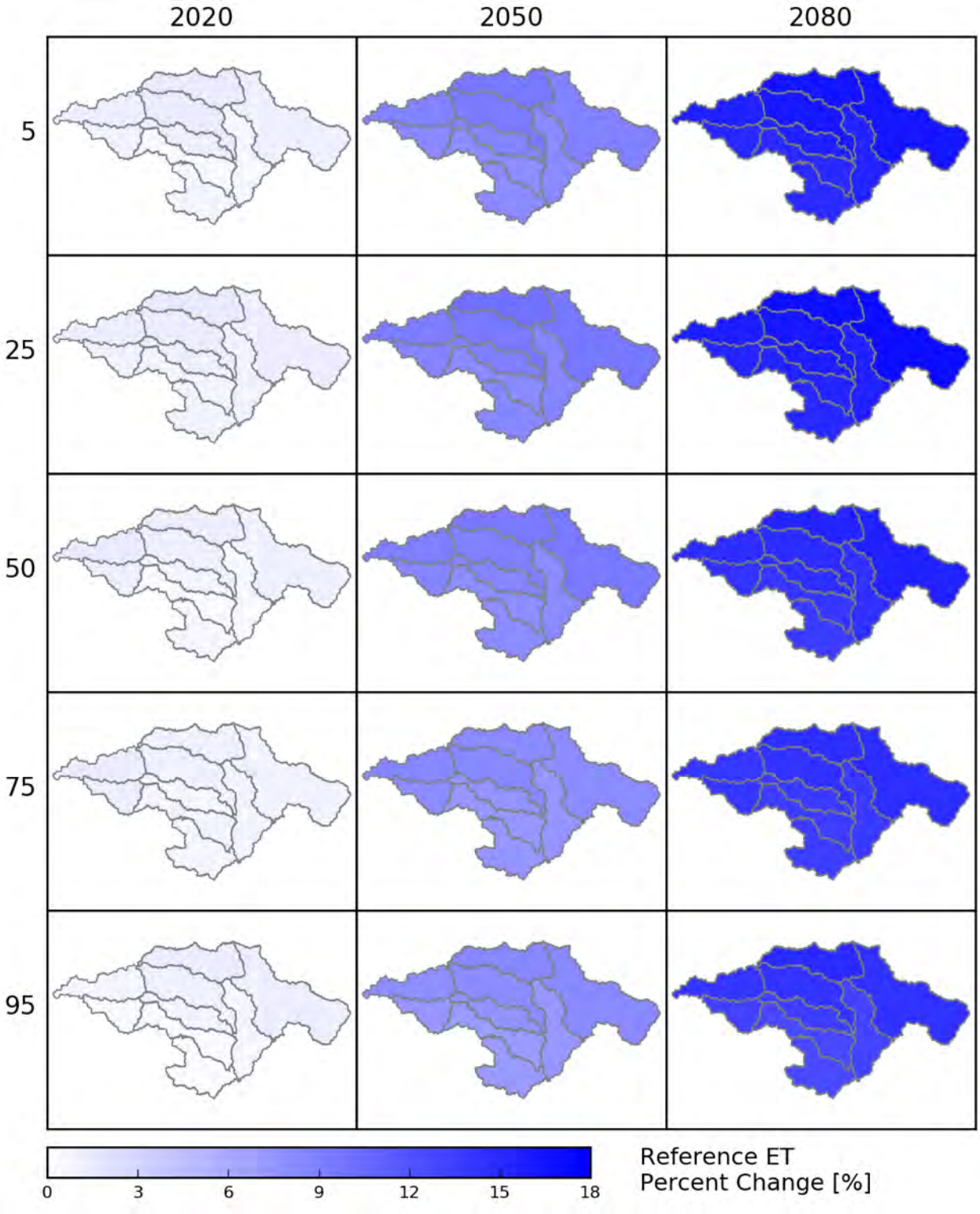

Figure 15 - Altus, Oklahoma Area – Spatial distribution of projected reference ET percent change for different percentiles and time periods.

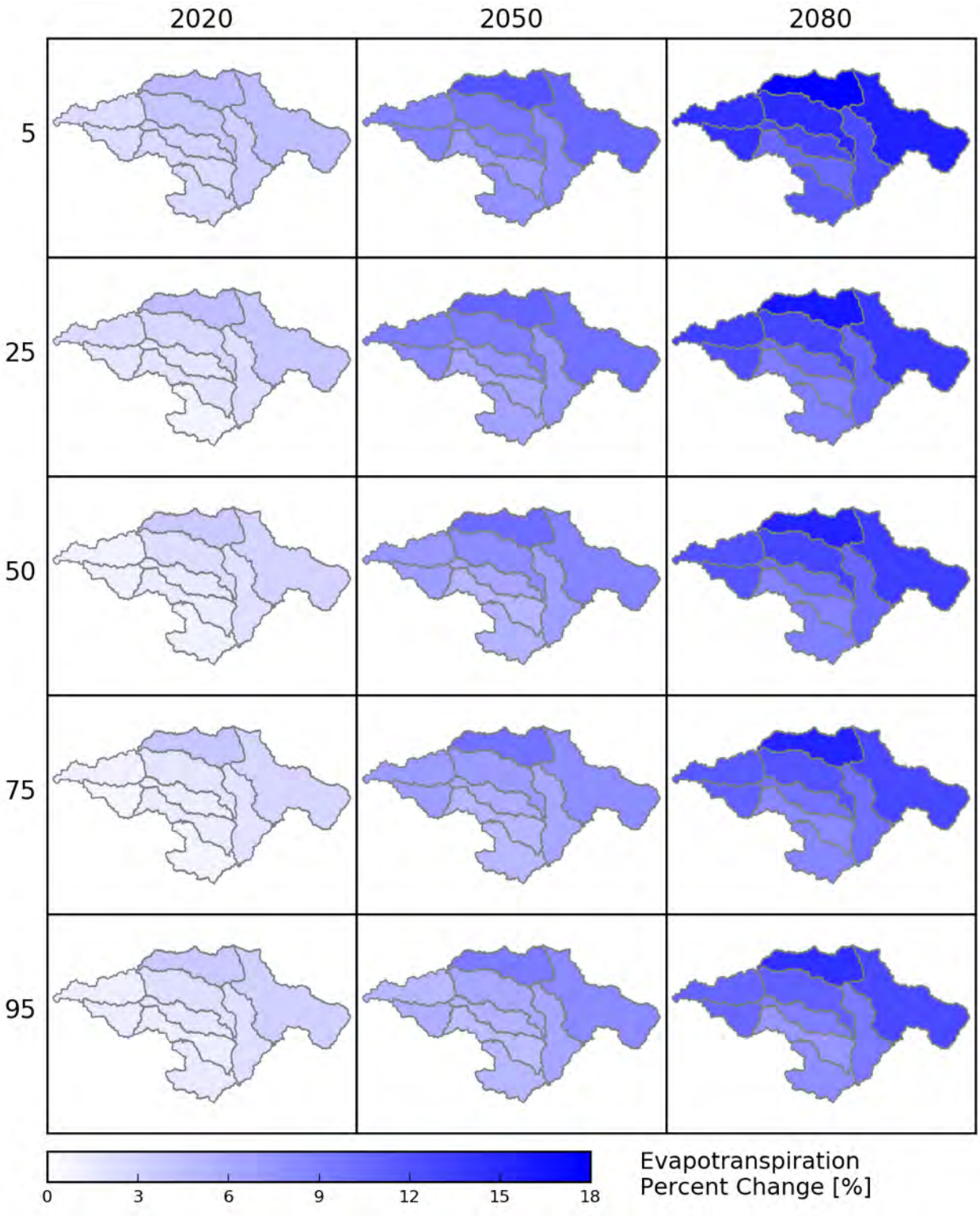

Figure 16 - Altus, Oklahoma Area – Spatial distribution of projected crop ET percent change for different percentiles and time periods.

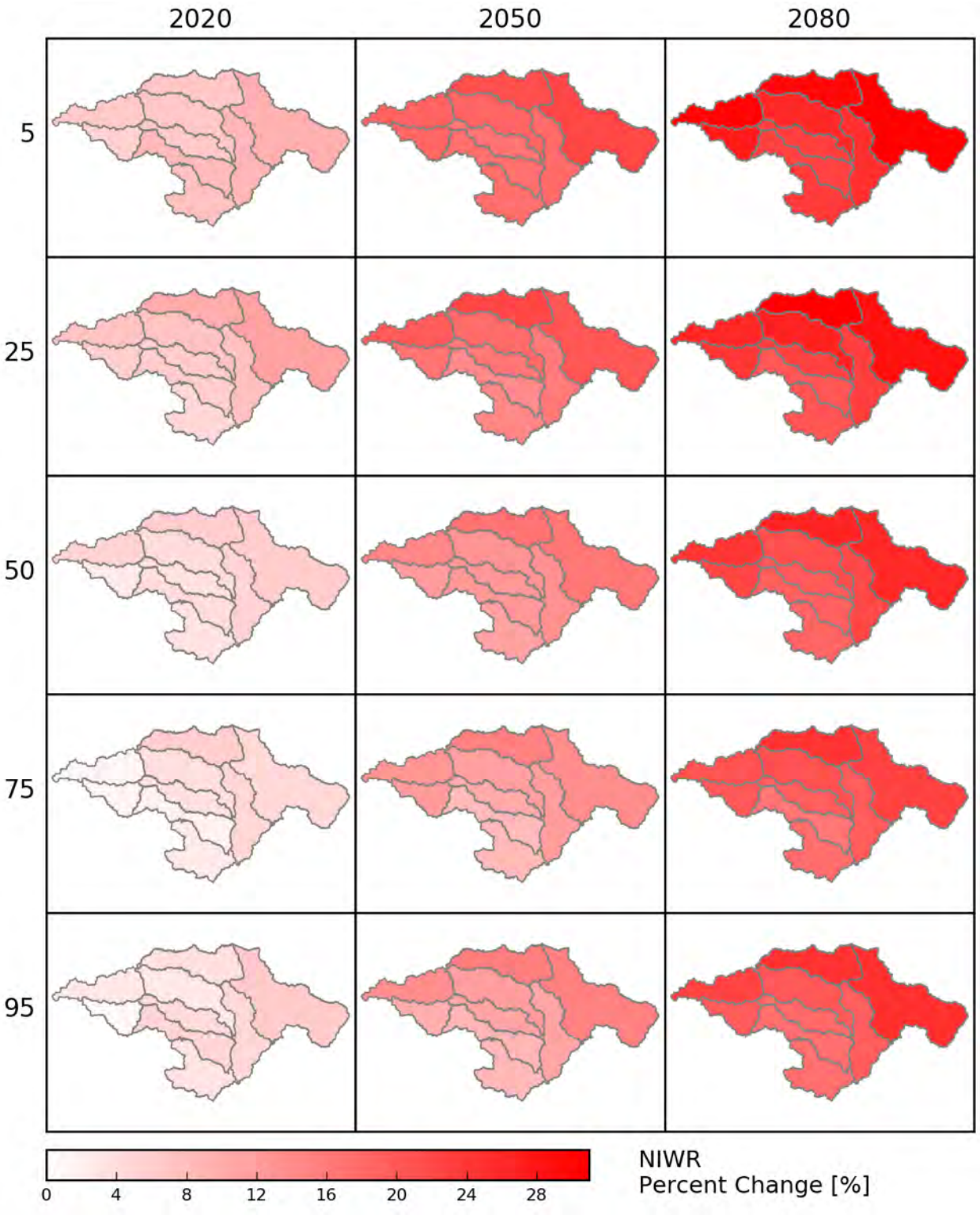

Figure 17 - Altus, Oklahoma Area – Spatial distribution of projected Net Irrigation Water Requirement percent change for different percentiles and time periods.

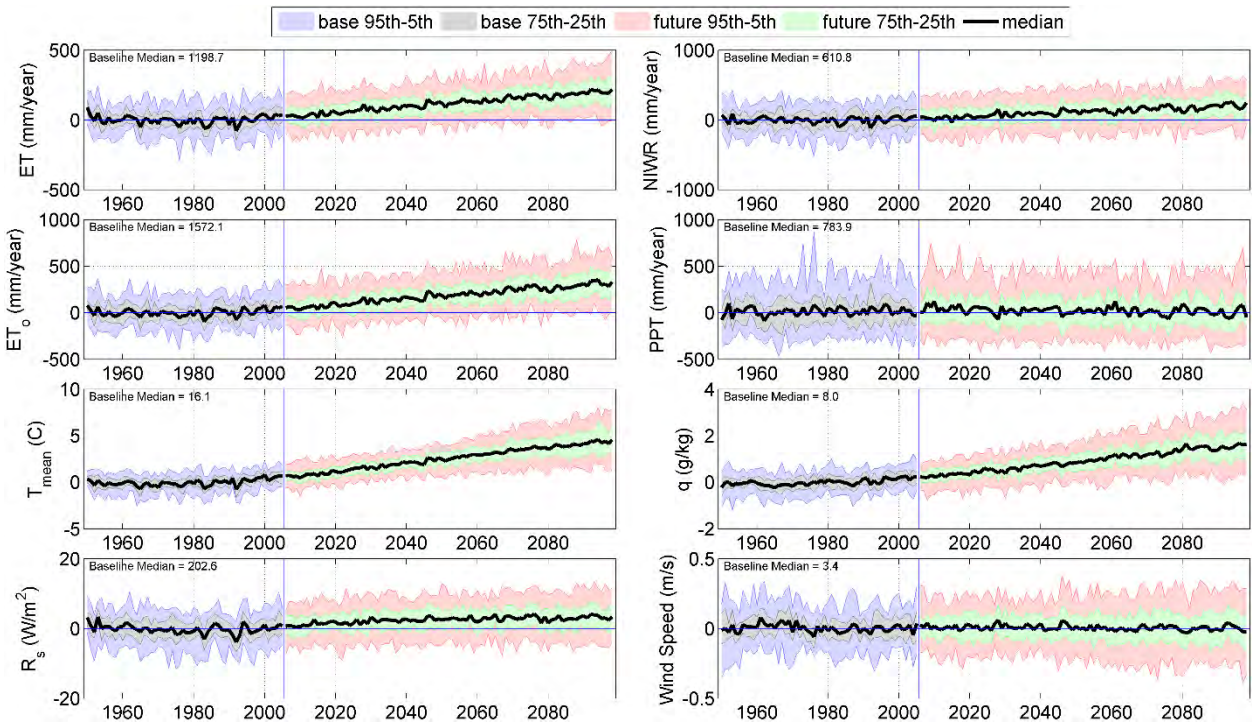

Figure 18 - Altus, Oklahoma Area – Transient time series anomaly plots of annual precipitation, temperature, solar radiation, humidity, wind speed, ET0, ETc, and NIWR for Metnode 336043 HUC 11130302 (near Fort Cobb).

Arkansas Basin

Figure 2 illustrates Metnodes that were used to estimate irrigation water demands, as well as HUC8 boundaries used to upscale Metnode estimates in the Arkansas basin. Figure 19 illustrates the spatial distribution of MACA derived baseline (1950–1999) average median precipitation (top left), temperature (top right), solar radiation (bottom left), and specific humidity (bottom right). Figure 20 illustrates the spatial distribution of MACA derived baseline (1950–1999) average median wind speed (top left), ET_0 (top right), ET_c (bottom left), and NIWR (bottom right). The spatial distribution of average median solar radiation is consistent with the distribution of precipitation and temperature – where there is less precipitation, solar radiation and temperature is higher. Figure 20 illustrates the spatial distribution of average median wind speed, where lower wind speed generally occurs in the central portion of the basin. Baseline median ET_0, ET_c, NIWR range from around 1300 to 1500, 800 to 1100, and 450 to 800 mm/yr, respectively, with higher rates of ET_c and NIWR occurring in the southwestern and eastern portions of the basin. Figure 21 shows the spatial distribution of projected precipitation changes for different percentiles and time periods, where it is evident that projected precipitation changes generally increase during the 2020 period, and then decrease in 2050 and 2080 time periods relative to baseline conditions, with changes ranging from -22 to 8 percent. Figure 22 illustrates the spatial distribution of projected temperature change, which shows spatially uniform warming with time, ranging

from 1.2 to 4 ^{o}C. Figures 23 and 24 illustrate solar radiation and specific humidity percent changes, where solar radiation changes are minor, and specific humidity increasing from 6 to 22 percent. Figure 25 illustrates wind speed percent change, ranging from ~ 0 to -5 percent. Figure 26 shows the spatial distribution of projected ET_0 percent change, which is generally spatially uniform with time and ranges from 3 to 14 percent. Figure 27 illustrates projected ET_c percent change, which ranges from 3 to 18 percent. Spatial differences in the distribution of projected percent change in ET_c are largely due to differences in crop type, precipitation, and baseline ET_c rates. The northeastern, central, and eastern portions of the basin are projected to experience the largest percent change for all projected time periods. Perennial forage crops (e.g. alfalfa and grass hay) have relatively high acreage in these areas, and are projected to have earlier greenup, longer harvest periods (i.e., more cuttings), and later killing frosts, leading to longer growing seasons and increased ET_c. The spatial distribution of projected NIWR percent change for different percentiles and time periods is shown in Figure 28. The NIWR incorporates growing season and non-growing season soil moisture gains and losses from precipitation, bare soil evaporation, and ET_c, therefore spatial variations in the distribution of NIWR percent change for different time periods and scenarios are a function of respective ET_c (Figures 27) and precipitation (Figure 21) distributions. NIWR percent changes range from 1 to 30 percent, where the northwestern and eastern portions of the basin are projected to increase the most. Transient time series anomaly plots of annual precipitation, temperature, solar radiation, humidity, wind speed, ET_0, ET_c, and NIWR are shown in Figure 29 for Metnode 431552 (near the Colorado State University Experiment Station located in Rocky Ford, Colorado), which illustrates the general increase in all variables relative to the baseline, with the exception of wind speed, solar radiation, and precipitation.

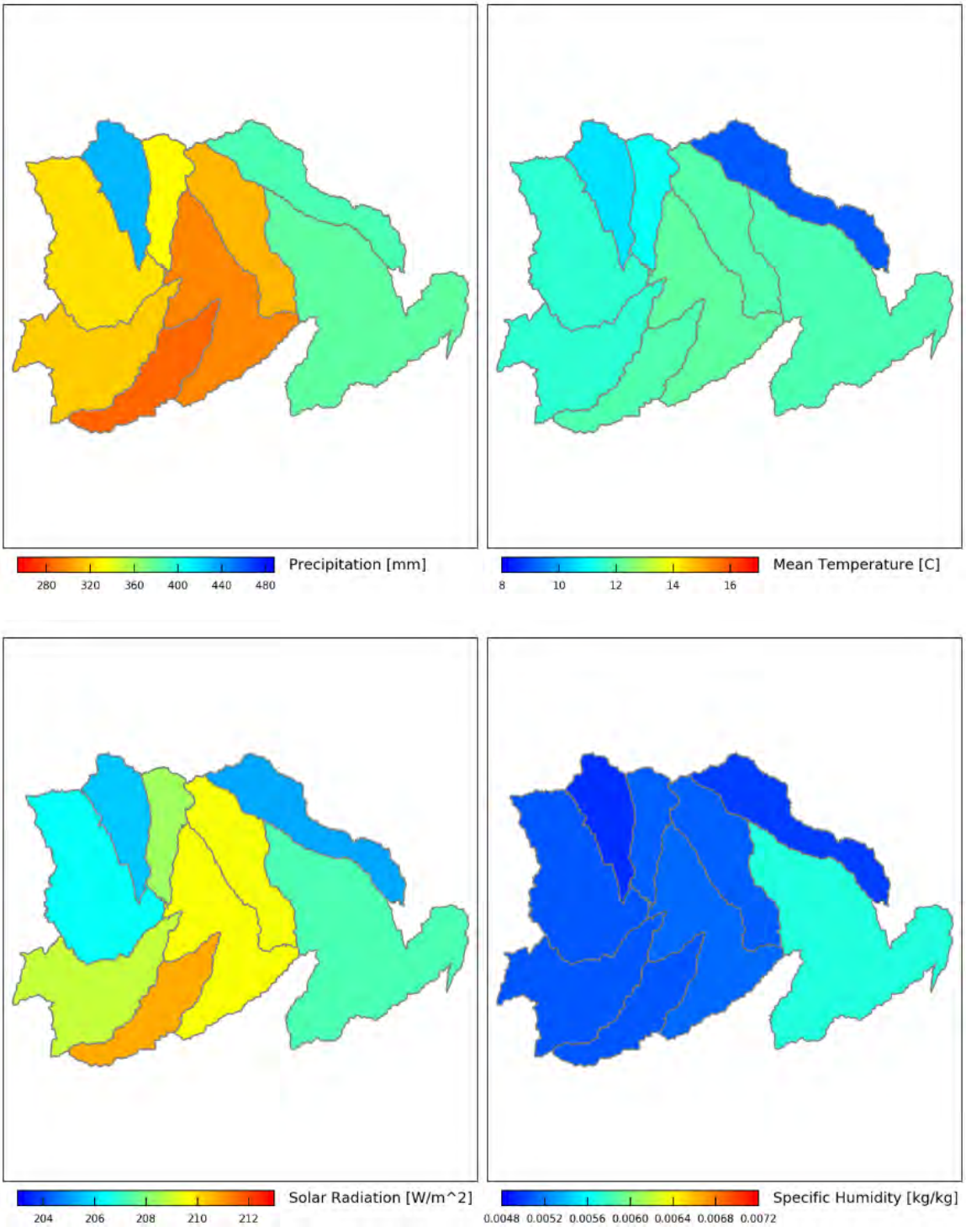

Figure 19 - Arkansas, Colorado Area – Spatial distribution of baseline precipitation, temperature, solar radiation, and humidity. Color scales are relative to baseline and future conditions.

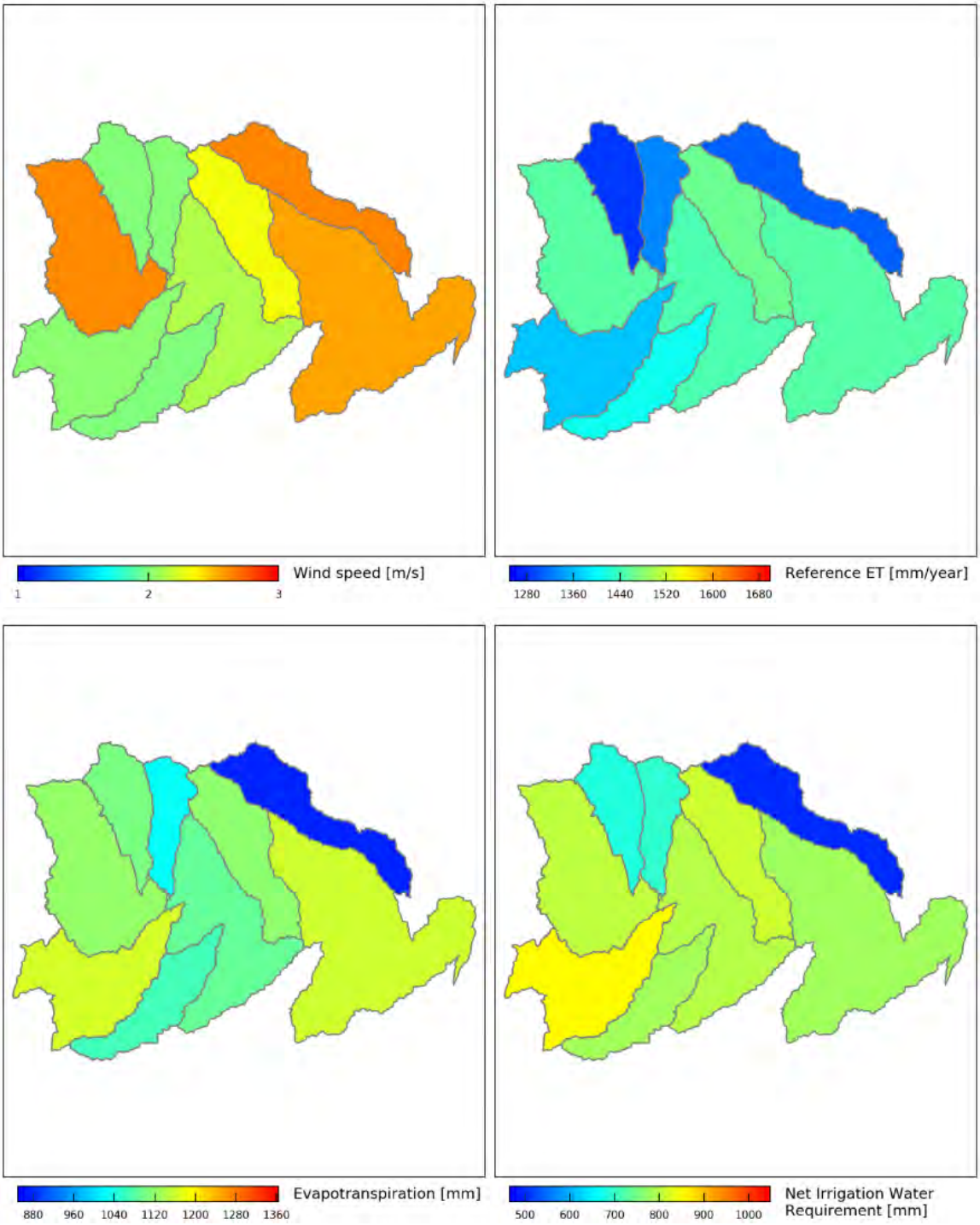

Figure 20 - Arkansas, Colorado Area – Spatial distribution of baseline wind speed, reference ET, crop evapotranspiration, and net irrigation water requirement.

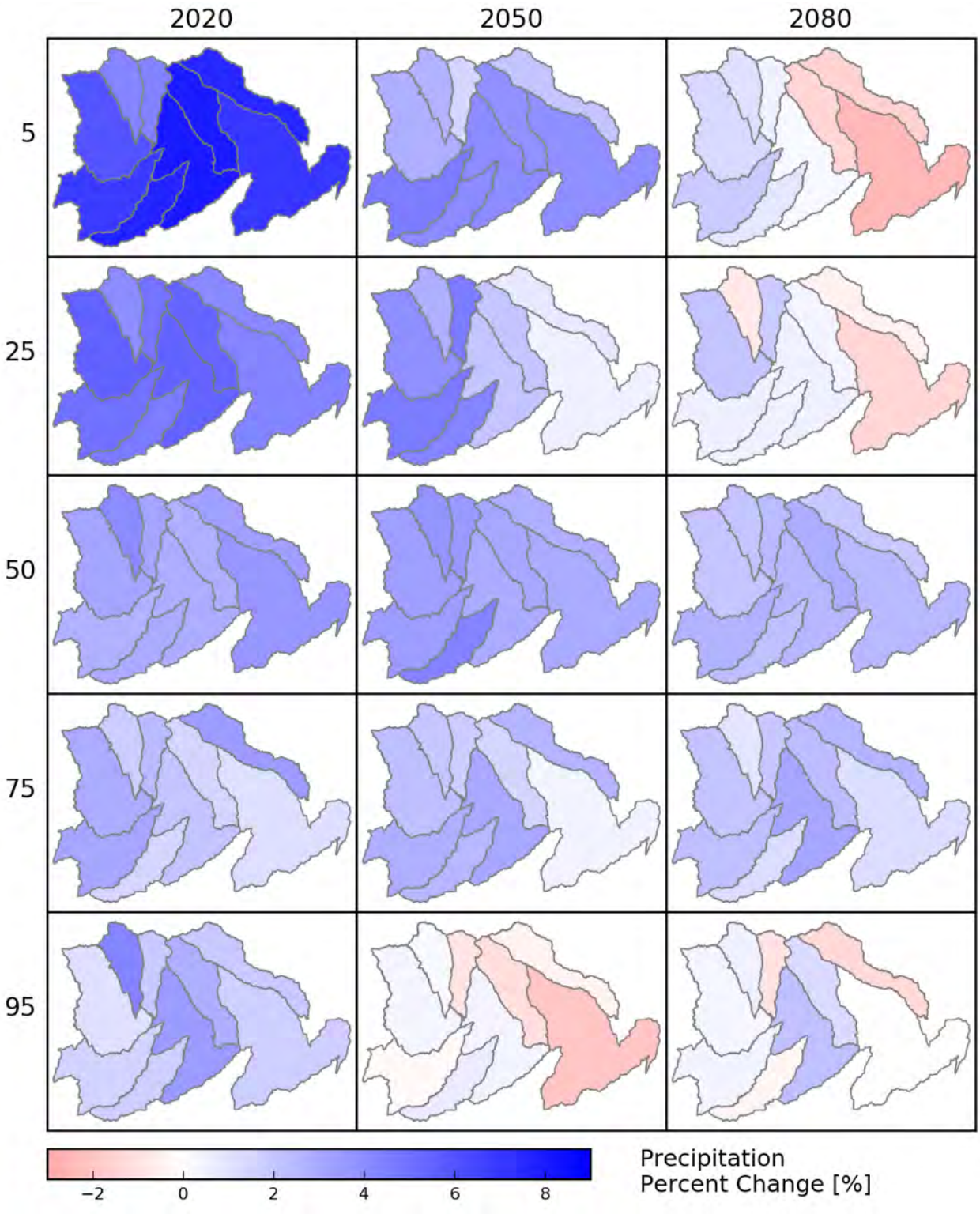

Figure 21 - Arkansas, Colorado Area – Spatial distribution of projected precipitation percent change for different percentiles and time periods.

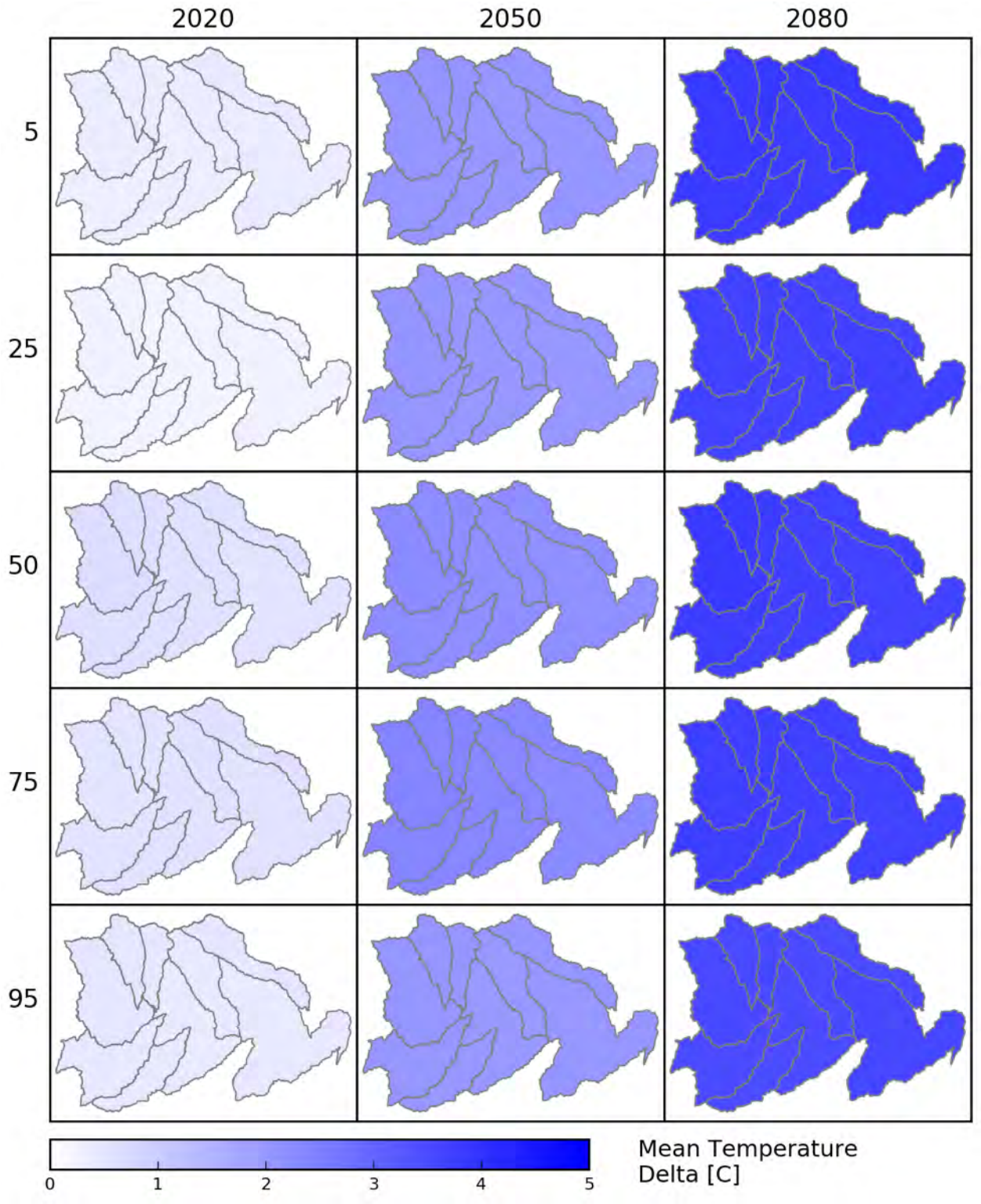

Figure 22 - Arkansas, Colorado Area – Spatial distribution of projected temperature change for different percentiles and time periods.

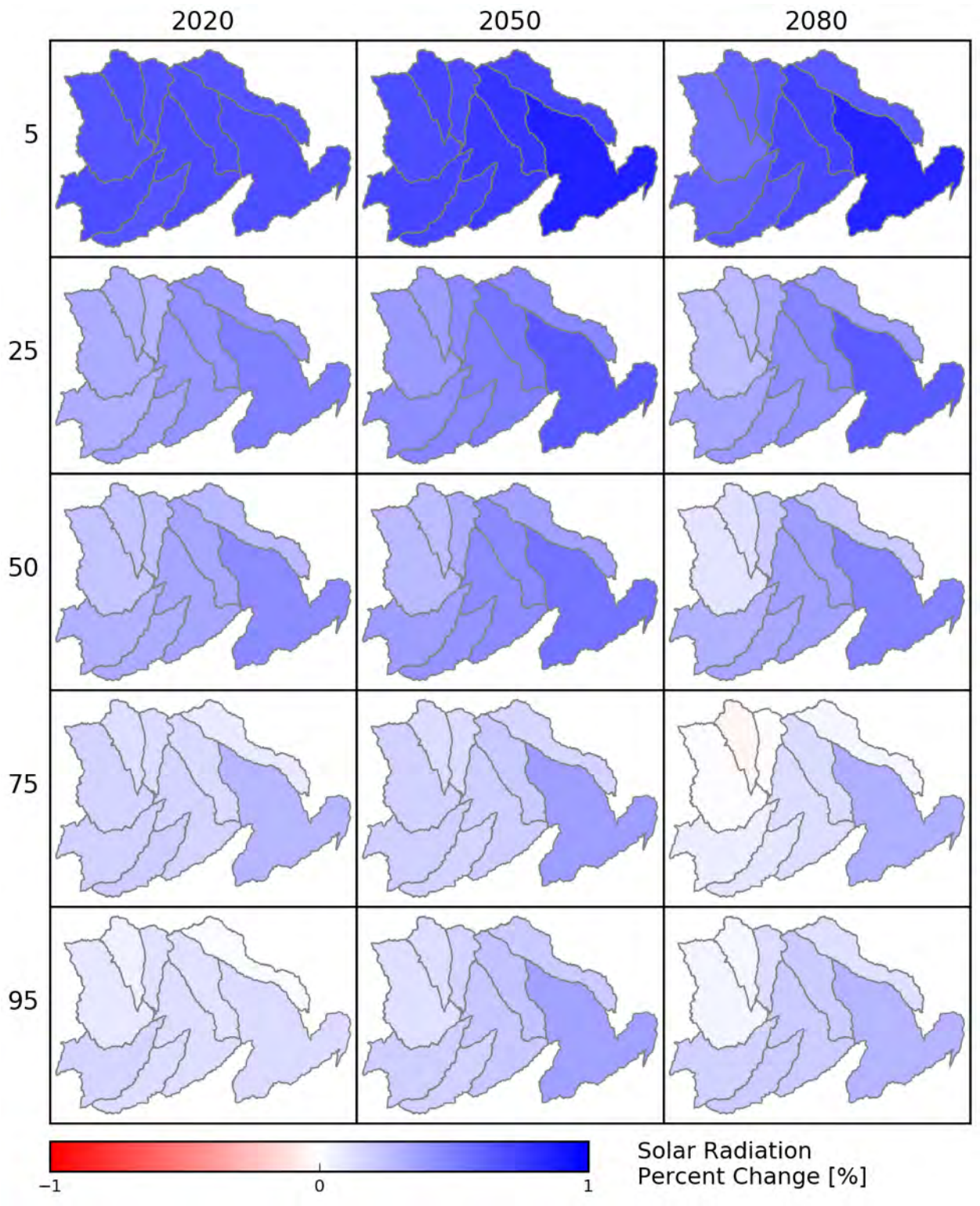

Figure 23 - Arkansas, Colorado Area – Spatial distribution of projected solar radiation percent change for different percentiles and time periods.

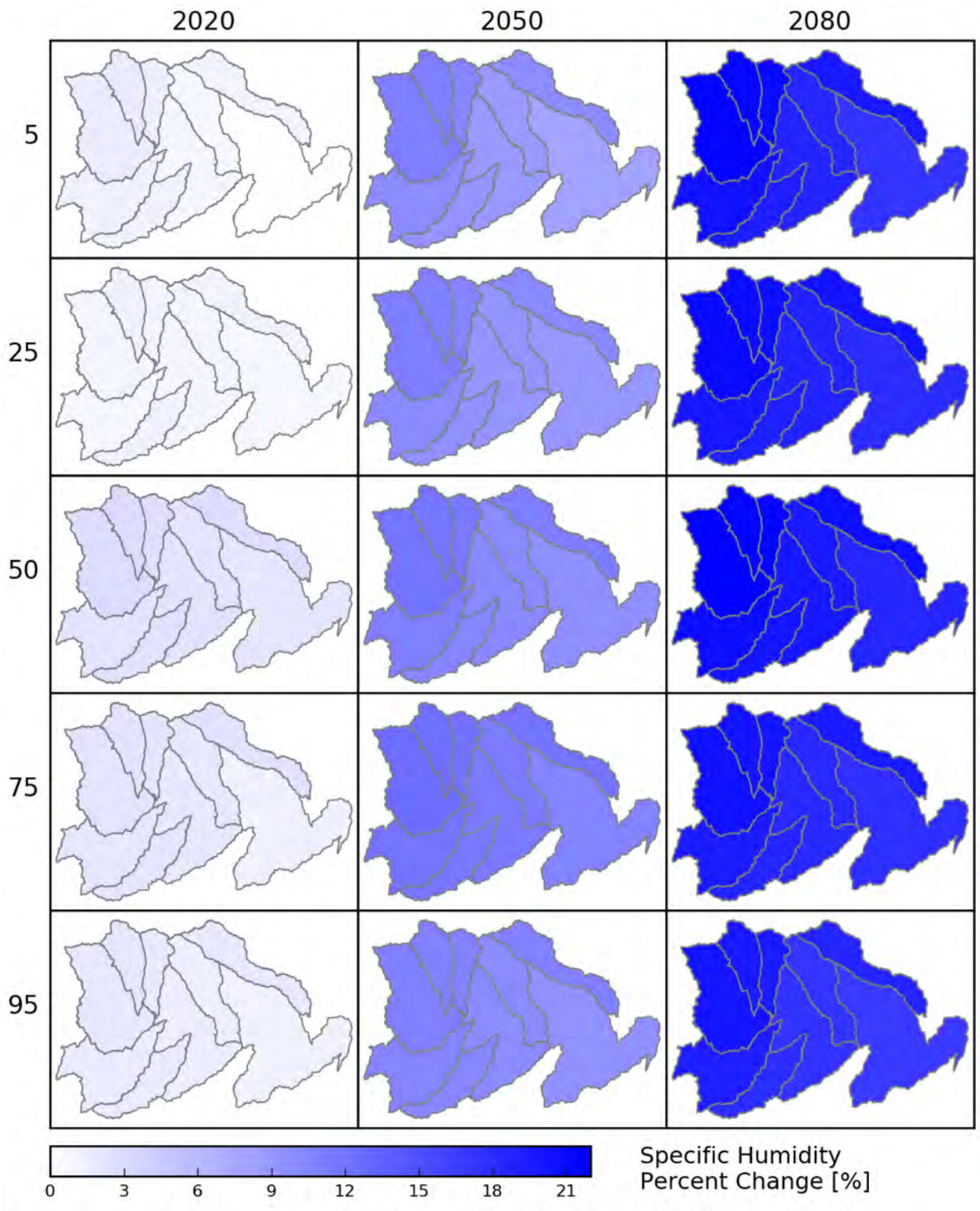

Figure 24 - Arkansas, Colorado Area – Spatial distribution of projected specific humidity percent change for different percentiles and time periods.

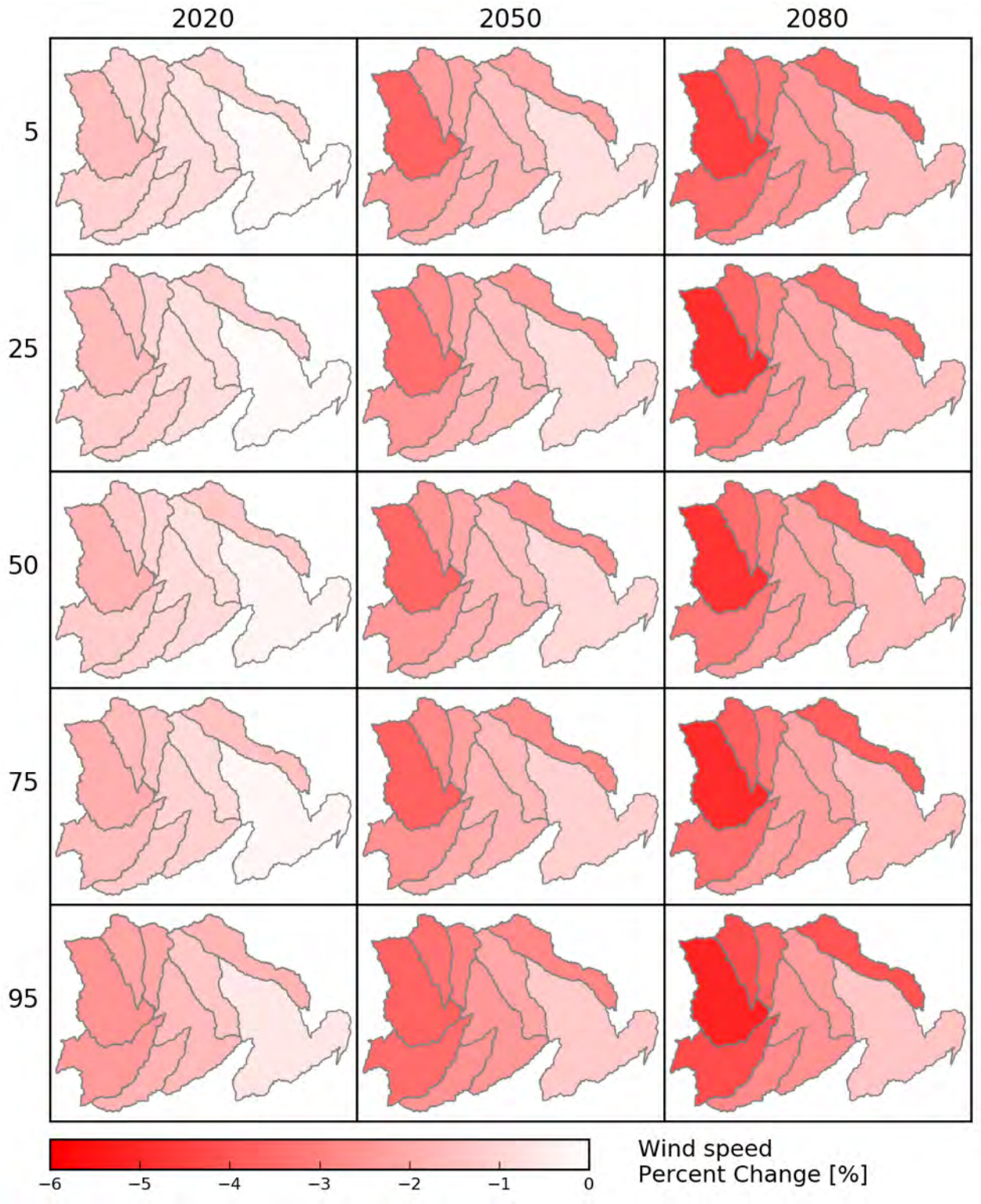

Figure 25 - Arkansas, Colorado Area – Spatial distribution of projected wind speed percent change for different percentiles and time periods.

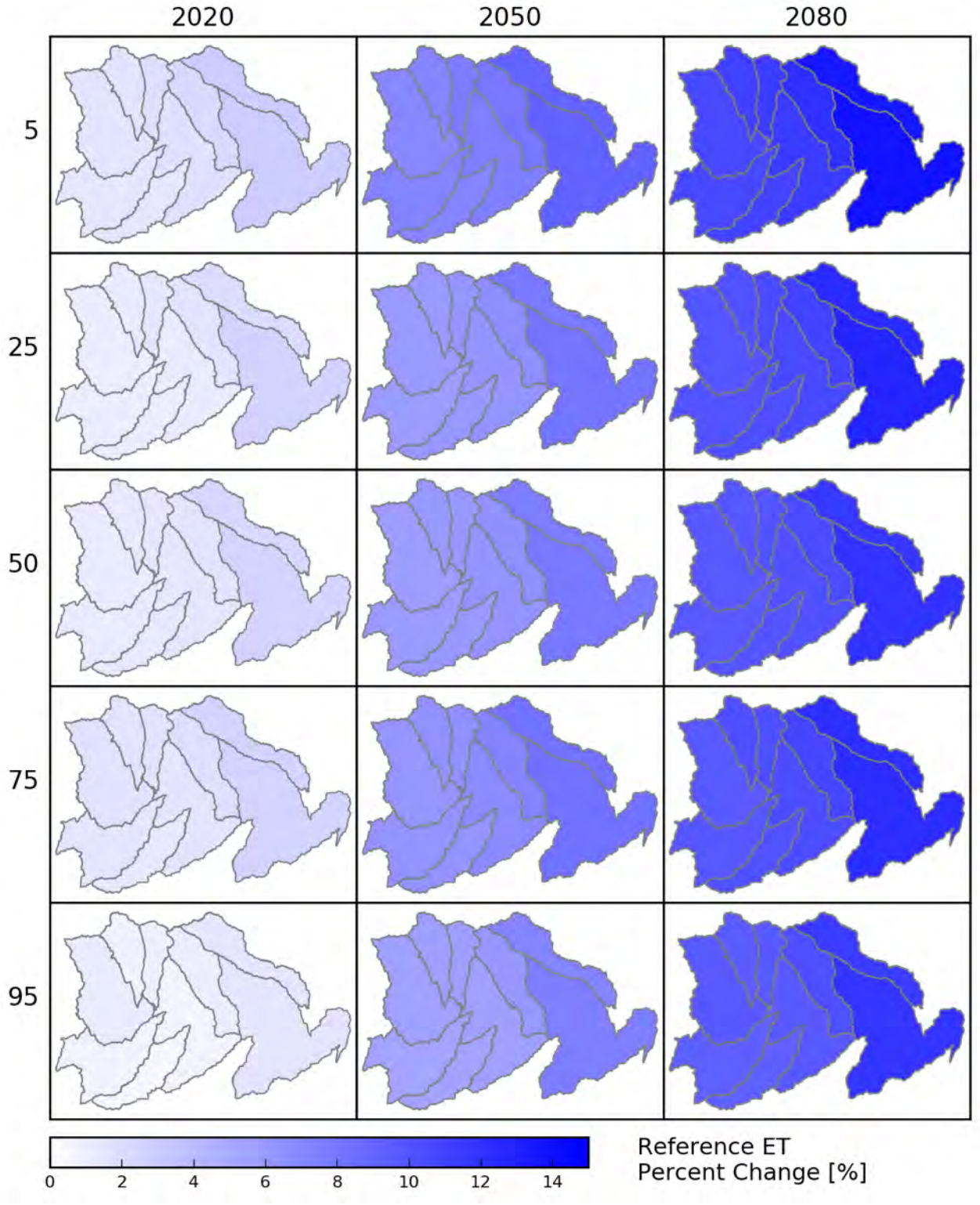

Figure 26 - Arkansas, Colorado Area – Spatial distribution of projected reference ET percent change for different percentiles and time periods.

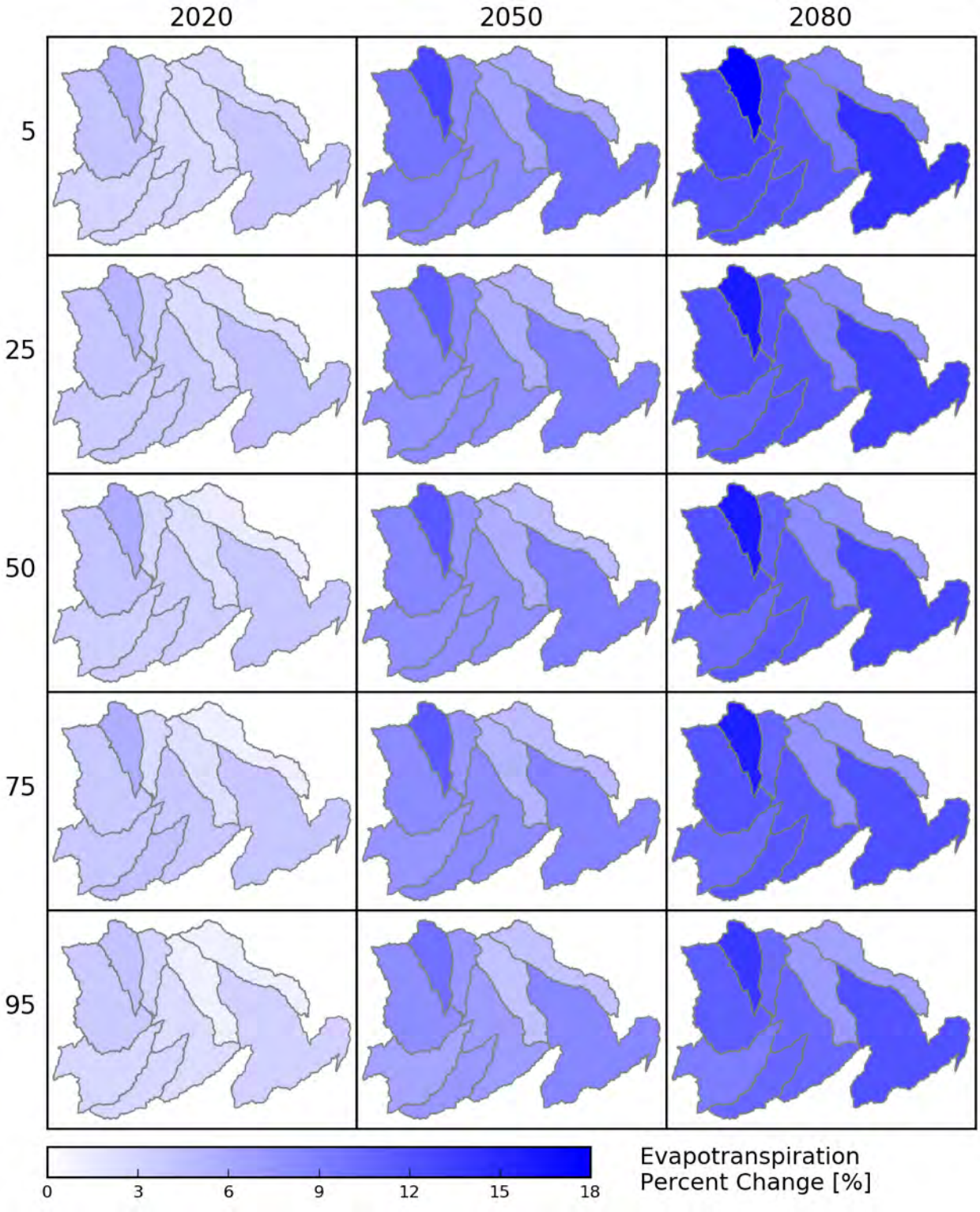

Figure 27 - Arkansas, Colorado Area – Spatial distribution of projected crop ET percent change for different percentiles and time periods.

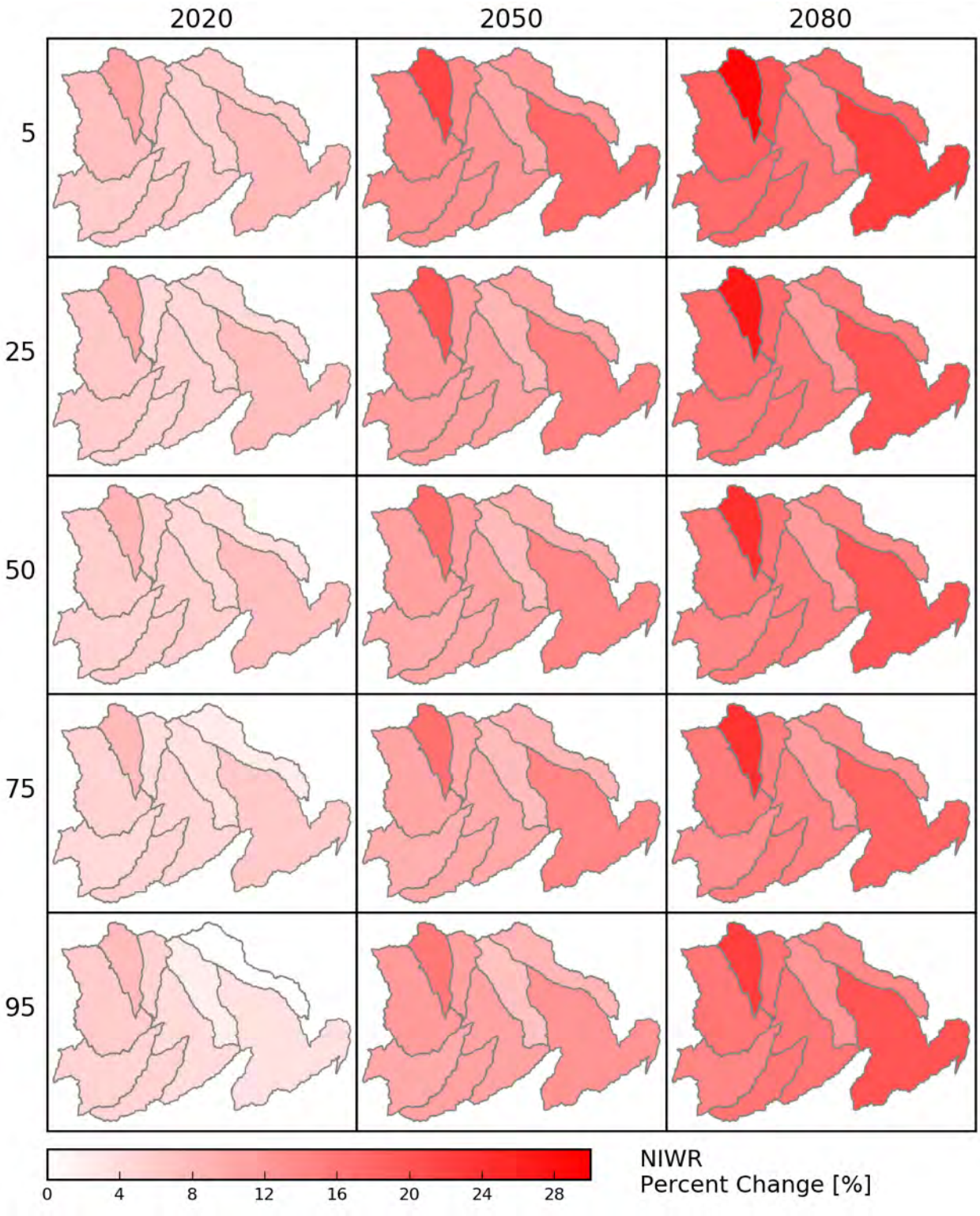

Figure 28 - Arkansas, Colorado Area – Spatial distribution of projected Net Irrigation Water Requirement percent change for different percentiles and time periods.

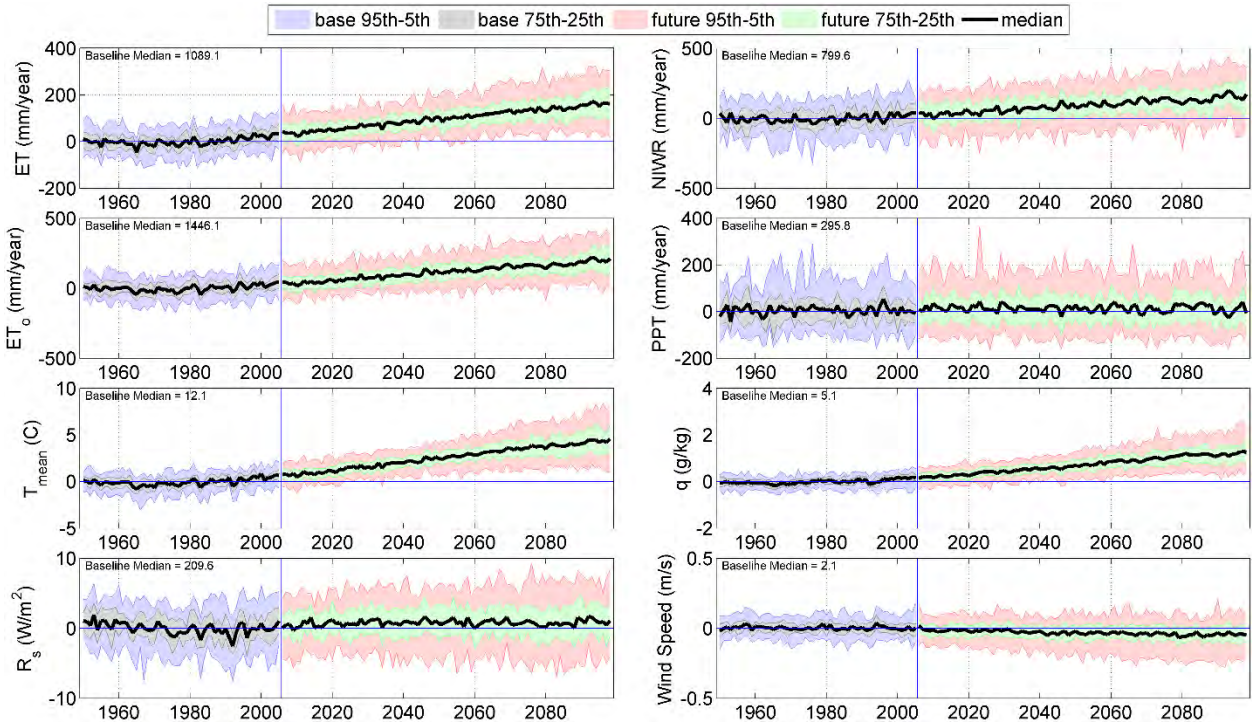

Figure 29 - Arkansas, Colorado Area – Transient time series anomaly plots of annual precipitation, temperature, solar radiation, humidity, wind speed, ET0, ETc, and NIWR for Metnode 431552, HUC8 11020005 (CSU Expt. Stn Rocky Ford).

Central Utah Area

Figure 3 illustrates Metnodes that were used to estimate irrigation water demands, as well as HUC8 boundaries used to upscale Metnode estimates in the Central Utah area. Figure 30 illustrates the spatial distribution of MACA derived baseline (1950–1999) average median precipitation (top left), temperature (top right), solar radiation (bottom left), and specific humidity (bottom right). Figure 31 illustrates the spatial distribution of MACA derived baseline (1950–1999) average median wind speed (top left), ET_0 (top right), ET_c (bottom left), and NIWR (bottom right). Baseline median ET_0, ET_c, NIWR estimates range from 1100 to 1300, 1000 to 1200, and 600 to 900 mm/yr, respectively, with higher rates of ET_c and NIWR occurring in the southern portions of the basin. Figure 32 shows the spatial distribution of projected precipitation changes for different percentiles and time periods, where it is evident that projected precipitation changes generally increase relative to baseline conditions, with changes ranging from 2 to 14 percent. Figure 33 illustrates the spatial distribution of projected temperature change ranging from 1.5 to 5 ^{o}C. Figures 34 and 35 illustrate solar radiation and specific humidity percent changes, with minor projected solar radiation changes, and specific humidity projected to increase by 7 to 25 percent, a reflection of projected increases in precipitation and likely increase in regional ET within the GCM. Figure 36 illustrates wind speed percent change, ranging from ~ -1 to -7 percent. Figure 37 and 38 illustrate the spatial distribution of projected ET_0 and ET_c percent change, ranging

from 3 to 15, and from 4 to 26 percent, respectively. Spatial differences in projected ET_c changes are primarily due to differences in crop type, precipitation projections, and baseline ET_c rates. The largest percent change occurs for a high elevation HUC8 where baseline ET_c is relatively low, while other large changes are projected to occur in areas with relatively high acreages of perennial forage crops (e.g. alfalfa and grass hay). Perennial forage crops are projected to have earlier greenup, longer harvest periods (i.e., more cuttings), and later killing frosts, leading to longer growing seasons and increased ET_c. The spatial distribution of projected NIWR percent change for different percentiles and time periods is shown in Figure 39. The NIWR incorporates growing season and non-growing season soil moisture gains and losses from precipitation, bare soil evaporation, and ET_c, therefore spatial variations in the distribution of NIWR percent change for different time periods and scenarios are a function of respective ET_c and precipitation distributions. NIWR percent changes range from 3 to 32 percent, with the greatest change occurring in high elevation HUC8s where baseline NIWR values are relatively low. Transient time series anomaly plots of annual precipitation, temperature, solar radiation, humidity, wind speed, ET_0, ET_c, and NIWR are shown in Figure 40 for Metnode 518672 (near USU Agmet station Murray GC), which illustrates the general increase in all variables relative to the baseline, with the exception of wind speed, solar radiation, and precipitation.

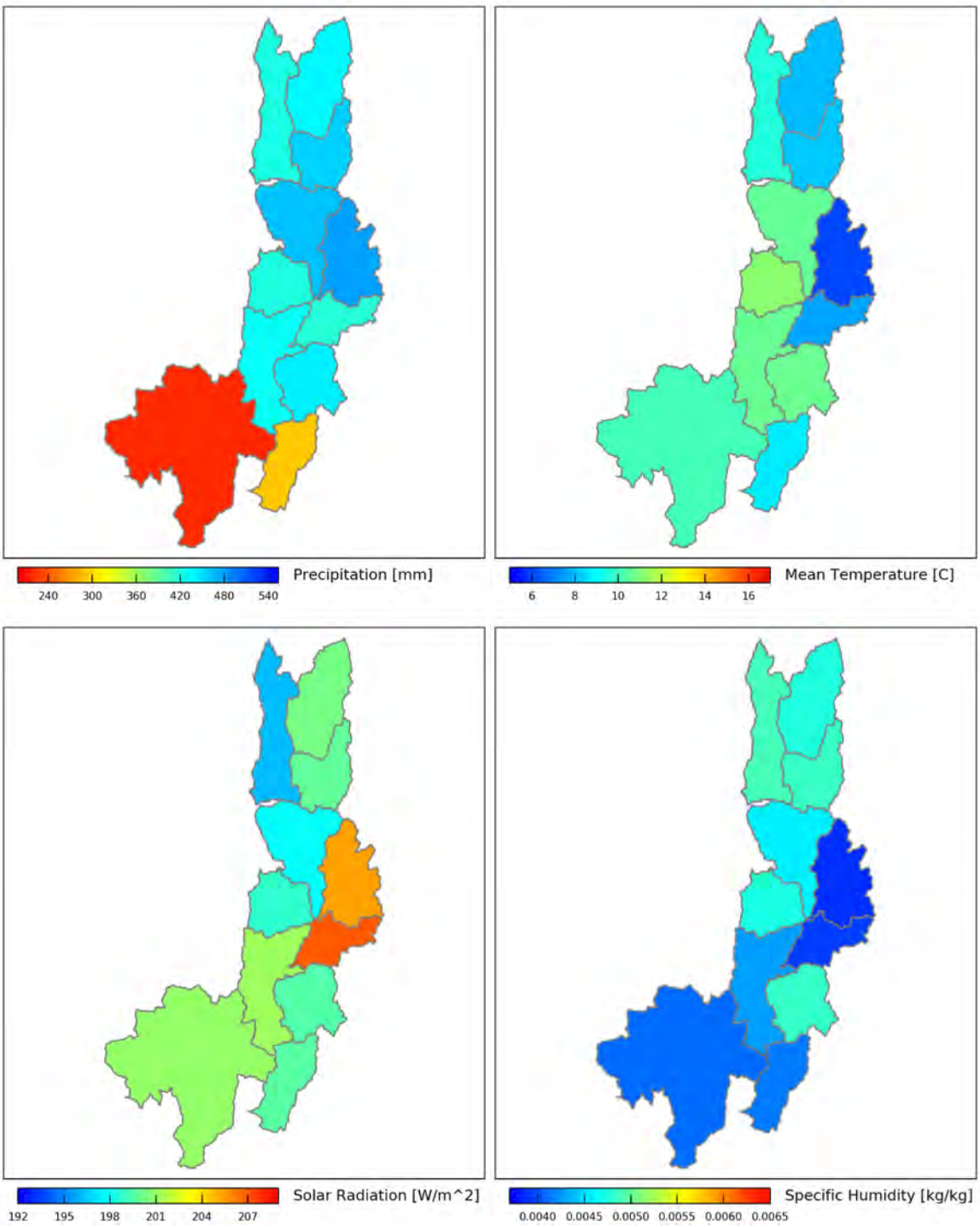

Figure 30 - Central Utah Area – Spatial distribution of baseline precipitation, temperature, solar radiation, and humidity. Color scales are relative to baseline and future conditions.

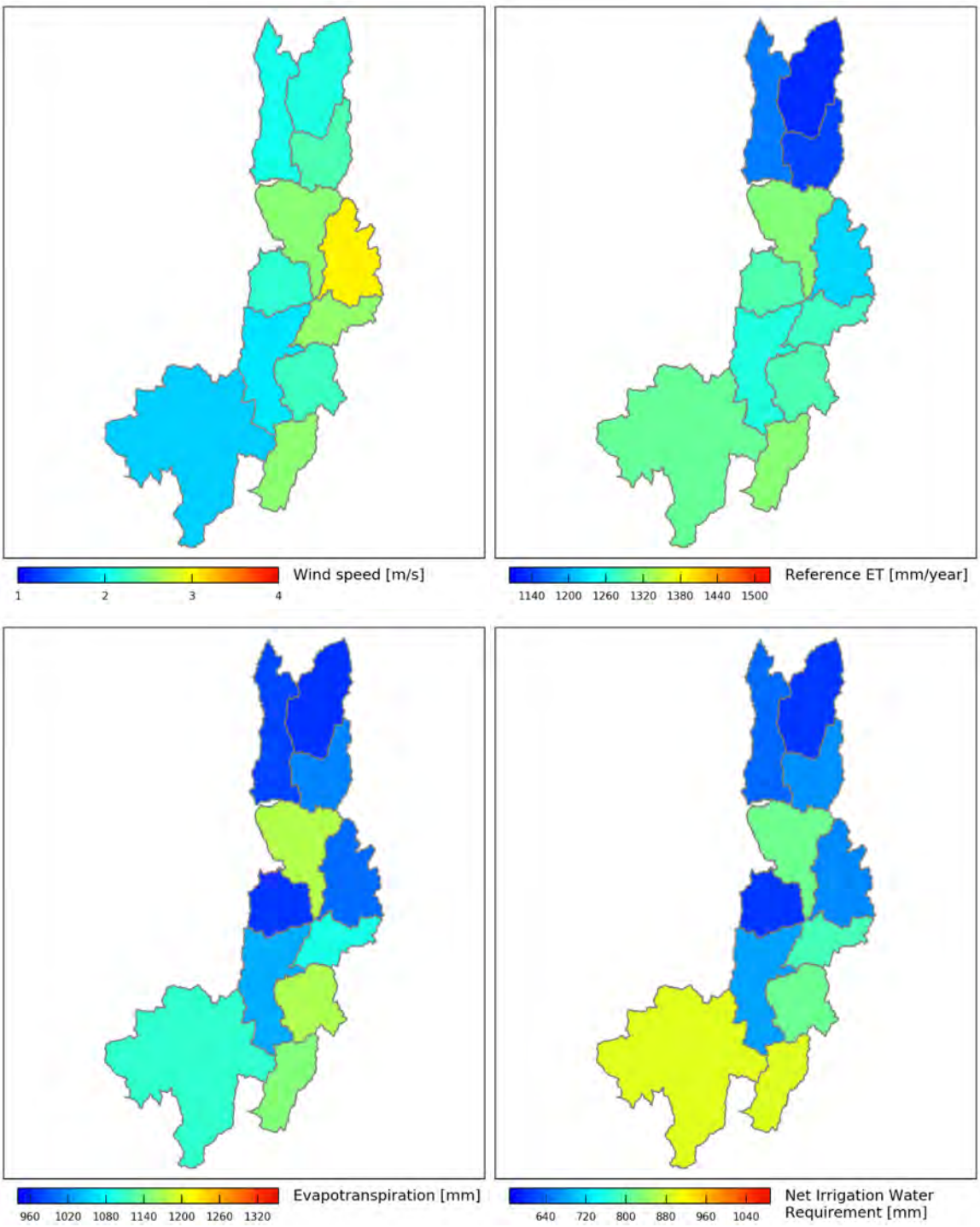

Figure 31 - Central Utah Area – Spatial distribution of baseline wind speed, reference ET, crop evapotranspiration, and net irrigation water requirement.

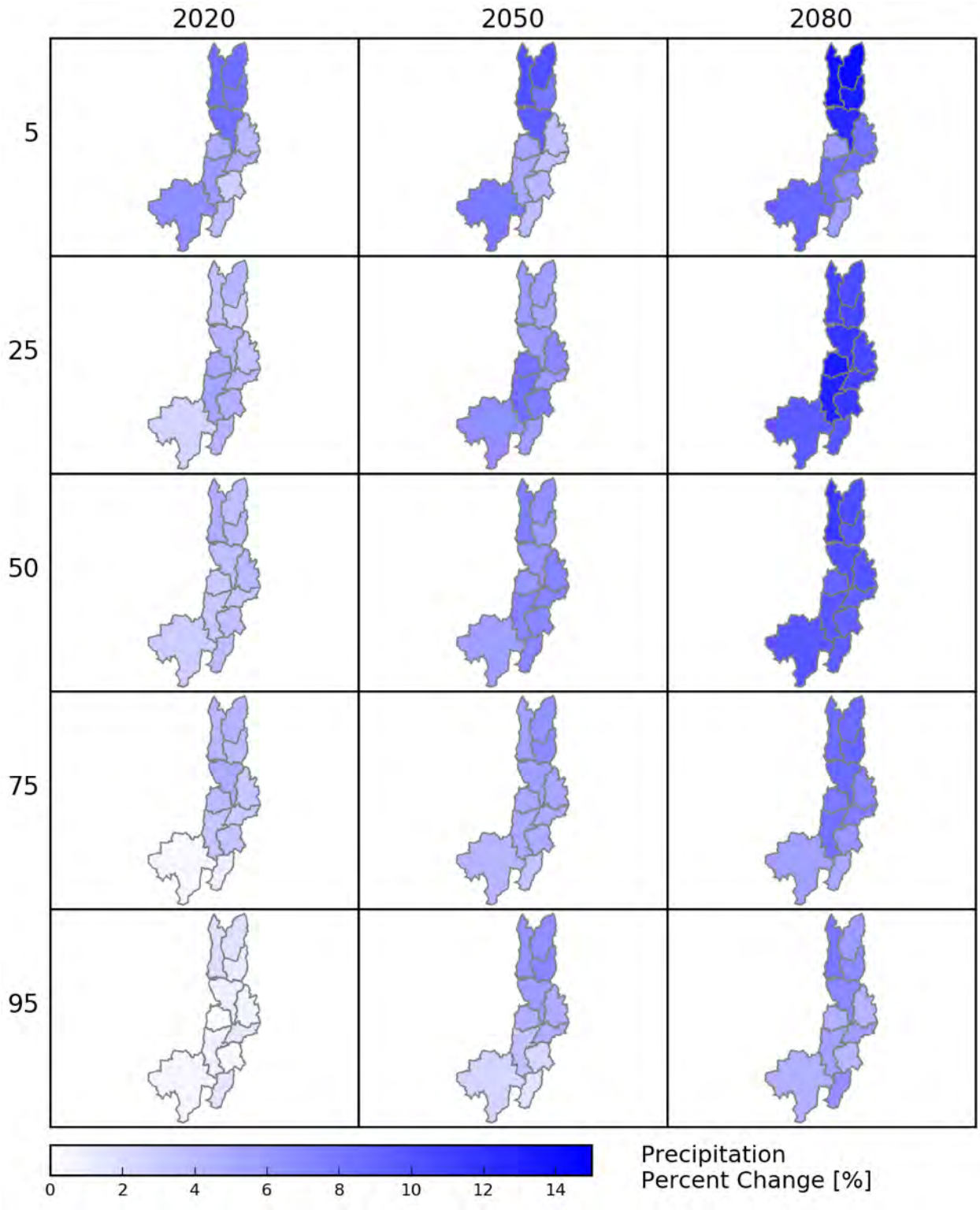

Figure 32 - Central Utah Area – Spatial distribution of projected precipitation percent change for different percentiles and time periods.

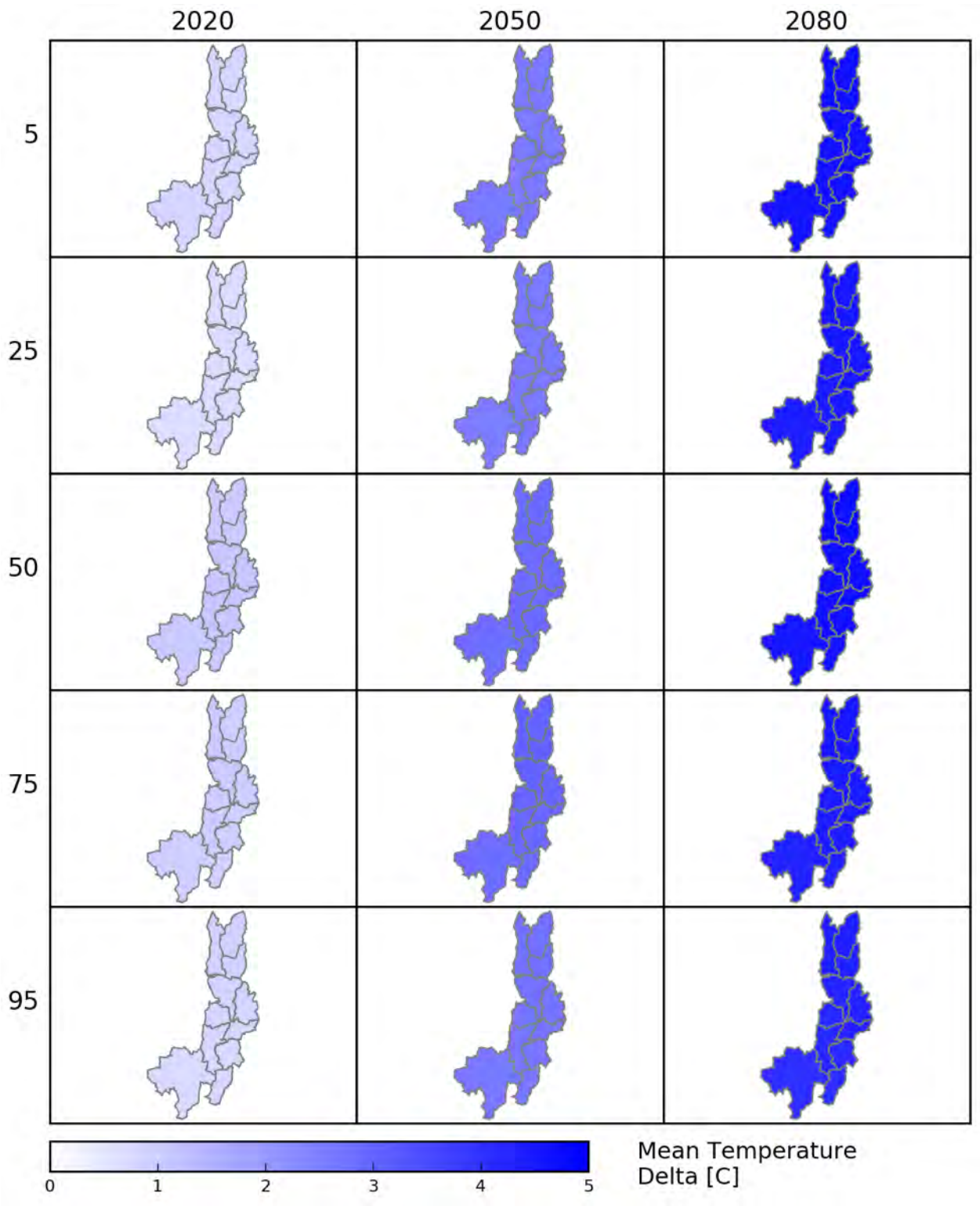

Figure 33 - Central Utah Area – Spatial distribution of projected temperature change for different percentiles and time periods.

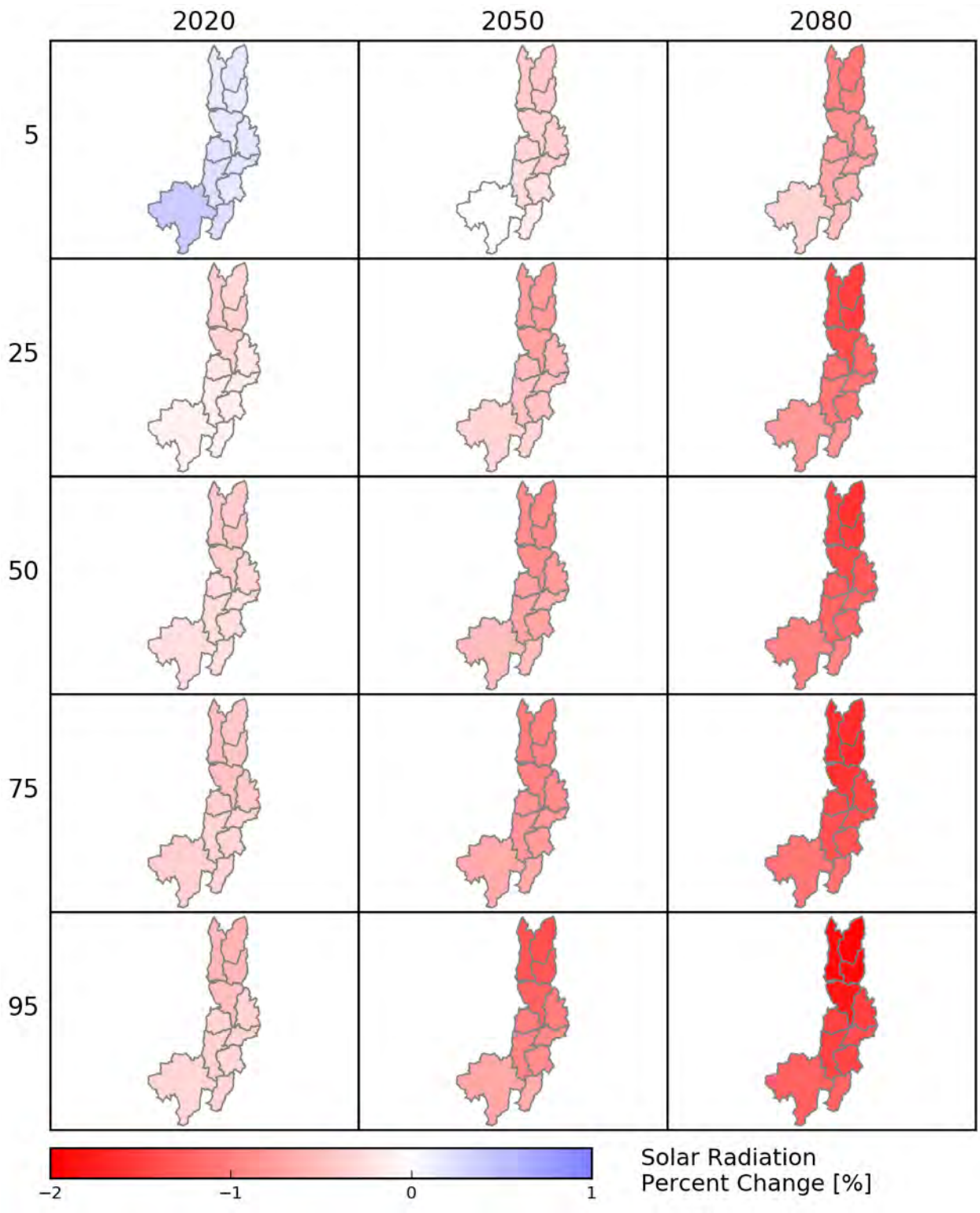

Figure 34 - Central Utah Area – Spatial distribution of projected solar radiation percent change for different percentiles and time periods.

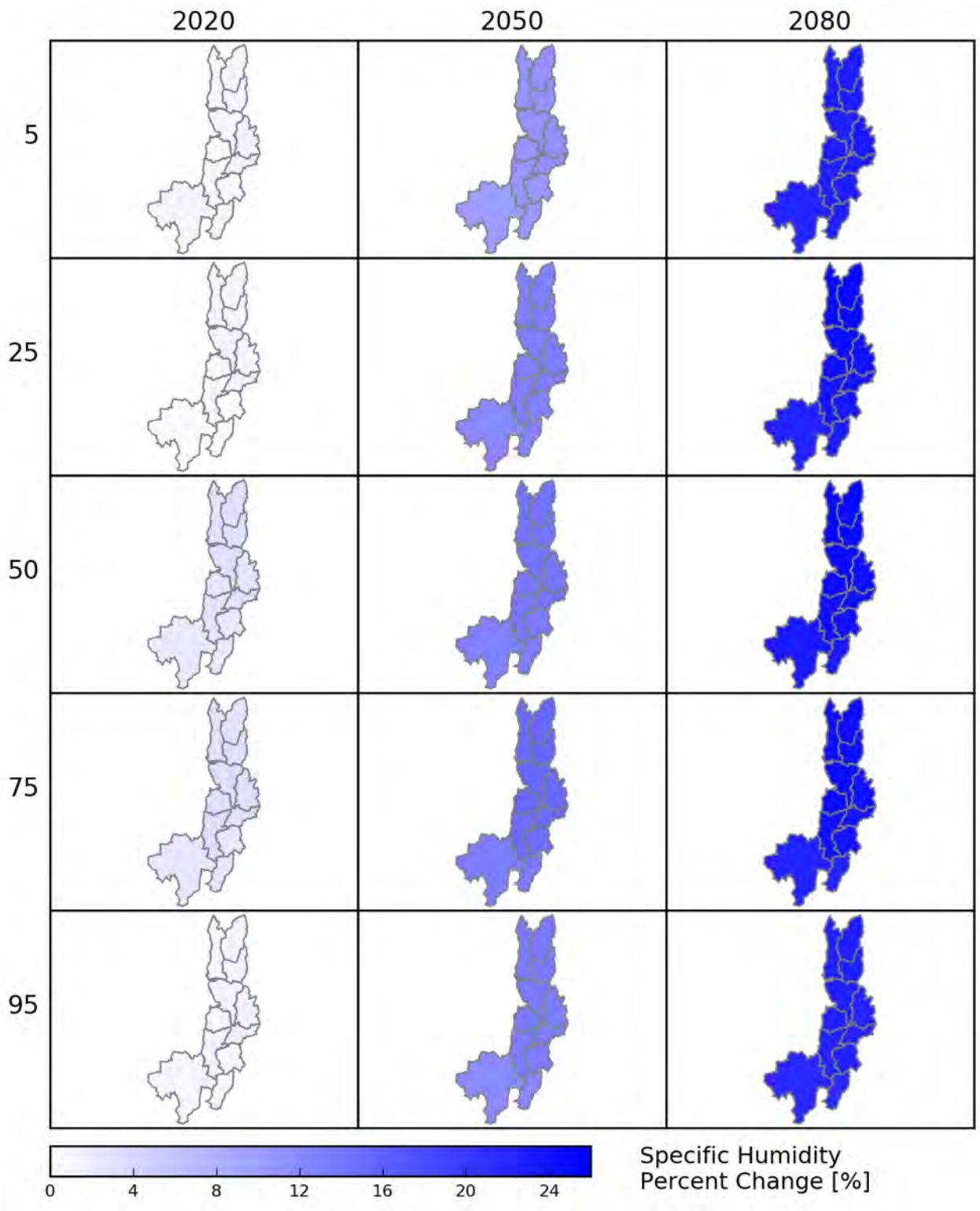

Figure 35 - Central Utah Area – Spatial distribution of projected specific humidity percent change for different percentiles and time periods.

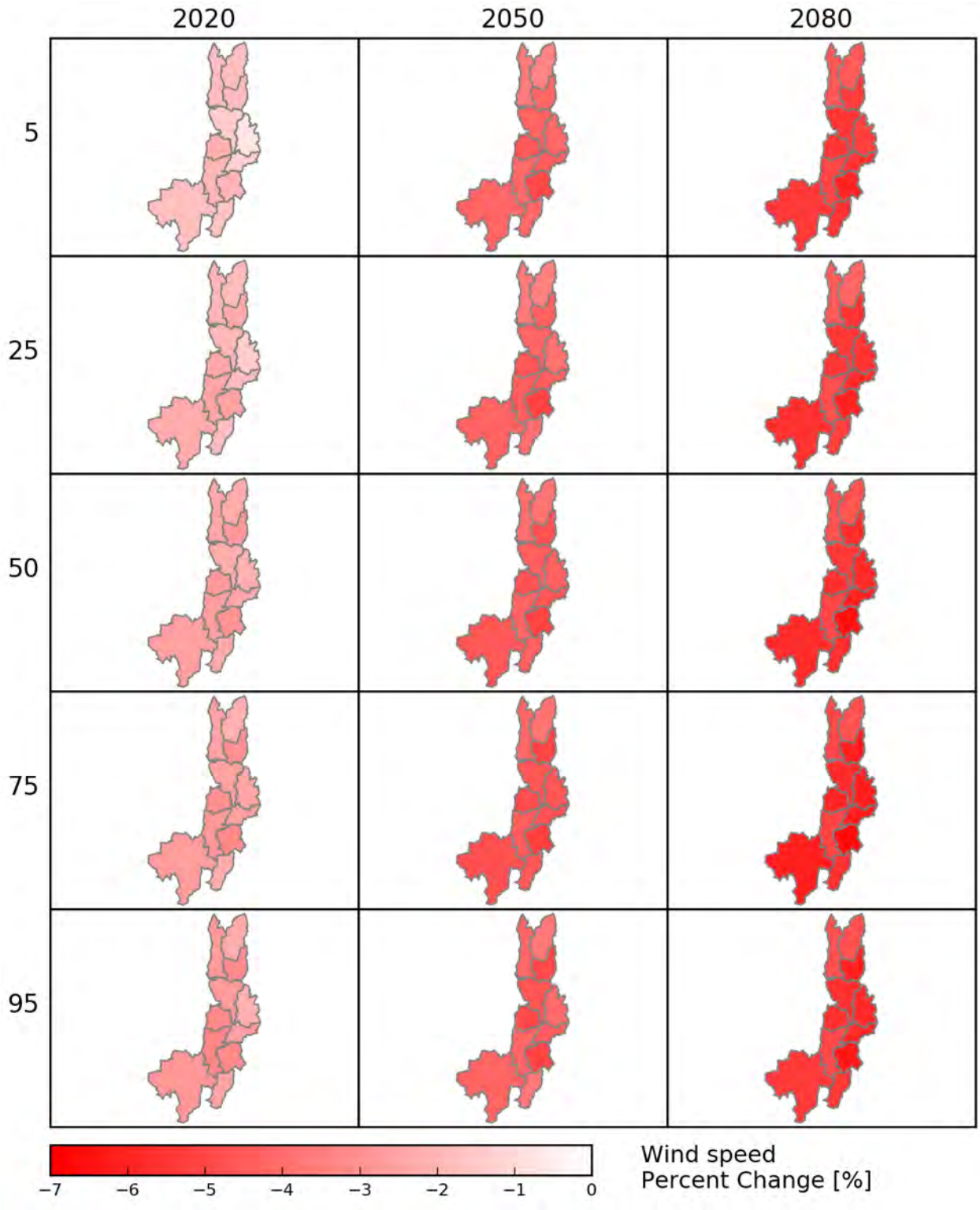

Figure 36 - Central Utah Area – Spatial distribution of projected wind speed percent change for different percentiles and time periods.

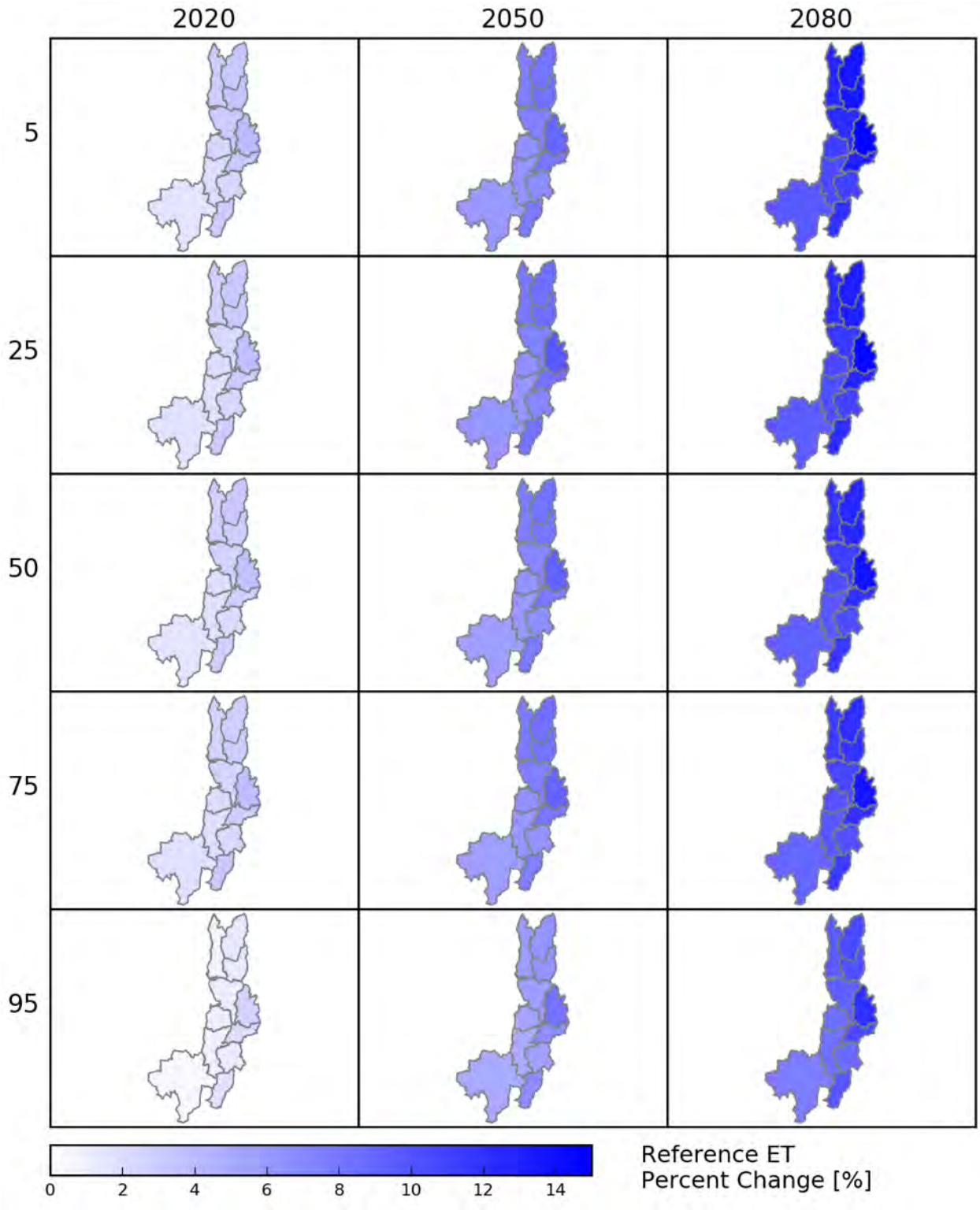

Figure 37 - Central Utah Area – Spatial distribution of projected reference ET percent change for different percentiles and time periods.

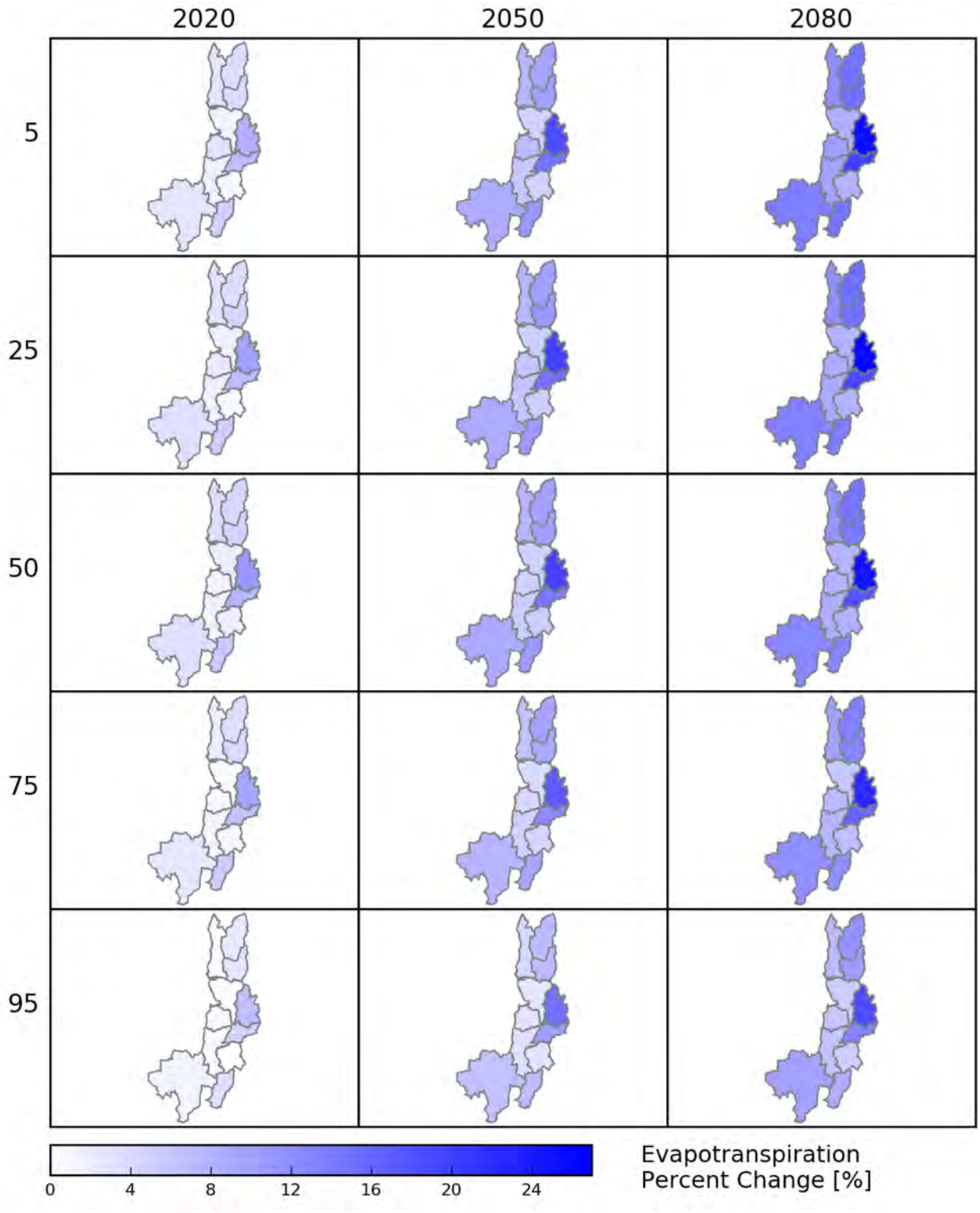

Figure 38 - Central Utah Area – Spatial distribution of projected crop ET percent change for different percentiles and time periods.

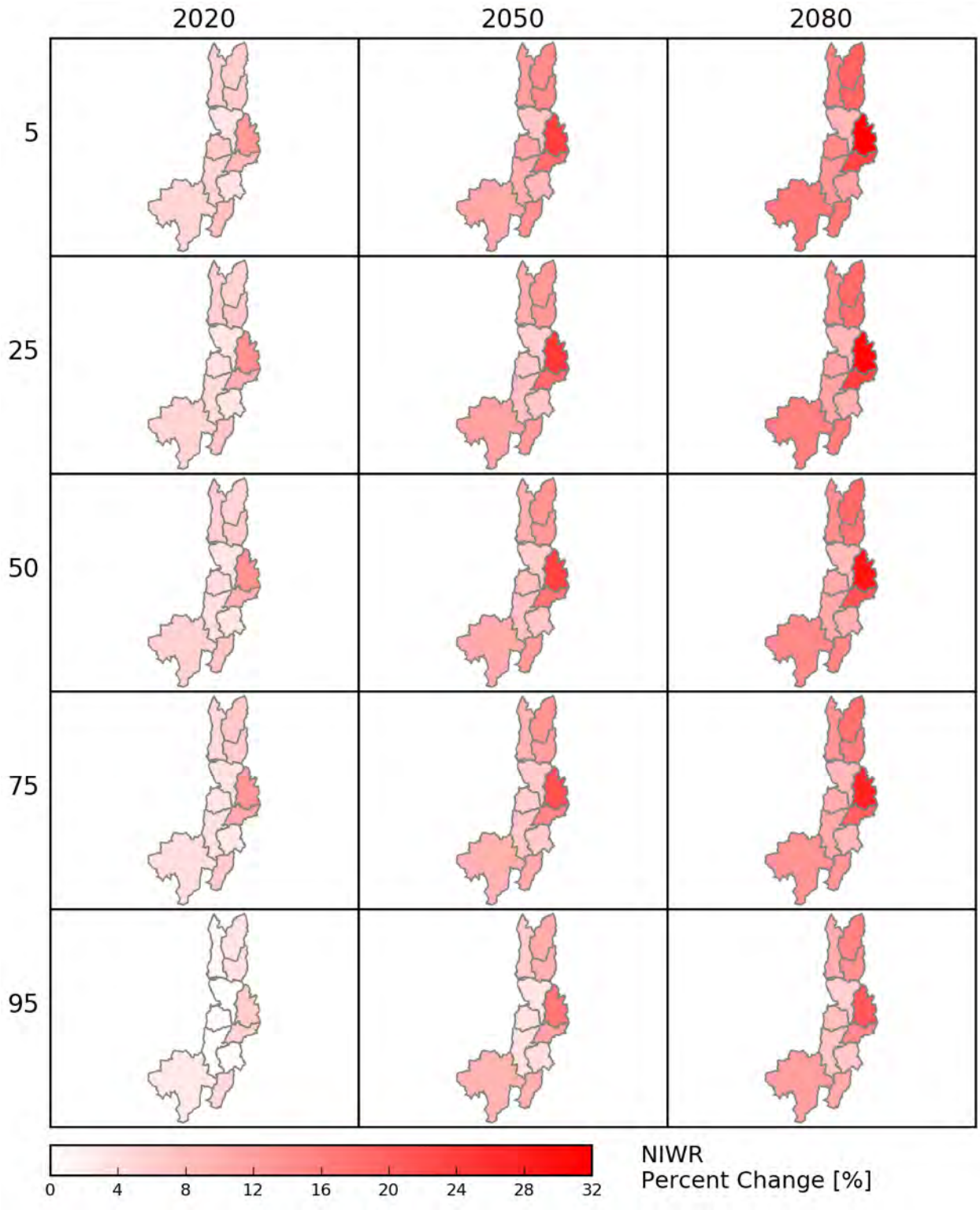

Figure 39 - Central Utah Area – Spatial distribution of projected Net Irrigation Water Requirement percent change for different percentiles and time periods.

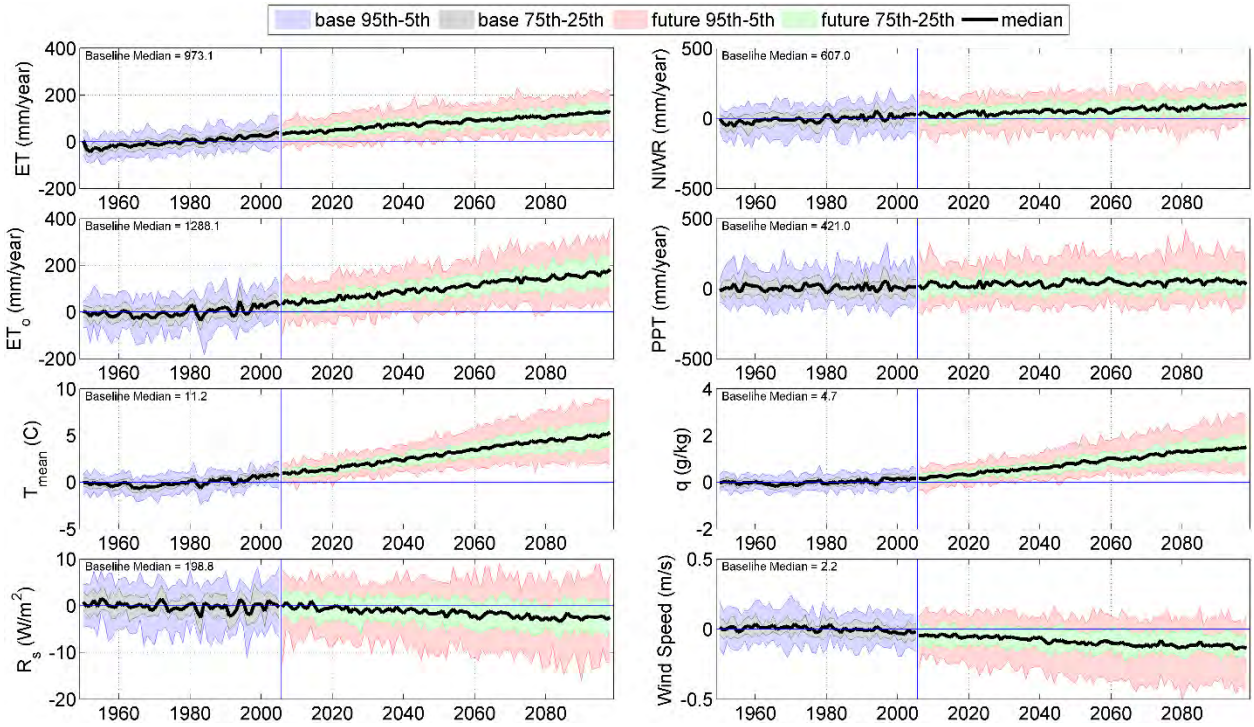

Figure 40 - Central Utah Area – Transient time series anomaly plots of annual precipitation, temperature, solar radiation, humidity, wind speed, ET0, ETc, and NIWR for Metnode 518672, HUC8 16020204 (near USU Agmet station Murray GC).

San Angelo Area

Figure 4 illustrates the single Metnode that was used to estimate irrigation water demands, as well as the HUC8 boundary used to upscale Metnode estimates in the San Angelo area. Figure 41 illustrates MACA derived baseline (1950–1999) average median temperature (top left), precipitation (top right), solar radiation (bottom left), and specific humidity (bottom right). Figure 42 illustrates MACA derived baseline (1950–1999) average median wind speed (top left), ET_0 (top right), ET_c (bottom left), and NIWR (bottom right). Baseline median ET_0, ET_c, NIWR estimates range from 1824, 1150, and 700 mm/yr respectively. Figure 43 shows projected precipitation changes for different percentiles and time periods, where it is evident that projected precipitation generally increases and then decreases with time, ranging from 5 to -5 percent relative to baseline. Figure 44 illustrates projected temperature change, ranging from 1.5 to 4 ^oC. Figures 45 and 46 illustrate solar radiation and specific humidity percent changes, which both show uniform positive changes with time and are consistent with respective declines in precipitation and higher regional ET likely being simulated by the GCMs. Figure 36 illustrates wind speed percent change, and are minimal. Figures 48 and 49 illustrates projected ET_0 and ET_c percent changes, ranging from 3 to 15 and 4 to 26 percent, respectively. The magnitude in projected percent change in ET_c

is largely due to crop type, precipitation, and baseline ET_c rates. The dominant crop types in the San Angelo basin are cotton and winter wheat, where higher ET_o combined with declines in precipitation leads to more frequent simulated irrigations, and subsequent higher bare soil evaporation and ET_c relative to baseline conditions. Projected NIWR percent change is shown in Figure 50. The NIWR incorporates growing season and non-growing season soil moisture gains and losses from precipitation, bare soil evaporation, and ET_c, therefore NIWR percent change for different time periods and scenarios are a function of respective ET_c and precipitation changes. NIWR percent changes range from 4 to 25 percent. Transient time series anomaly plots of annual precipitation, temperature, solar radiation, humidity, wind speed, ET_0, ET_c, and NIWR are shown in Figure 51 for Metnode 214033 (near Veribest, TX), which illustrates the general increase in all variables relative to the baseline, with the exception of wind speed and precipitation.

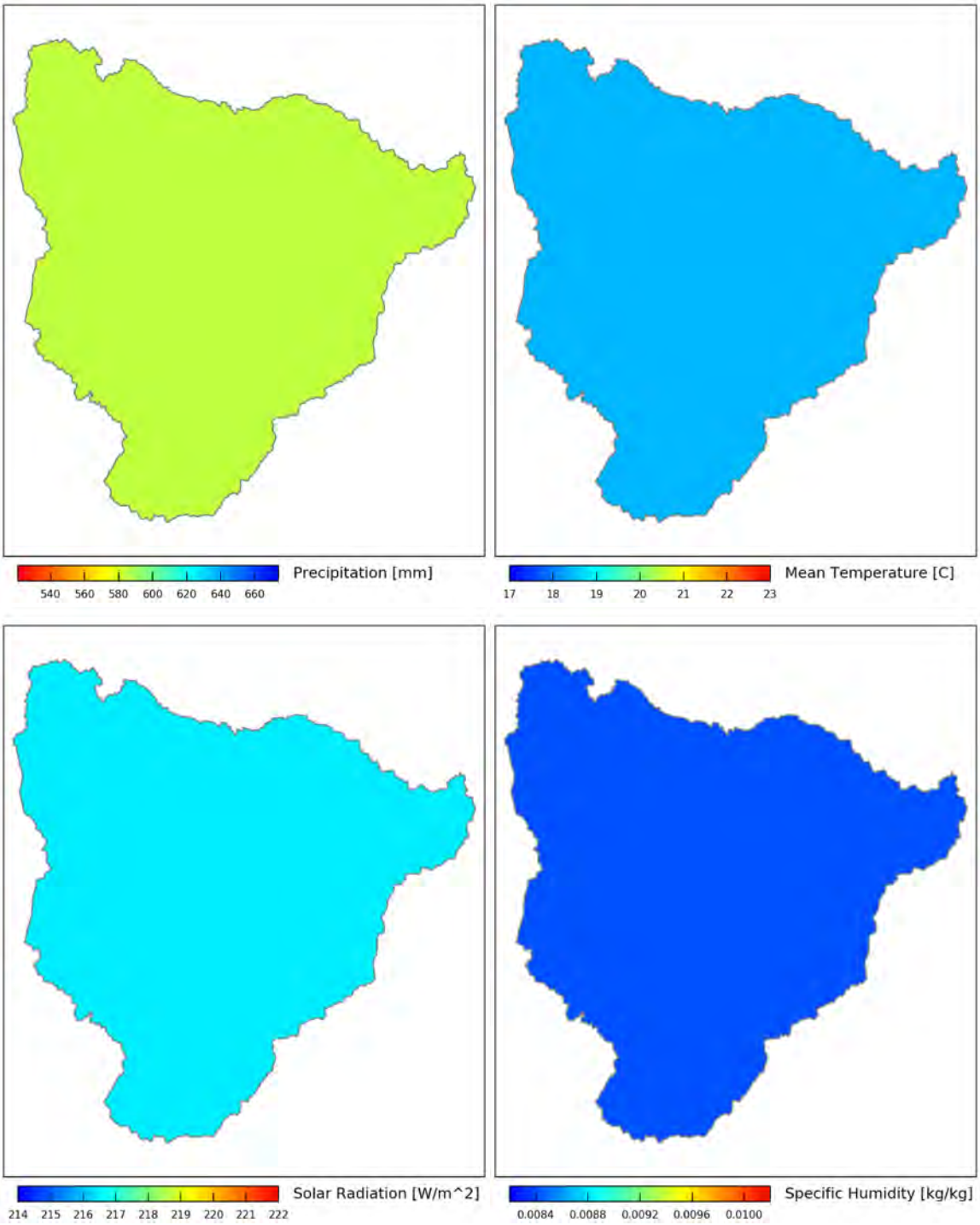

Figure 41 - San Angelo, Texas Area – Spatial distribution of baseline precipitation, temperature, solar radiation, and humidity. Color scales are relative to baseline and future conditions.

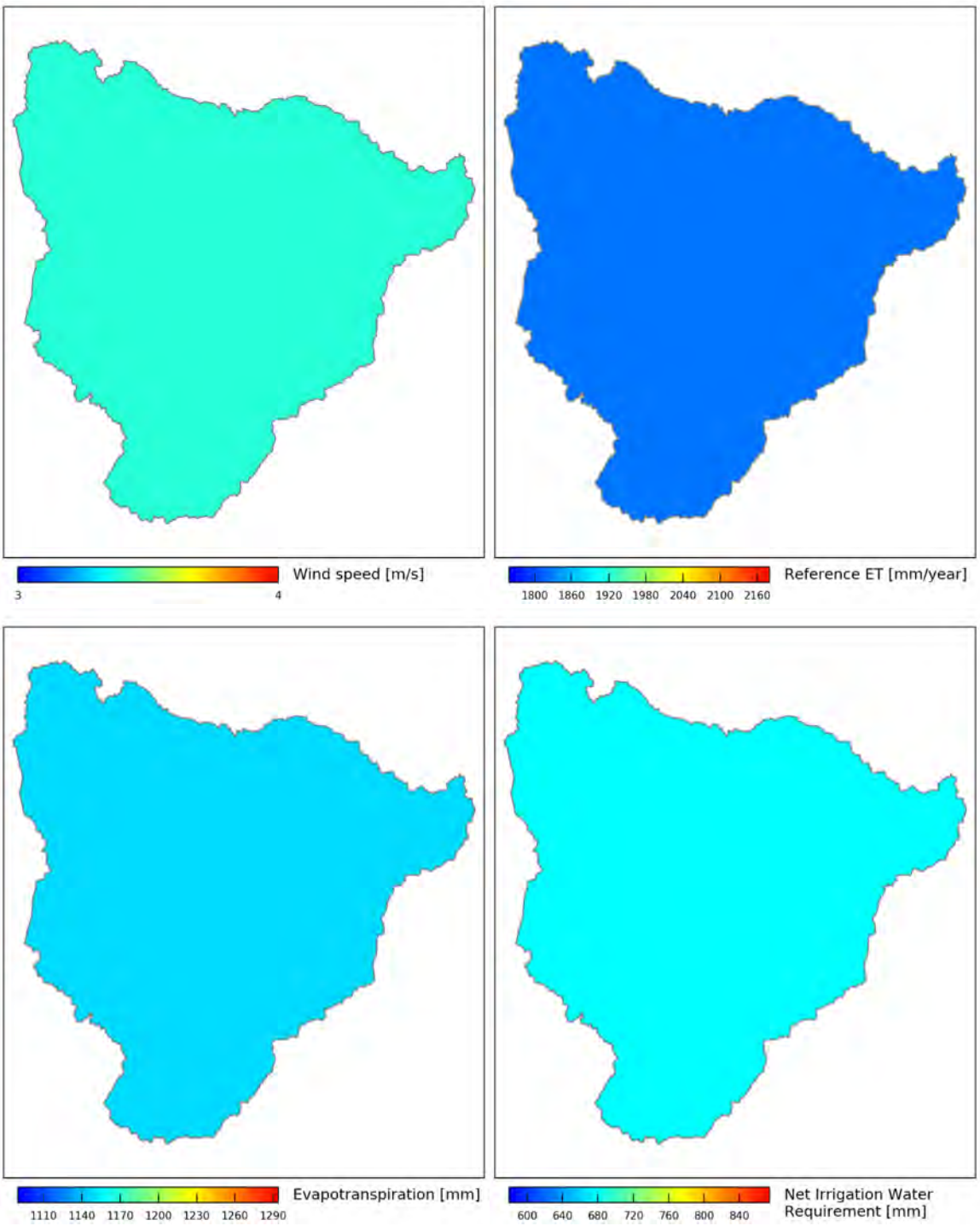

Figure 42 - San Angelo, Texas Area – Spatial distribution of baseline wind speed, reference ET, crop evapotranspiration, and net irrigation water requirement.

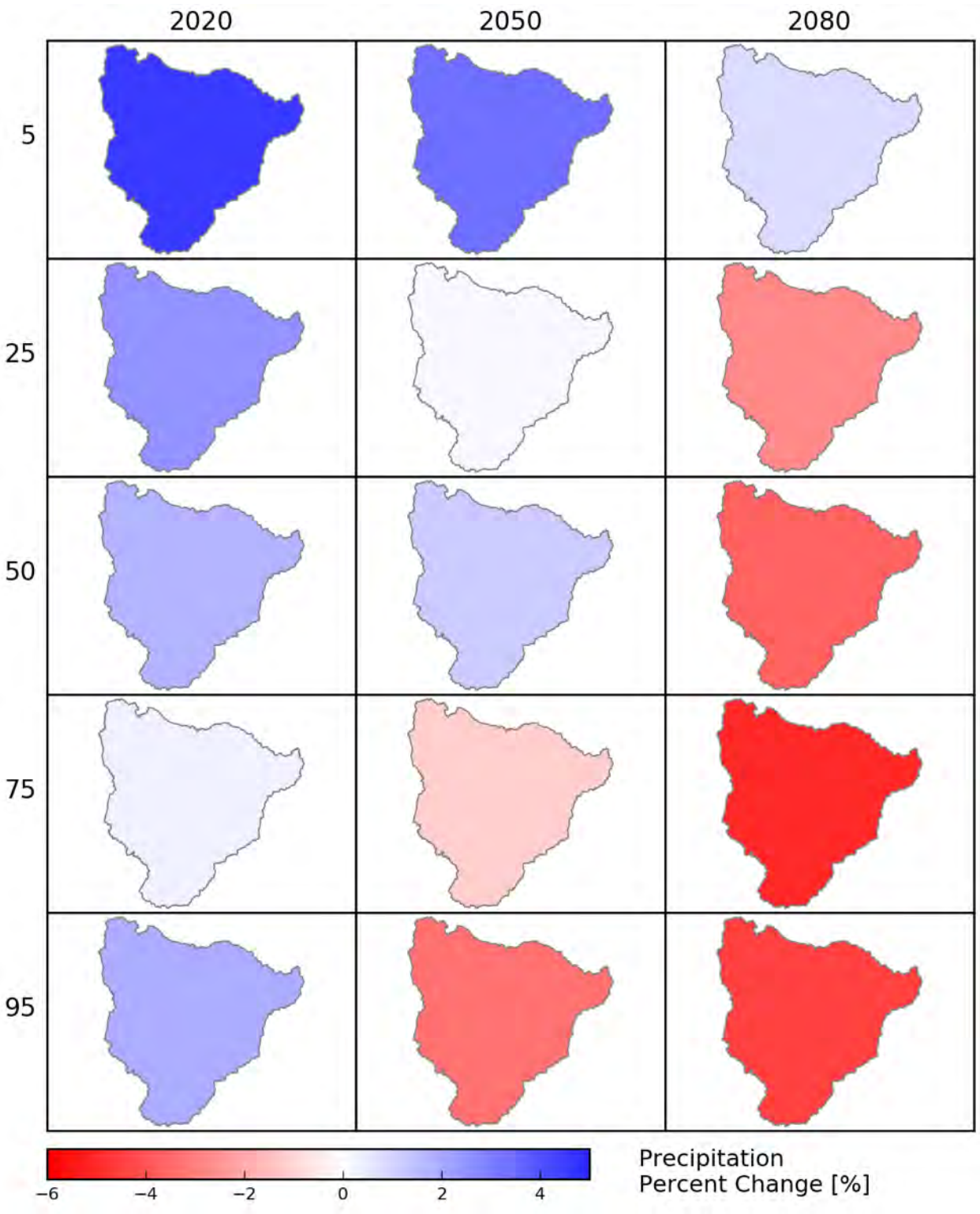

Figure 43 - . San Angelo, Texas Area – Spatial distribution of projected precipitation percent change for different percentiles and time periods.

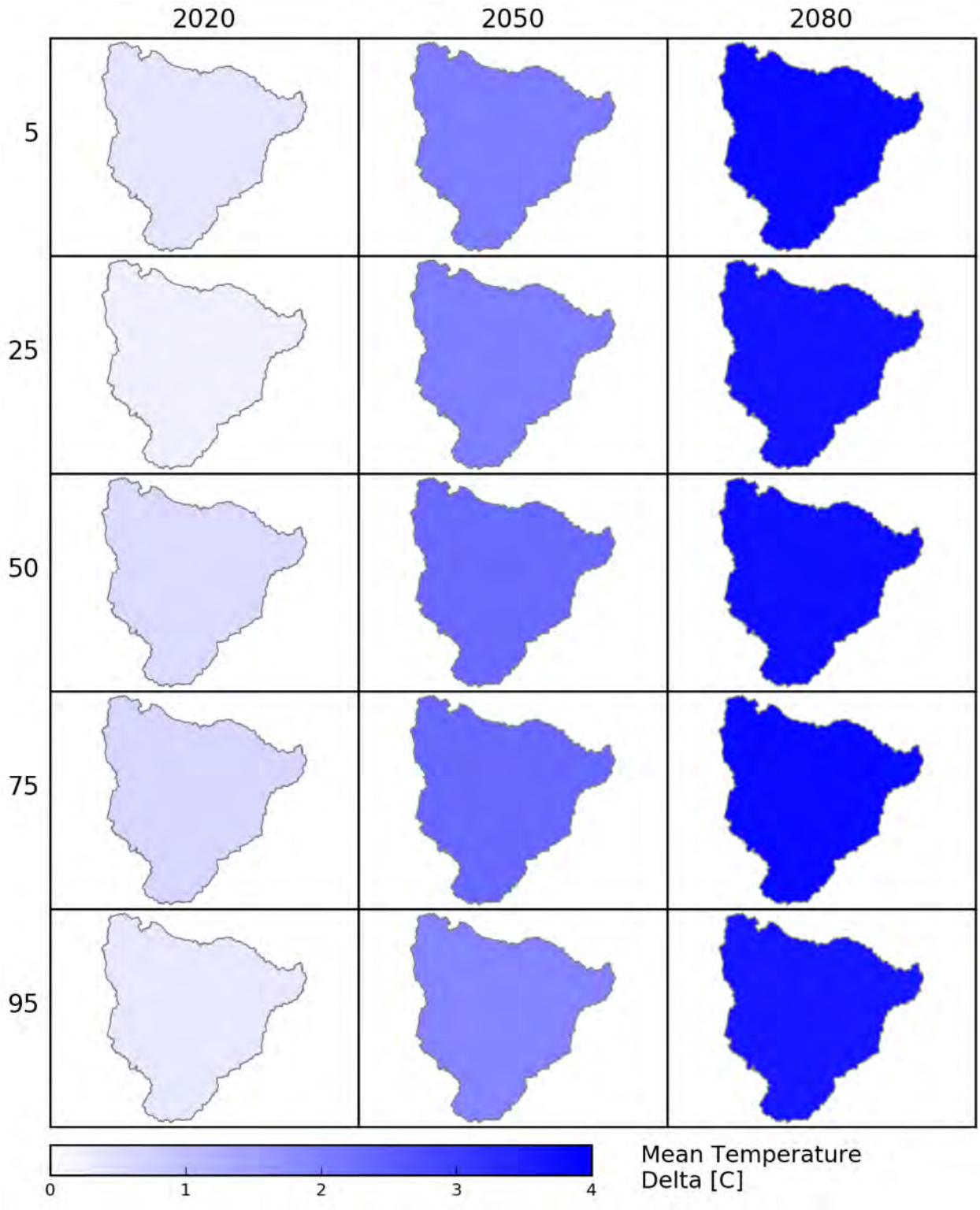

Figure 44 - San Angelo, Texas Area – Spatial distribution of projected temperature change for different percentiles and time periods.

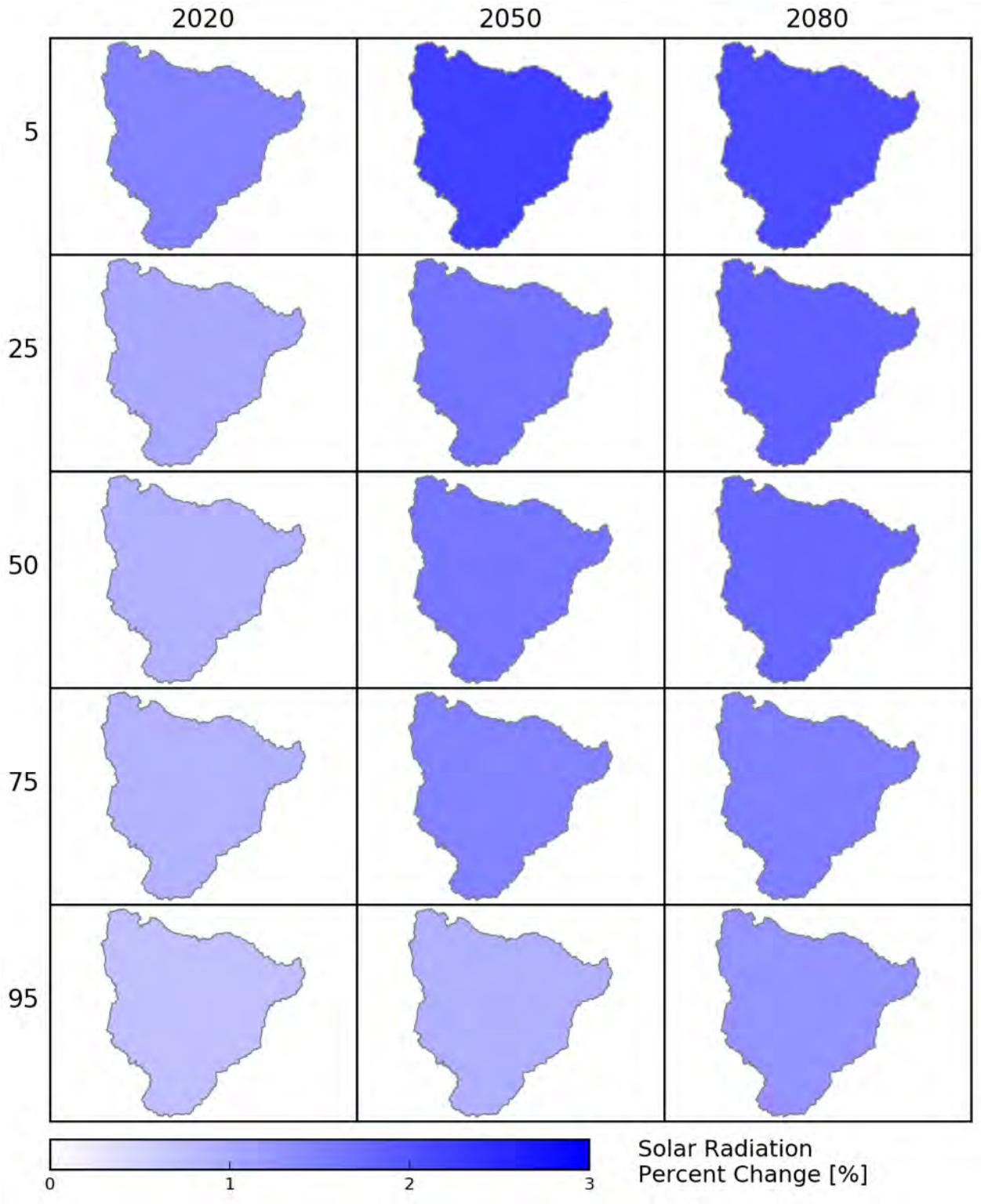

Figure 45 - San Angelo, Texas Area – Spatial distribution of projected solar radiation percent change for different percentiles and time periods.

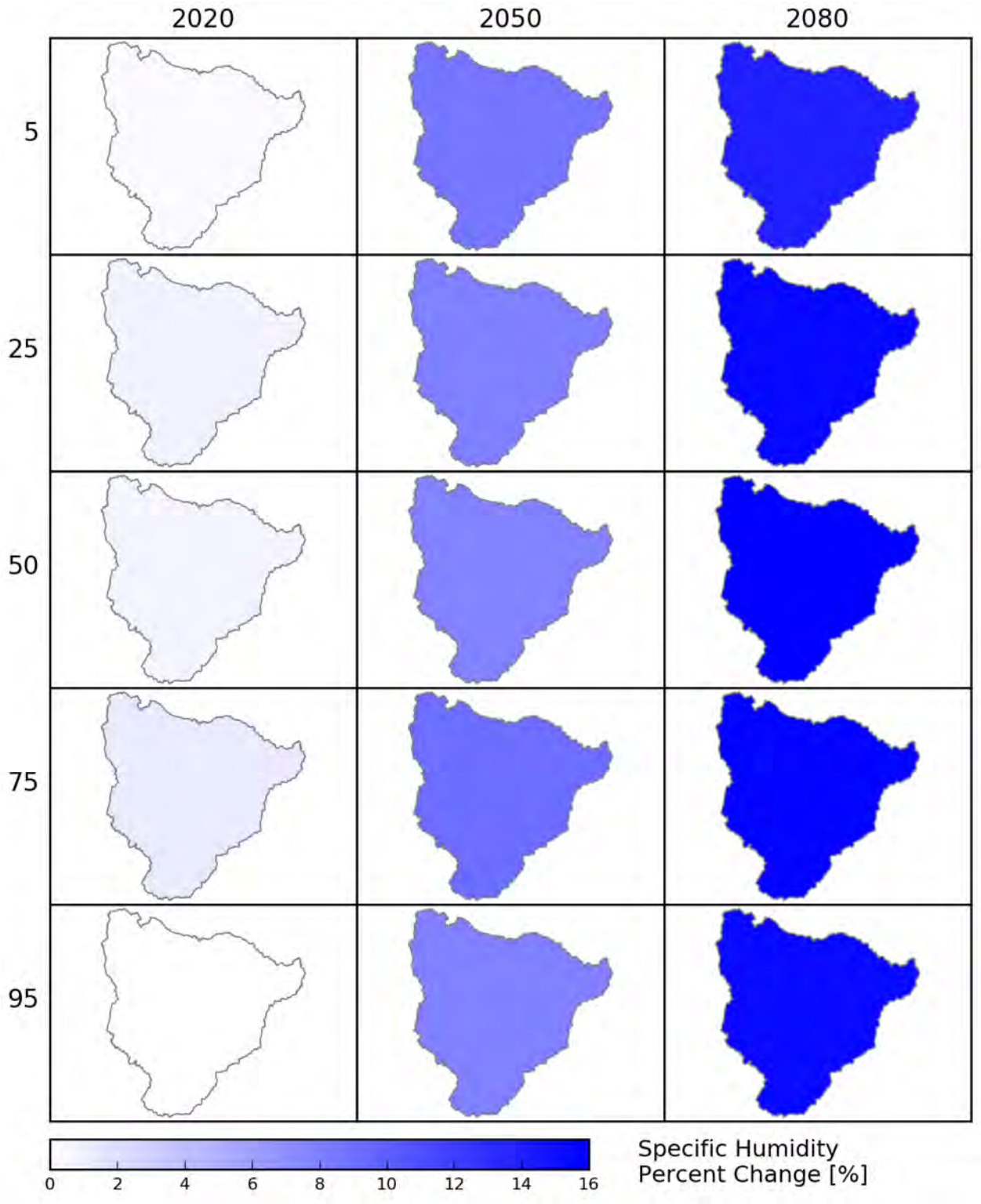

Figure 46 - San Angelo, Texas Area – Spatial distribution of projected specific humidity percent change for different percentiles and time periods.

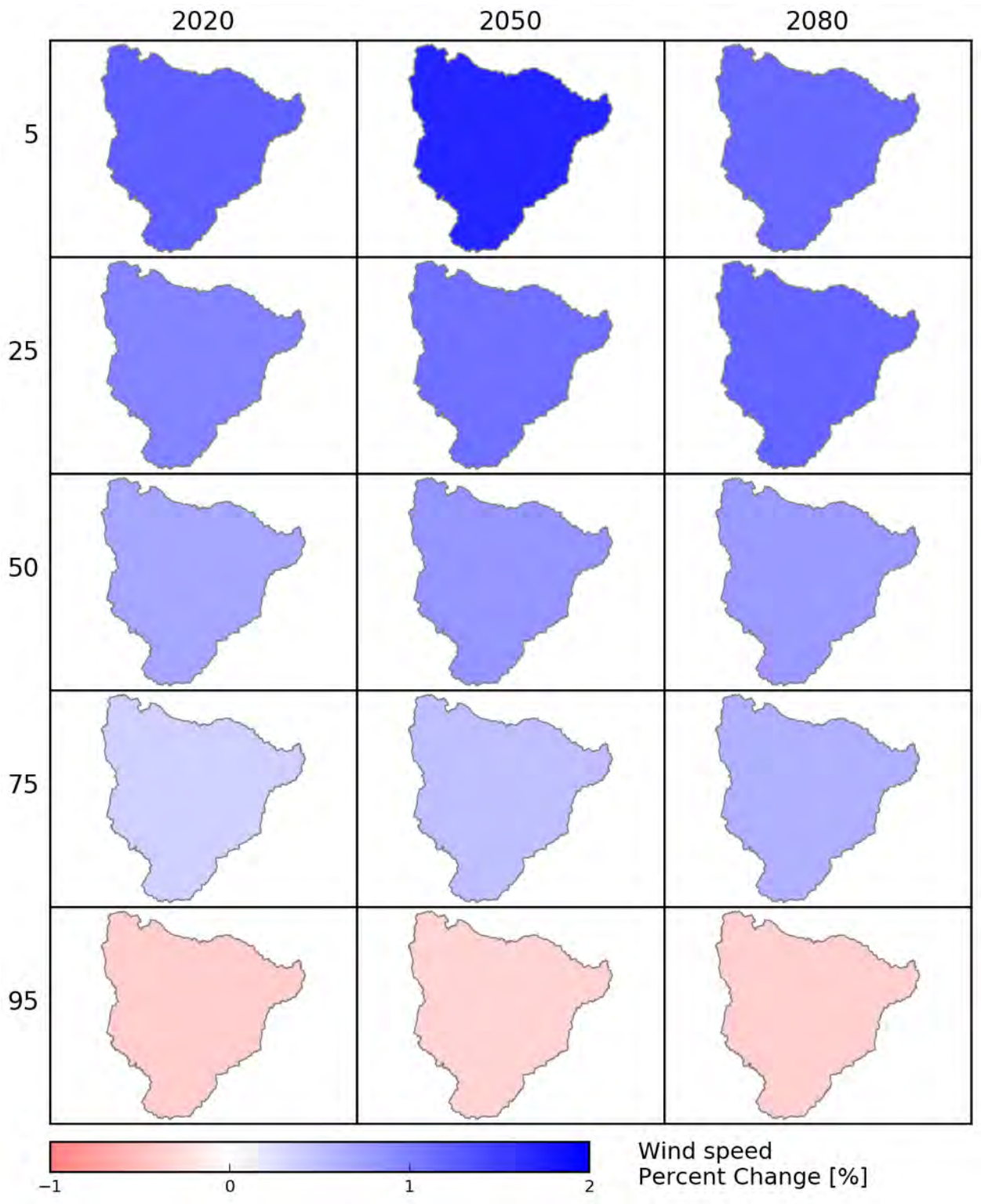

Figure 47 - San Angelo, Texas Area – Spatial distribution of projected wind speed percent change for different percentiles and time periods.

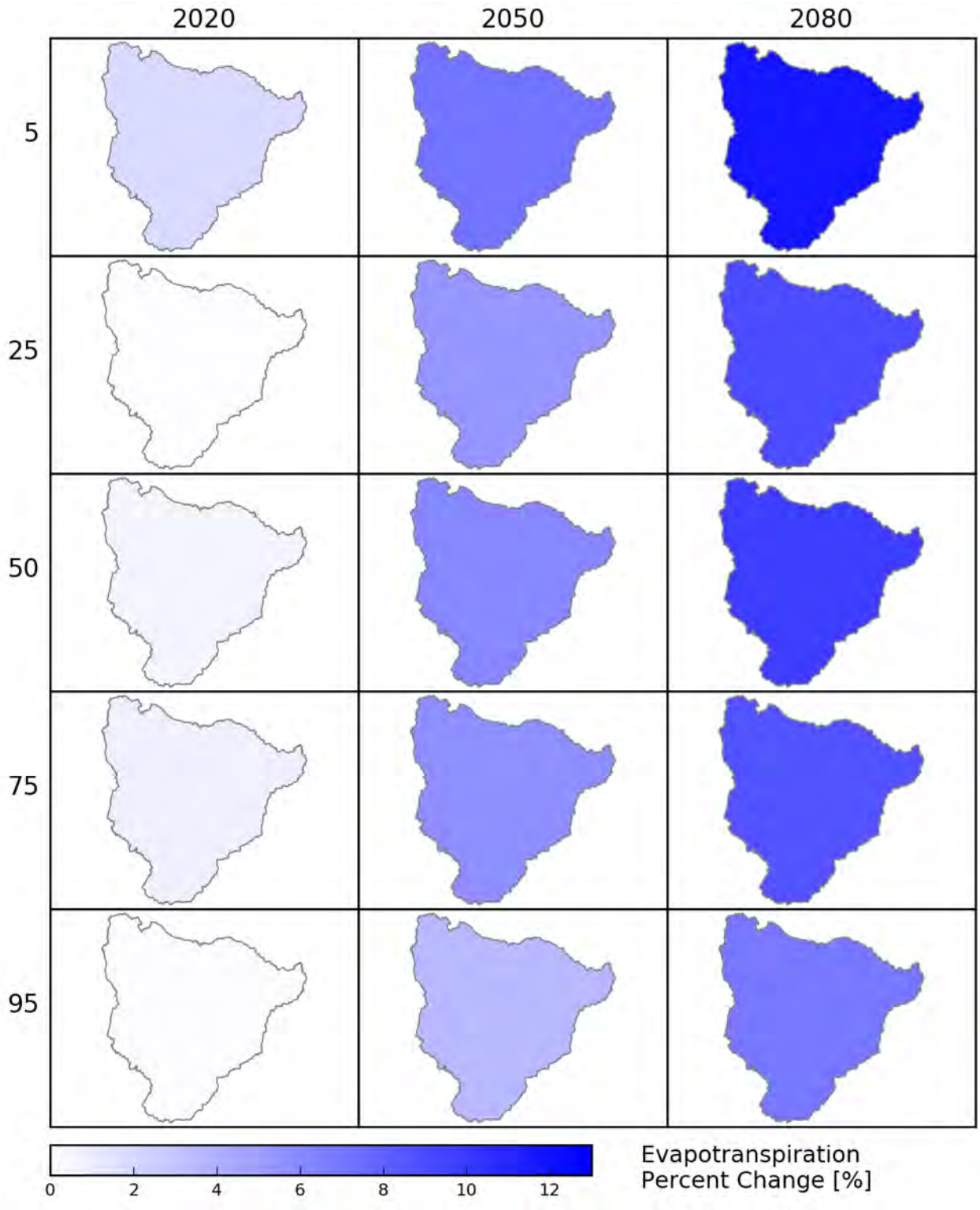

Figure 48 - San Angelo, Texas Area – Spatial distribution of projected reference ET percent change for different percentiles and time periods.

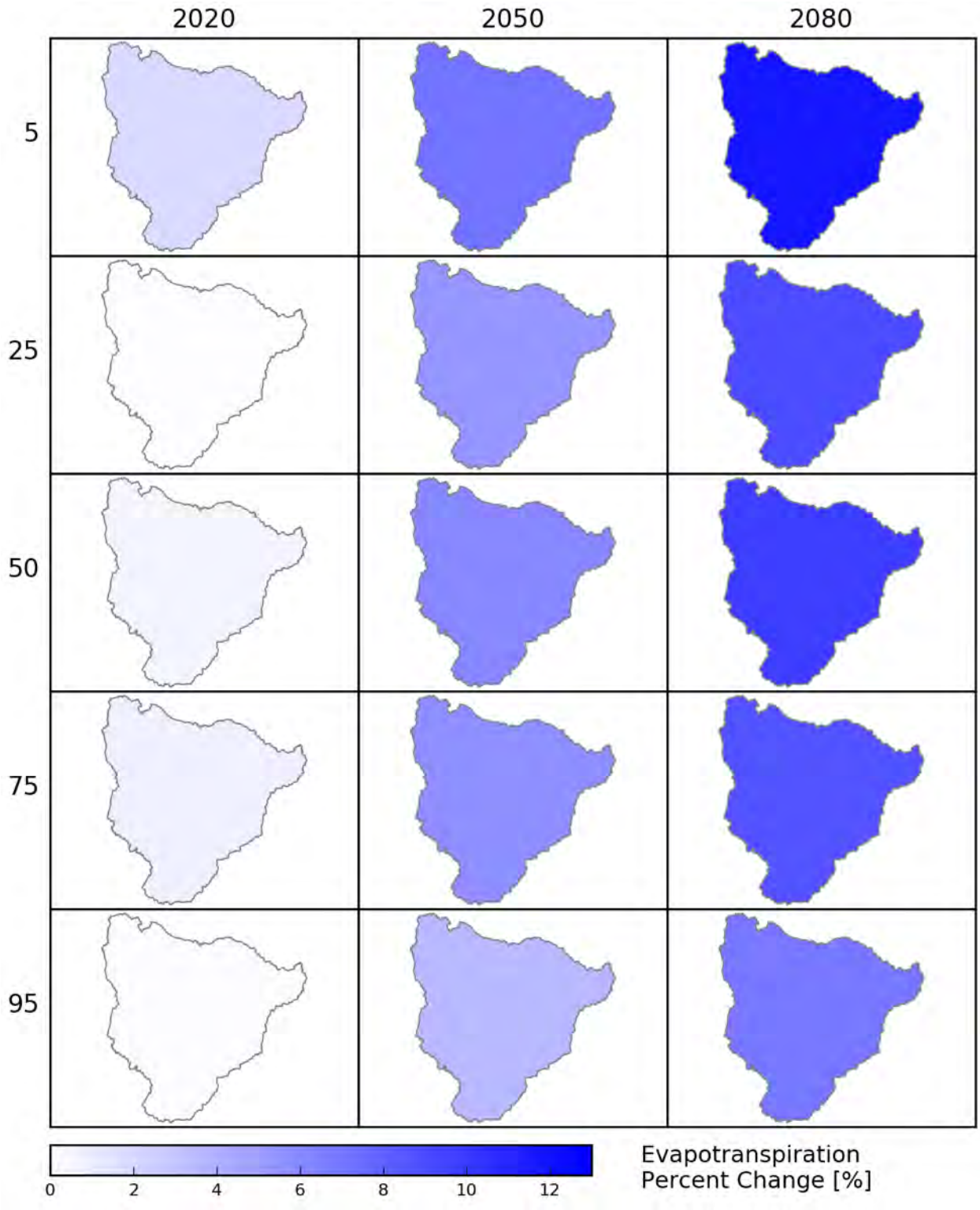

Figure 49 - San Angelo, Texas Area – Spatial distribution of projected crop ET percent change for different percentiles and time periods.

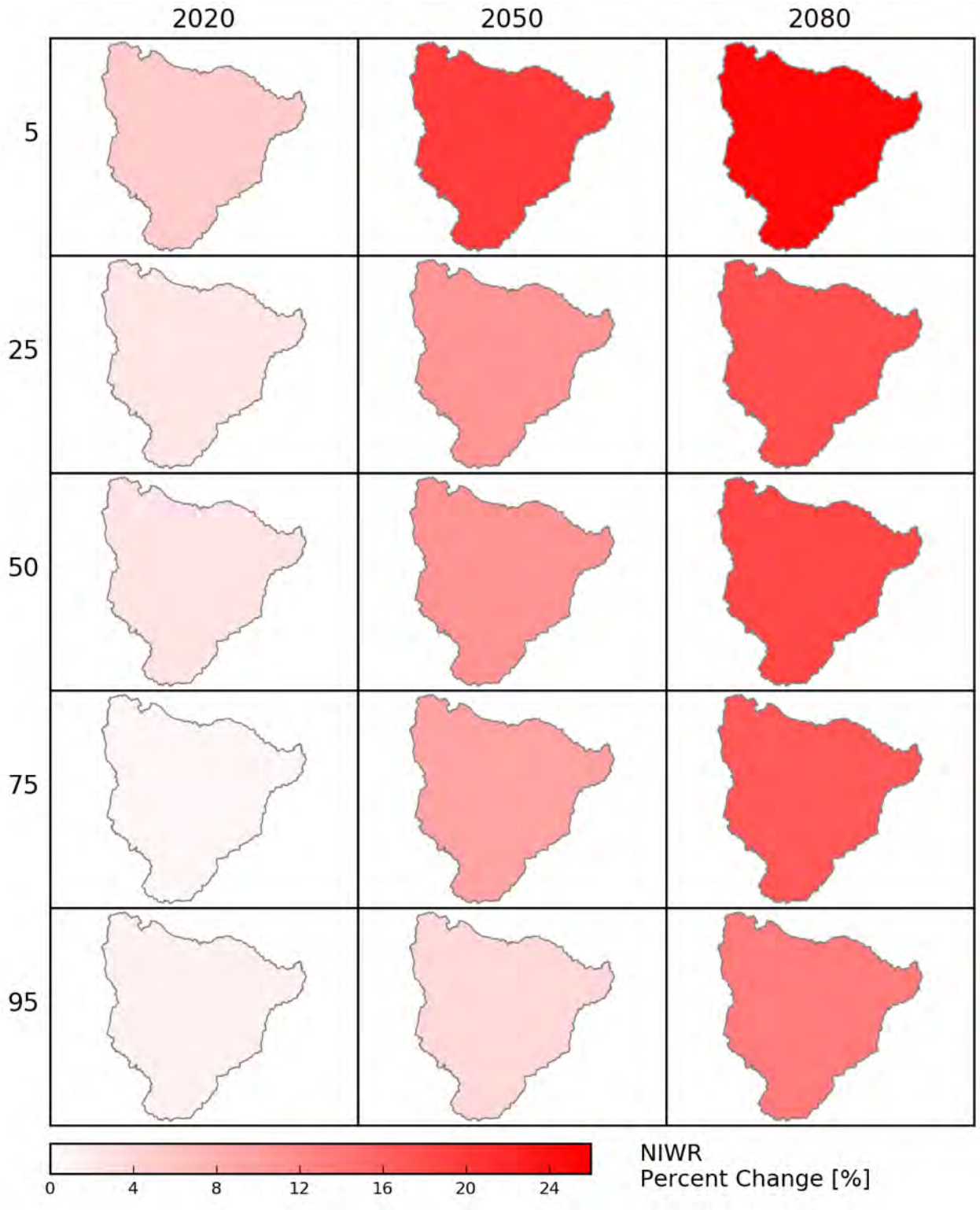

Figure 50 - . San Angelo, Texas Area – Spatial distribution of projected Net Irrigation Water Requirement percent change for different percentiles and time periods.

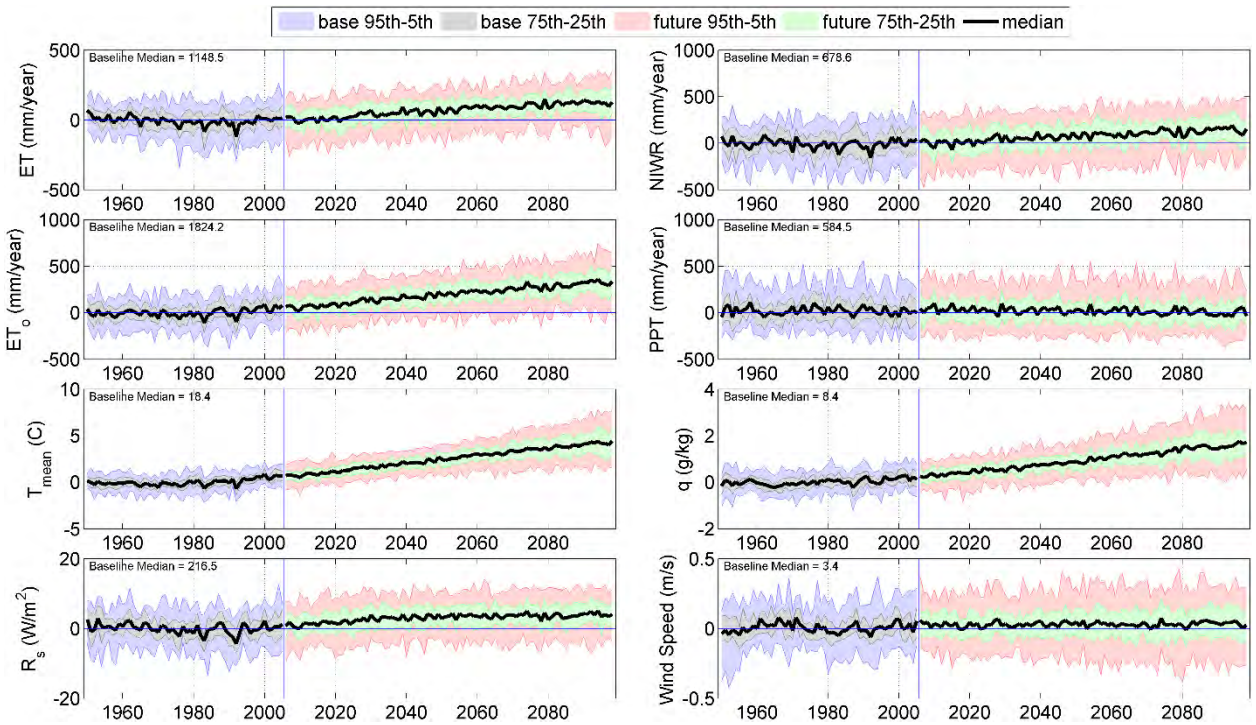

Figure 51 - San Angelo, Texas Area – Transient time series anomaly plots of annual precipitation, temperature, solar radiation, humidity, wind speed, ET0, ETc, and NIWR for Metnode 214033, HUC 12090105 (near Veribest, TX).

TCWLH Basins

Figure 5 illustrates Metnodes that were used to estimate irrigation water demands, as well as HUC8 boundaries used to upscale Metnode estimates in the TCWLH basins. Figure 52 illustrates the spatial distribution of MACA derived baseline (1950–1999) average median precipitation (top left), temperature (top right), solar radiation (bottom left), and specific humidity (bottom right). Figure 53 illustrates the spatial distribution of MACA derived baseline (1950–1999) average median wind speed (top left), ET_0 (top right), ET_c (bottom left), and NIWR (bottom right). Baseline median ET_0, ET_c, NIWR estimates range from 800 to 1200, 600 to 1100, and 500 to 1000 mm/yr, respectively, with higher rates of ET_c and NIWR occurring in lower elevation and eastern portions of the study area. Figure 54 shows the spatial distribution of projected precipitation changes for different percentiles and time periods, where it is evident that projected precipitation changes generally increase relative to baseline conditions, with changes ranging from -3 to 13 percent. Figure 55 illustrates the spatial distribution of projected temperature change ranging from 1.2 to 4.2 ^{o}C. Figures 56 and 57 illustrate solar radiation and specific humidity percent changes, with minor declines solar radiation, and specific humidity projected to increase by 7 to 23 percent, a reflection of projected increases in precipitation and likely increase in regional ET within the GCM. Figure 58 illustrates wind speed percent change, ranging from ~ 0 to -5 percent. Figure 59 and 60 illustrate the spatial distribution of projected ET_0 and ET_c percent change, ranging

from 2 to 14, and from 3 to 30 percent, respectively. Large spatial differences in projected ET_c changes are primarily due to differences in crop type, precipitation projections, and baseline ET_c rates. The largest percent change occurs within Lake Tahoe and Bridgeport area HUC8s where baseline ET_c is relatively low and pasture grass is the primary crop type. Other large changes are projected to occur in areas with relatively high acreages of perennial forage crops (e.g. alfalfa, grass hay, pasture grass). Perennial forage crops are projected to have earlier greenup, longer harvest periods (i.e., more cuttings), and later killing frosts, leading to longer growing seasons and increased ET_c. The spatial distribution of projected NIWR percent change for different percentiles and time periods is shown in Figure 61. The NIWR incorporates growing season and non-growing season soil moisture gains and losses from precipitation, bare soil evaporation, and ET_c, therefore spatial variations in the distribution of NIWR percent change for different time periods and scenarios are a function of respective ET_c and precipitation distributions. NIWR percent changes range from 3 to 39 percent, with the greatest change occurring in high elevation HUC8s where baseline NIWR values are relatively low and irrigated pasture grass is the primary crop type. Transient time series anomaly plots of annual precipitation, temperature, solar radiation, humidity, wind speed, ET_0, ET_c, and NIWR are shown in Figure 62 and 63 for Metnodes 478314 (Fallon, NV) and 468580 (Tahoe City, CA) which illustrate the general increase in all variables relative to the baseline, with the exception of wind speed and solar radiation.

A comparison of TCWLH results from this work was made to those from the recent WWCRA study by Huntington et al. (2015) for baseline and 2080 time periods to evaluate potential differences in ensemble median ET_0, ET_c, NIWR estimates, and evaluate the causes of potential differences. Comparison results indicate that ensemble median WWCRA ET_0, ET_c, NIWR estimates are higher than the current study for baseline and 2080 time periods. The difference is primarily due to higher WWCRA ET_0 estimates for baseline and 2080 time periods. In WWCRA applications, ET_0 was computed using gridded T_{max} and T_{min} data that was bias corrected to National Weather Service (NWS) Cooperative Observer (COOP) station data. These stations are not located in well-watered irrigated environments. Although mean monthly agricultural station based dewpoint depression and wind speed estimates were used for computing ET_0 for WWCRA applications, T_{max} and T_{min} were representative of COOP station locations. The ASCE-PM equation for estimating ET_0 is highly sensitive to temperature, making WWCRA estimated ET_0 higher than ET_0 estimated in the current CAT grant work. In the current work, rather than bias correcting individual ET_0 components (temperature, solar radiation, humidity, wind speed), METDATA estimated ET_0 was bias corrected based on mean monthly ratios of agricultural station measured ET_0 to METDATA estimated ET_0. Mean growing season (April-October) bias correction factors within the TCWLH applied to METDATA and MACA estimated ET_0 range from 0.72 to 0.83, thus reducing METDATA and MACA estimated ET_0 to provide more representative agricultural station based estimates of ET_0. Reduced ET_0 translates to reduced ET_c and NIWR when compared to WWCRA results. Comparisons are graphically summarized for baseline and

2080 time periods in Figures 64 and 65. Another factor making future ET_c and NIWR lower in this work when compared to WWCRA results, is the consideration of CO_2 reductions in transpiration. Figure 6 highlights the correction factors applied over time to K_{cb}. WWCRA estimated precipitation is fairly similar to MACA baseline precipitation, however, future projections of precipitation within the TCWLH region are higher than WWCRA estimates, further reducing NIWR estimated in this work. Results from this comparison highlight the need for careful consideration of well-watered agricultural climate conditions when estimating ET_0, ET_c, and NIWR. The TCWLH study area is likely an extreme example of "conditioning" of ET_0 due to the fact that irrigated lands are surrounded by relatively hot dry deserts. In areas where more regional precipitation and ET occurs, differences between ambient and irrigated agriculture ET_0 (and its forcings) are less.

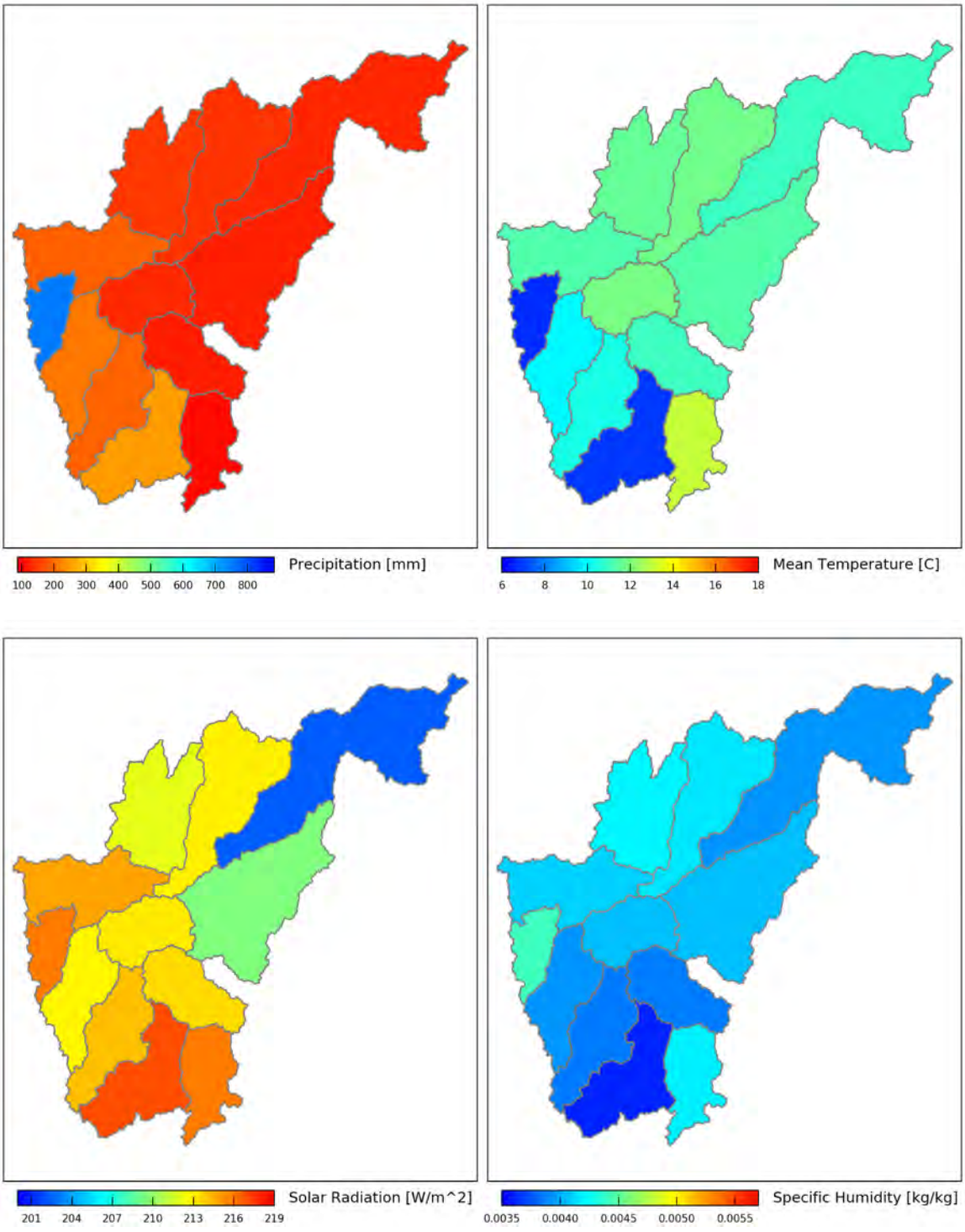

Figure 52 - TCWLH, Nevada-California Areas – Spatial distribution of baseline precipitation, temperature, solar radiation, and humidity. Color scales are relative to baseline and future conditions.

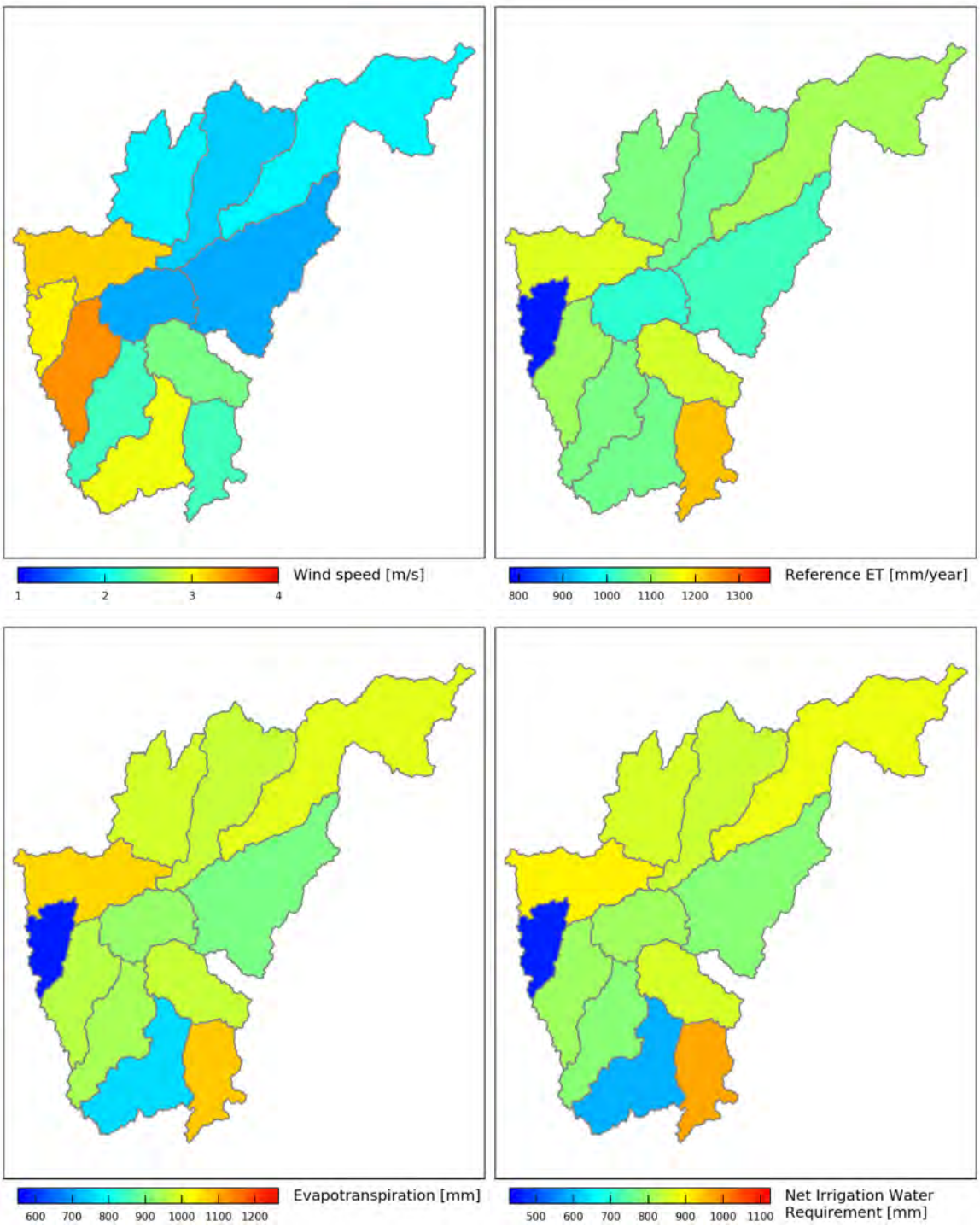

Figure 53 - TCWLH, Nevada-California Areas – Spatial distribution of baseline wind speed, reference ET, crop evapotranspiration, and net irrigation water requirement.

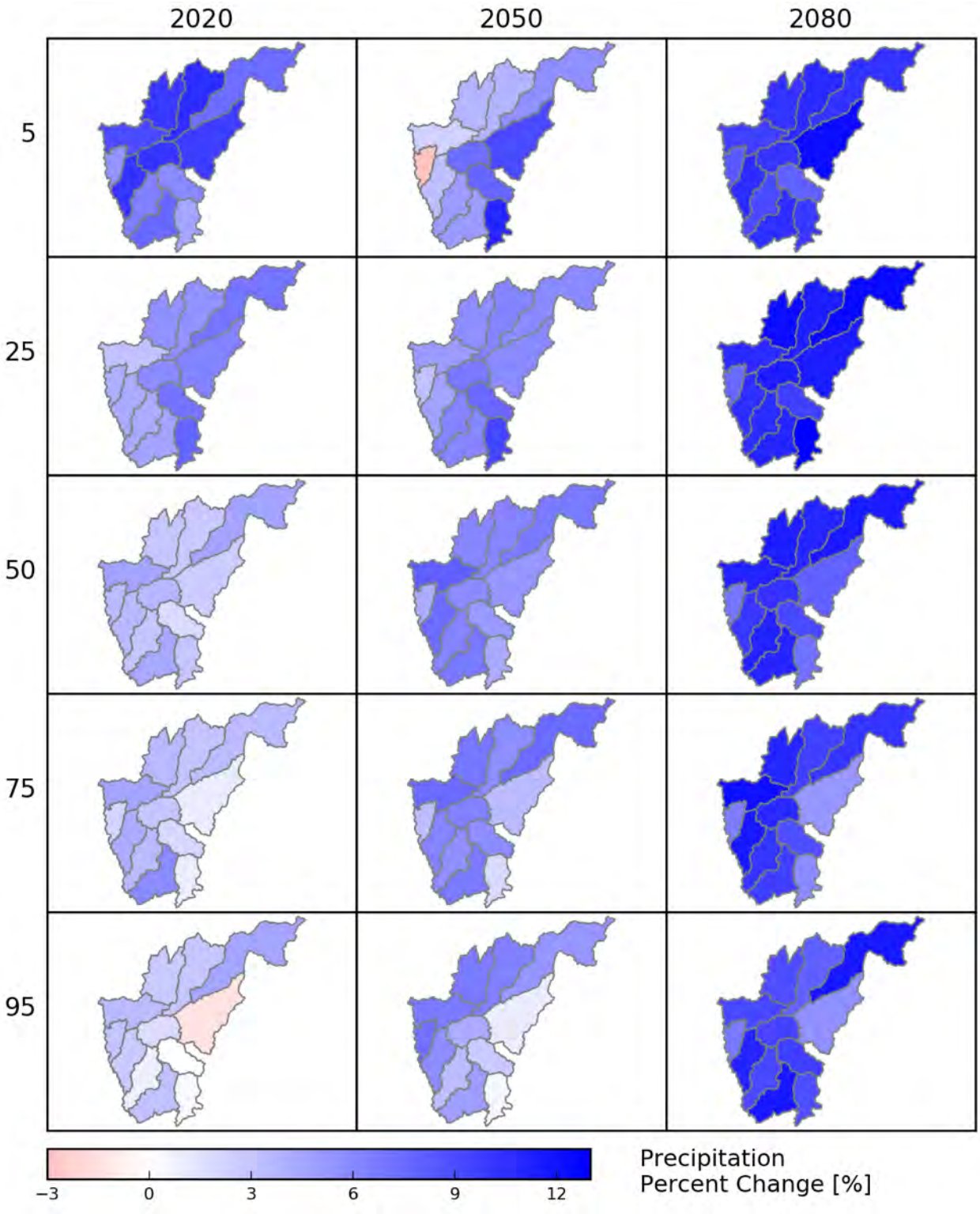

Figure 54 - TCWLH, Nevada-California Areas – Spatial distribution of projected precipitation percent change for different percentiles and time periods.

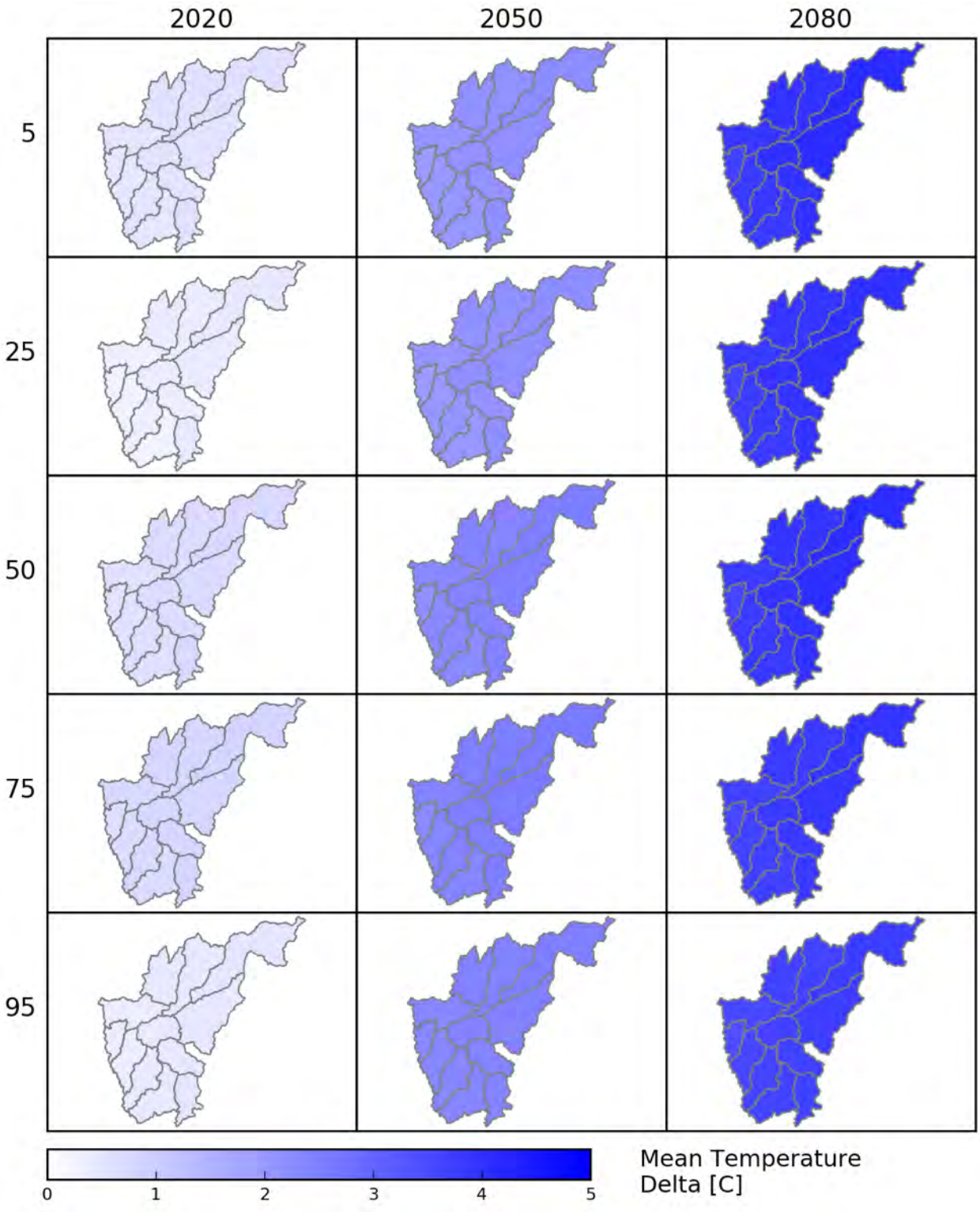

Figure 55 - TCWLH, Nevada-California Areas – Spatial distribution of projected temperature change for different percentiles and time periods.

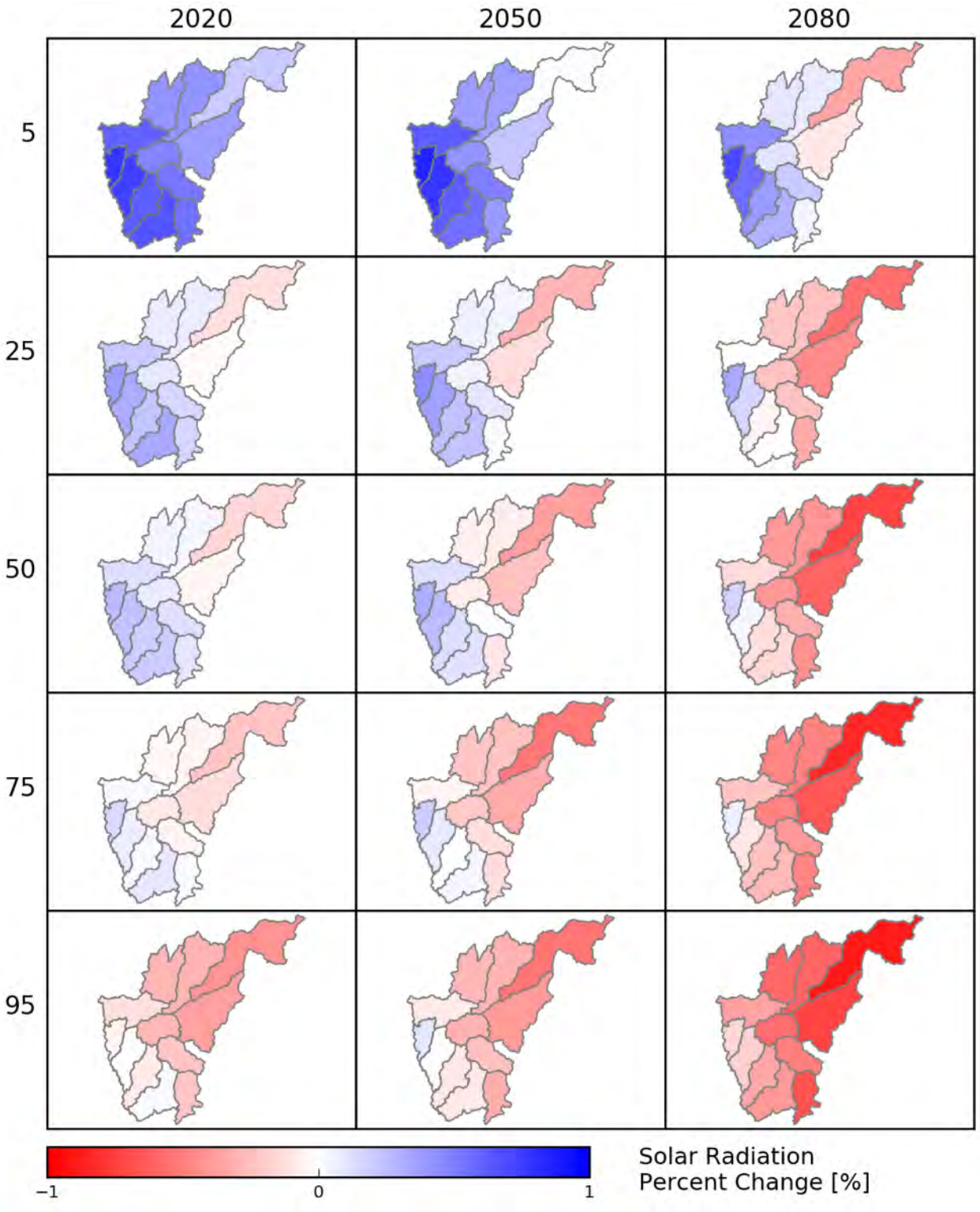

Figure 56 - TCWLH, Nevada-California Areas – Spatial distribution of projected solar radiation percent change for different percentiles and time periods.

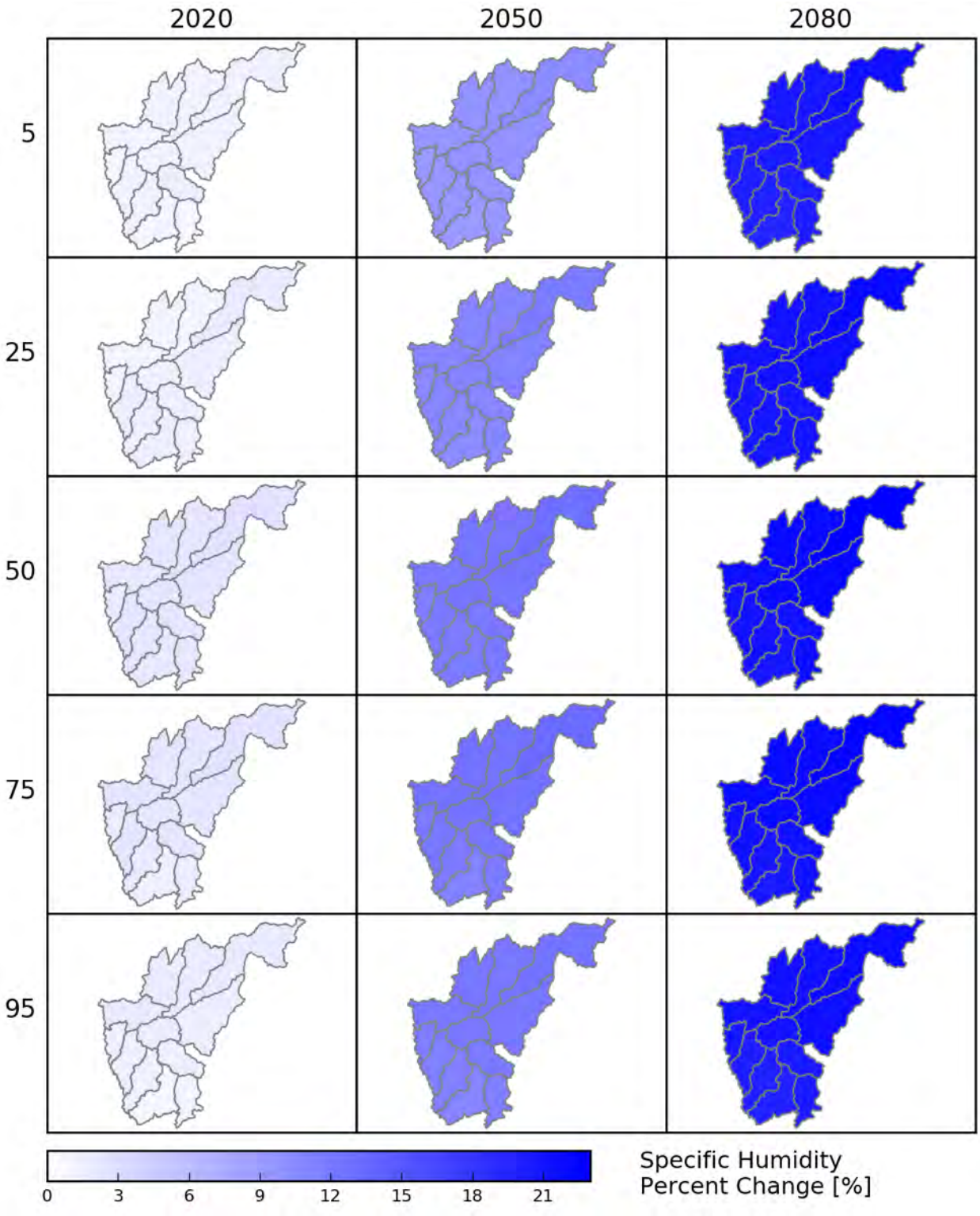

Figure 57 - TCWLH, Nevada-California Areas – Spatial distribution of projected specific humidity percent change for different percentiles and time periods.

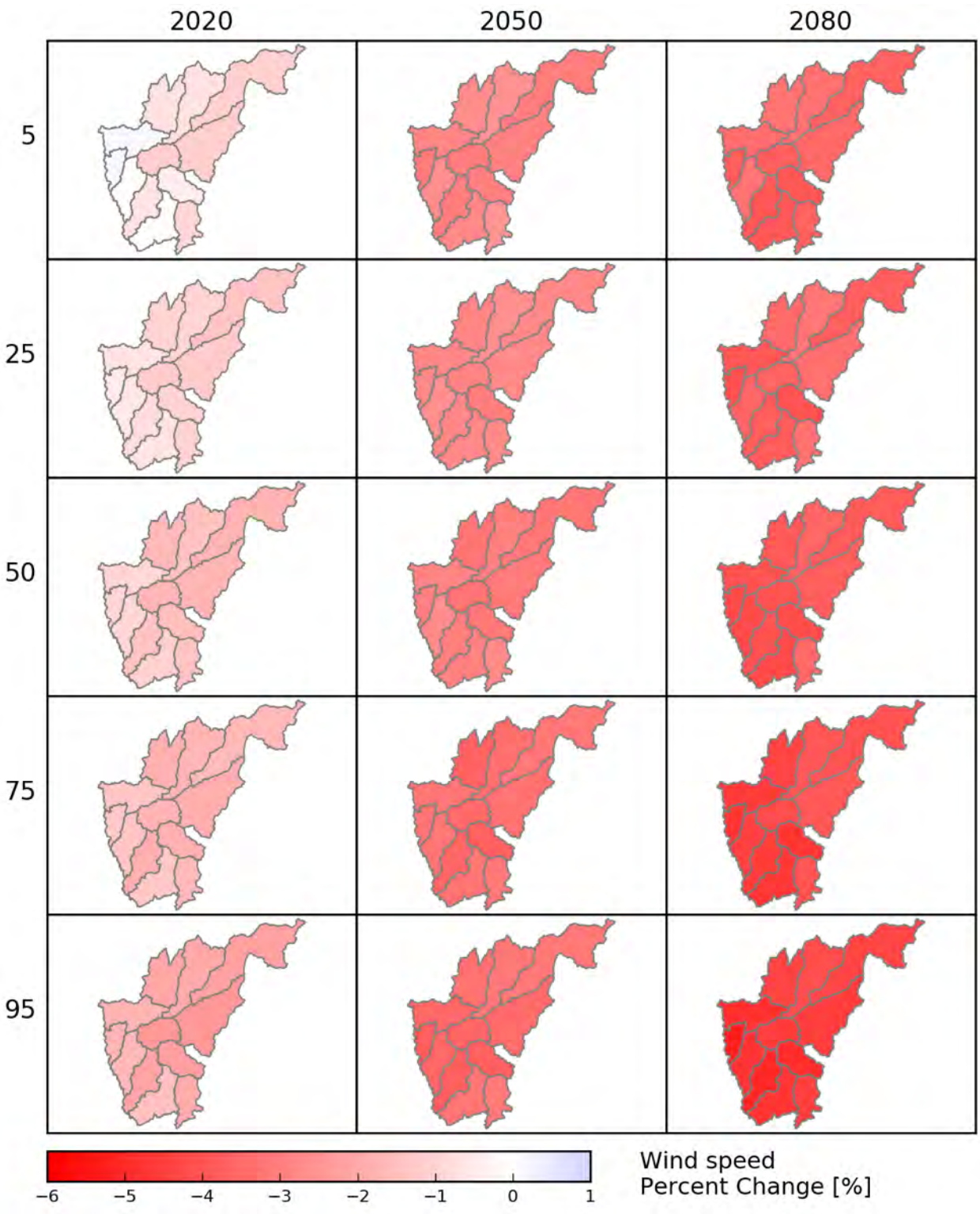

Figure 58 - TCWLH, Nevada-California Areas – Spatial distribution of projected wind speed percent change for different percentiles and time periods.

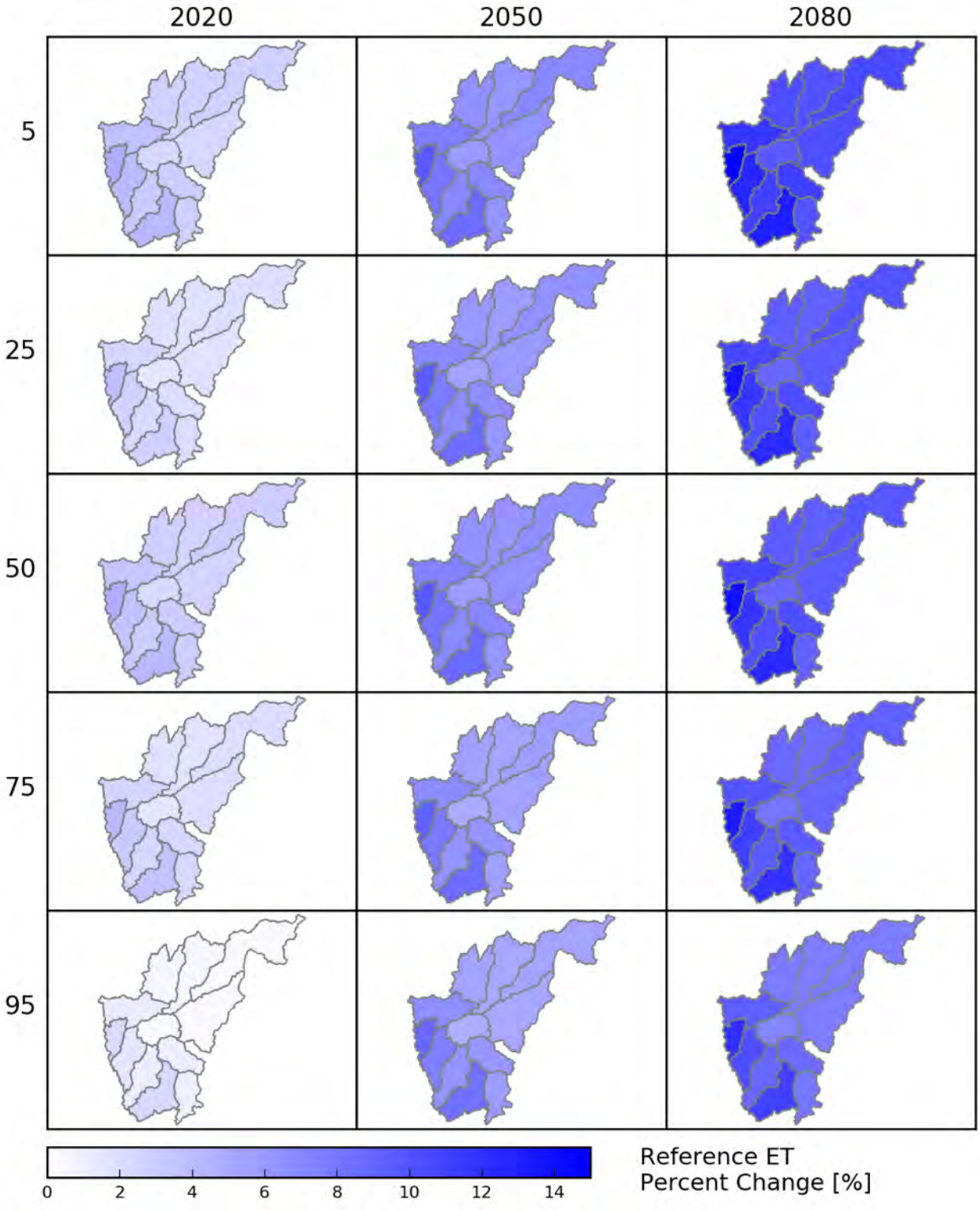

Figure 59 - TCWLH, Nevada-California Areas – Spatial distribution of projected reference ET percent change for different percentiles and time periods.

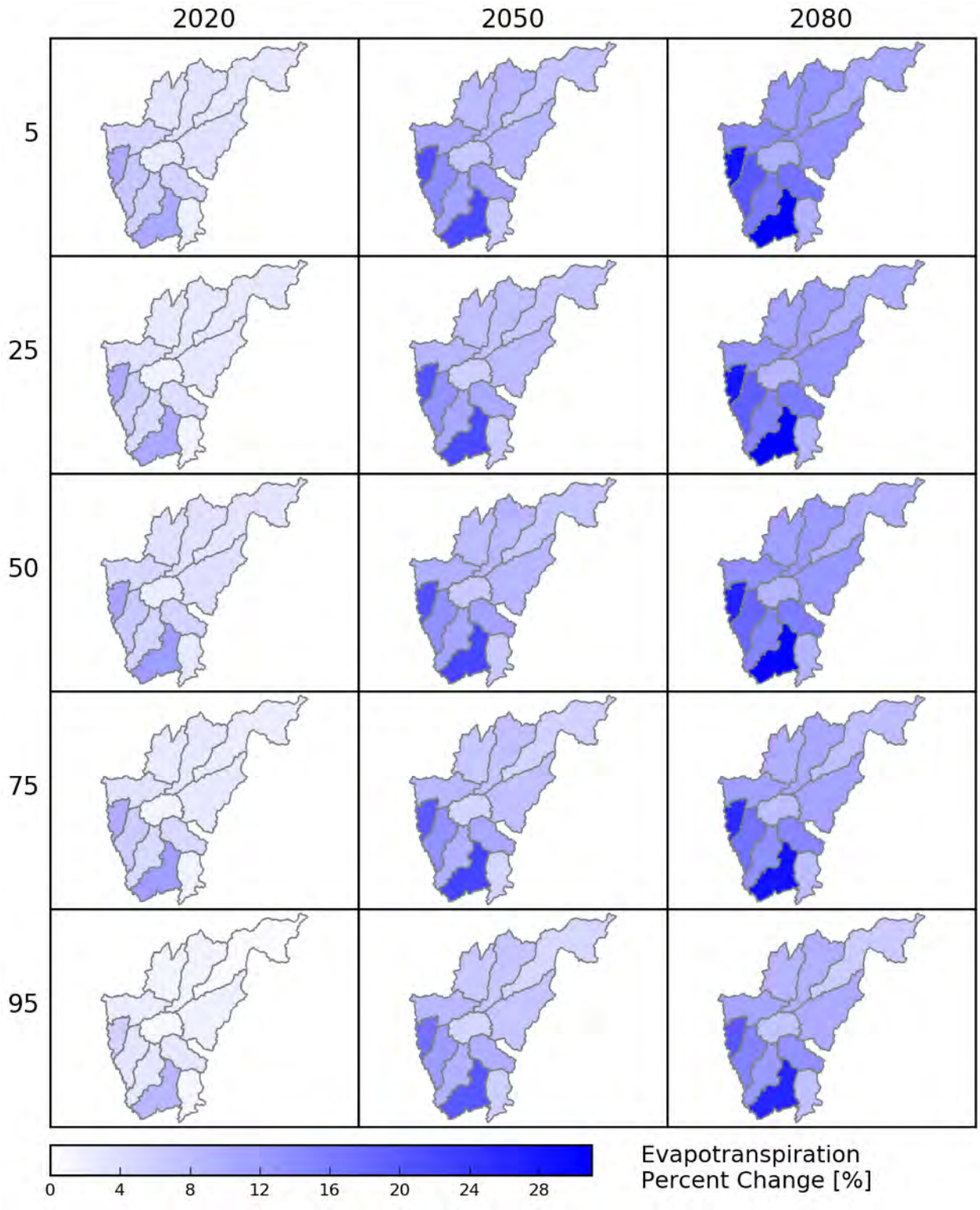

Figure 60 - TCWLH, Nevada-California Areas – Spatial distribution of projected crop ET percent change for different percentiles and time periods.

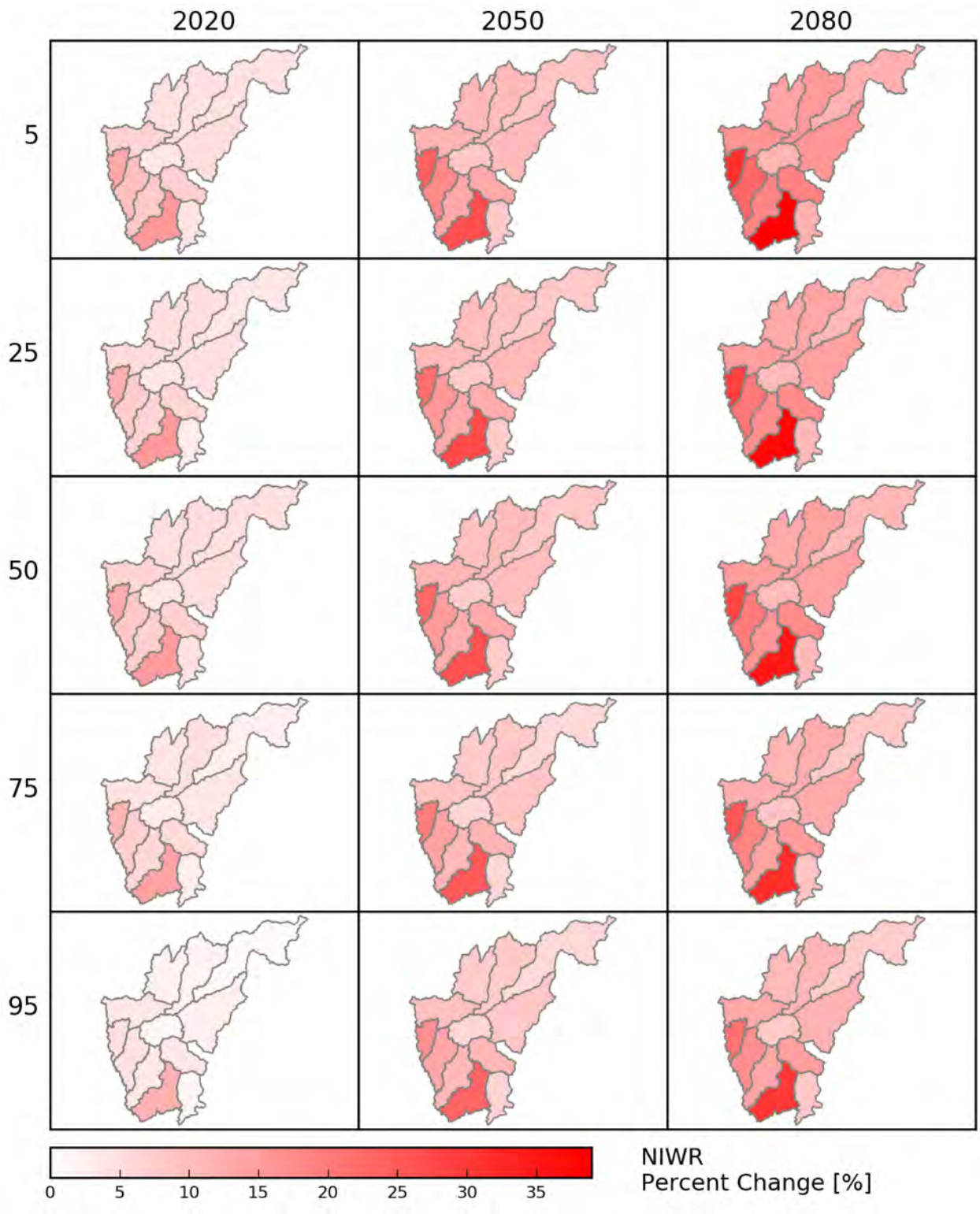

Figure 61 - TCWLH, Nevada-California Areas – Spatial distribution of projected Net Irrigation Water Requirement percent change for different percentiles and time periods.

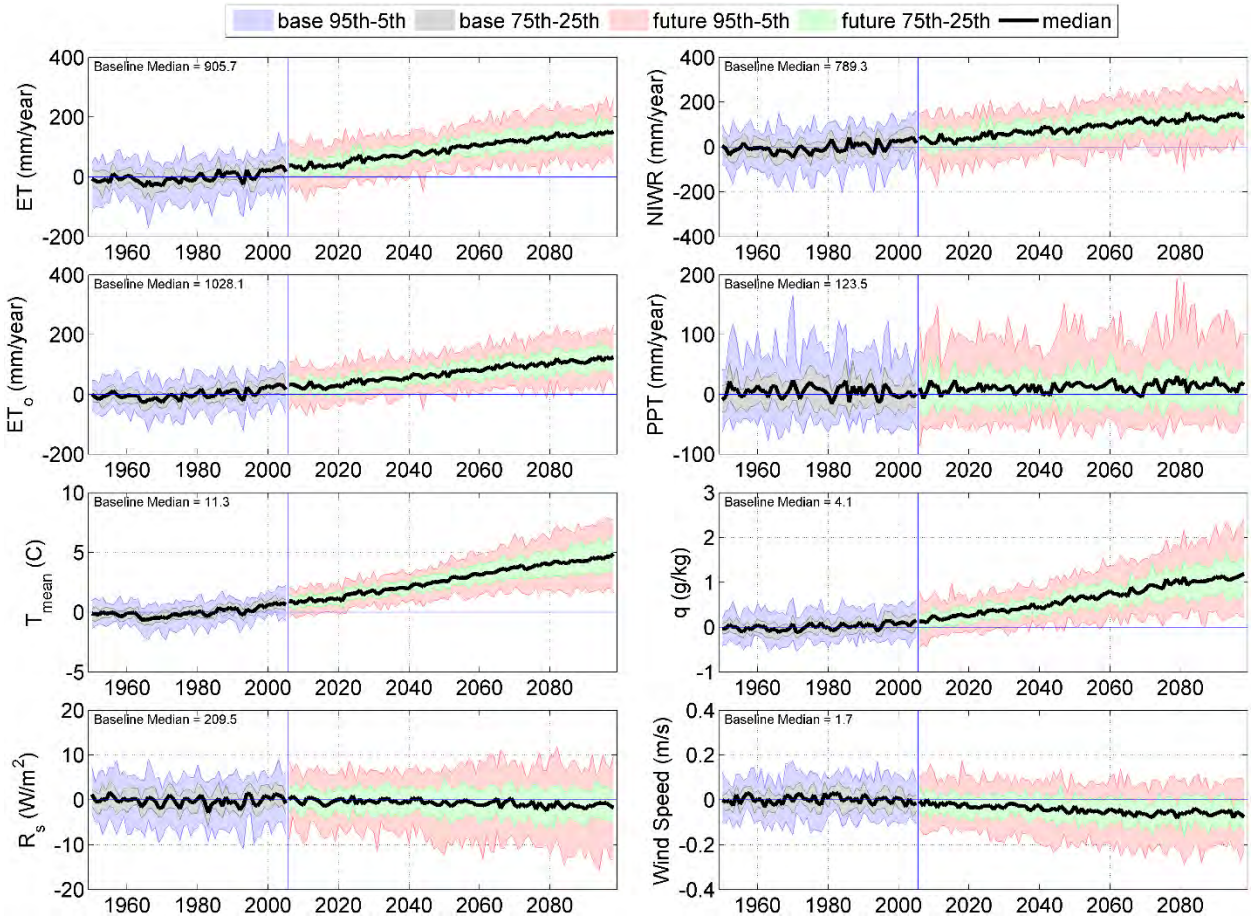

Figure 62 - TCWLH, Nevada-California Areas – Transient time series anomaly plots of annual precipitation, temperature, solar radiation, humidity, wind speed, ET0, ETc, and NIWR for Metnode 478314, HUC8 16050203 (Fallon, NV).

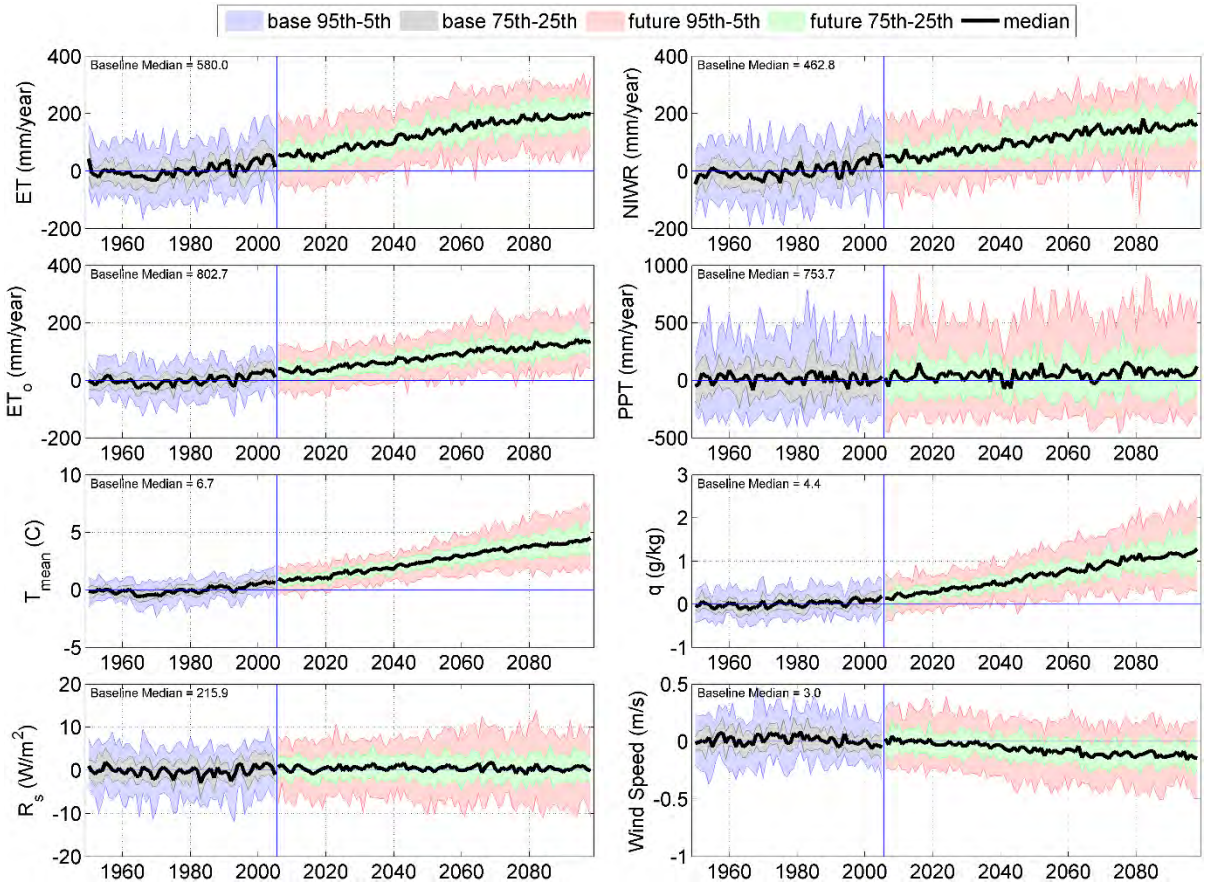

Figure 63 - TCWLH, Nevada-California Areas – Transient time series anomaly plots of annual precipitation, temperature, solar radiation, humidity, wind speed, ET0, ETc, and NIWR for Metnode 468580, HUC 16050101 (Tahoe City, CA).

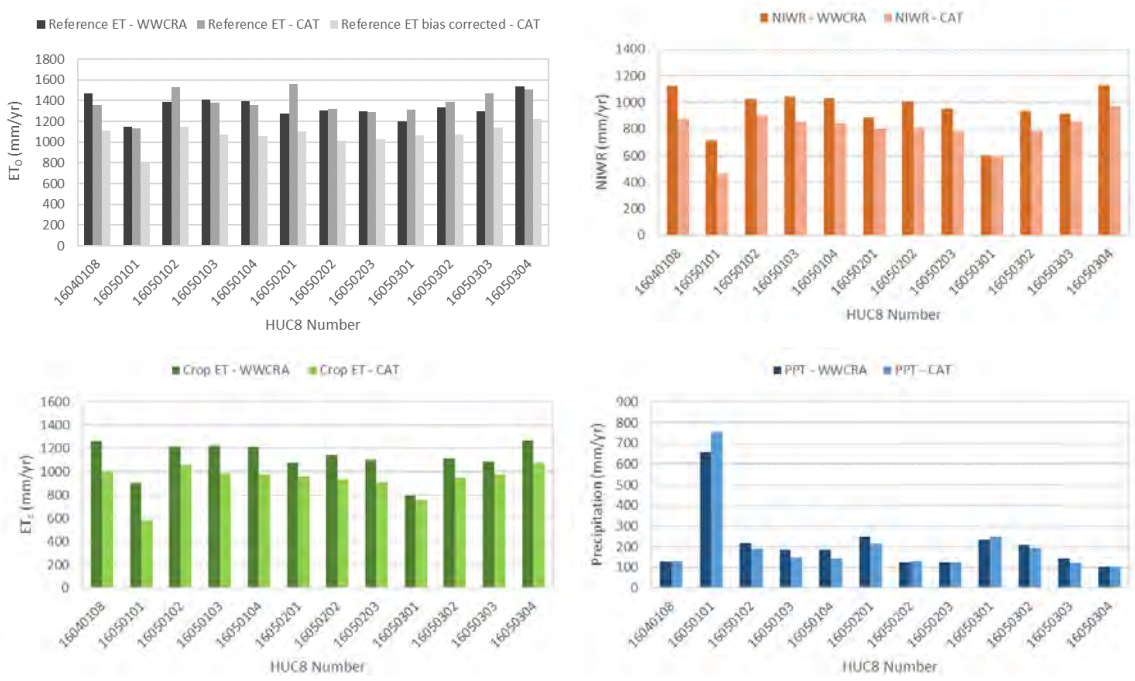

Figure 64 - TCWLH, Nevada-California Areas – Comparison of baseline reference ET, crop ET, net irrigation water requirement, and precipitation estimates derived from the WWCRA study, and this study (i.e. CAT).

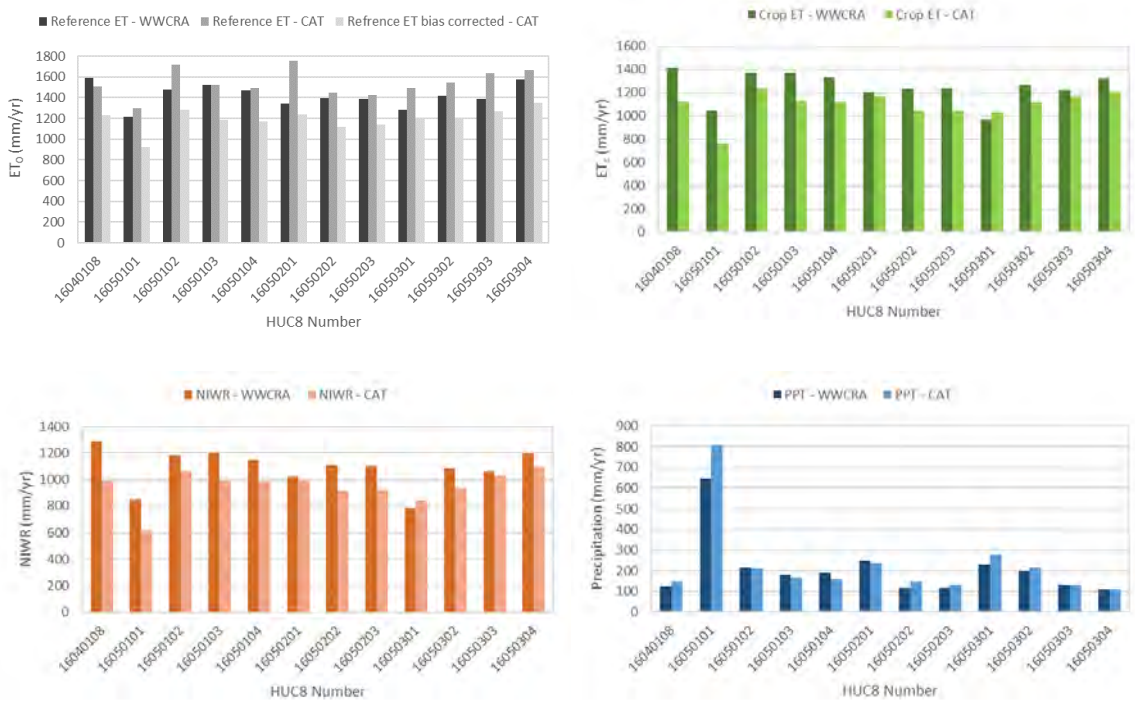

Figure 65 - TCWLH, Nevada-California Areas – Comparison of 2080 median reference ET, crop ET, net irrigation water requirement, and precipitation estimates derived from the WWCRA study, and this study (i.e. CAT).

SUMMARY

This section briefly summarizes the findings on irrigation demands. The impacts across the five basins vary, but general consistencies in results are summarized in the following:

- Precipitation projections are highly variable and basin dependent, with the ensemble medians showing both slight increases and decreases within most basins.
- Temperature shows a persistent increasing trend from the baseline level.
- Reference ET is projected to increase in all basins.
- Crop evapotranspiration is projected to increase in all basins, especially areas where perennial crops are grown, and with smaller increases in areas where annual crops are grown.
- Because the NIWR incorporates growing season and non-growing season soil moisture gains and losses from precipitation, bare soil evaporation, and crop ET, projections of NIWR largely reflect changes of crop ET, but it is uncertain and dependent on the projected precipitation.
- Comparisons between TCWLH baseline and future projections of crop ET and NIWR from this study are generally lower than from a previous study using different climate projection information. Lower estimates of crop ET and NIWR are primarily due to lower reference ET when compared to WWCRA estimates of reference ET.

UNCERTAINTIES

Including 20 different climate models and 2 different climate scenarios in this analysis was designed to provide a quantitative representation of how irrigation water demand in the study basins may respond to a range of future climate projections. The analysis was designed to take advantage of best available datasets and modeling tools and to follow methodologies documented in peer-reviewed literature. However, there are a number of analytical uncertainties that should be understood in interpreting results, including uncertainties associated with the following analytical areas that can be grouped under two categories—climate projection information and assessing irrigation demand. Climate projection information is largely uncertain with respect to four major categories: global climate forcing, global climate simulation, climate projection bias correction, and climate projection spatial downscaling. Projected irrigation demand information is largely uncertain with respect to four major categories: modeling of irrigation demand, bias and calibration, spatial resolution, and temporal resolution.

Climate Projection Information Uncertainty

Although the assessment of irrigation demands considers future climate projections representing a range of future greenhouse gas (GHG) emission paths, the uncertainties associated with these pathways were not explored. Such uncertainties include those introduced by assumptions about technological and economic developments, globally and regionally; how those assumptions translate into global energy use involving greenhouse gas emissions; and biogeochemical analysis to determine the fate of GHG emissions in the oceans, land, and atmosphere. The activity presented in this report considers climate projections produced by state-of-the-art coupled ocean-atmosphere climate models, which have shown an ability to simulate the influence of increasing GHG emissions on global climate (IPCC 2007). Despite utilizing the best available projections, there are still challenges with representing physical processes mathematically in an efficient manner given computational limitations and uncertainties concerning the scientific understanding of the physical processes that affect climate (e.g., atmospheric circulation, clouds, ocean circulation, deep ocean heat uptake, ice sheet dynamics, sea level change, land cover effects from water cycle, vegetative and other biological changes).

The irrigation demands analysis was designed on the philosophy that GCM biases toward being too wet, too dry, too warm, or too cool should be accounted for as bias-corrected climate projections data prior to use in impact studies to account for disparities in scale and climate between the global, regional, and local scales. Bias correction of GCM scale climate projections to place-based gridded METDATA observations through use of MACA climate projections was especially important since major irrigation demands simulation processes are temperature and precipitation dependent. However, uncertainties remain about the limitations of empirical downscaling methodologies. One potential limitation relates to how empirical methodologies require historical reference information on spatial climatic patterns, at the downscaled spatial resolution. These finer-grid patterns (e.g. in METDATA) are implicitly related to historical large-scale atmospheric circulation patterns, which presumably could somewhat change in the future. Application of the historical finer-grid spatial patterns to guide downscaling of future climate projections implies an assumption where the historical relationship between finer-grid surface climate patterns and large-scale atmospheric circulation is still valid under the future climate. In other words, the relationship is assumed to have statistical stationarity. However, it is possible that such stationarity will not hold at various space and time scales, over multiple locations, and for various climate variables. The significance of potential non-stationarity in empirical bias correction and downscaling methods (such as MACA), and the need to utilize alternative downscaling methodologies, remains to be established.

Uncertainty in Modeling Irrigation Demands

Uncertainties and limitations in modeling reference ET, crop ET, and NIWR under historical and future conditions are primarily due to uncertainty of how representative estimates of reference ET are with respect to well-watered reference conditions. Additionally, ET Demands model parameters and variables, such as basal crop coefficient curves, thermal based functions that simulate planting, crop development and harvest, crop dependent root depth and simulation of seasonal root growth, NRCS derived soil water holding capacity and runoff parameters, simulation of irrigation amount and frequency, and consideration of winter time surface cover and precipitation accumulation also have uncertainties. While numerous generalized parameters were used in this assessment, numerous primary variables and parameters, such as basal crop coefficients and thermal parameters defining growing season length and crop development, were based from detailed field scale lysimeter and crop water use studies and calibration to documented greenup, planting, and harvest dates. Also, while there are more complex and physically based crop growth and water use models available that inherently require more parameters and assumptions, the ET Demands model structure considers most important crop water use processes, such as consideration of reference crop daily energy balance, daily soil water balance, seasonal crop development and harvest for different crop types, bare soil evaporation, temperature dependent growing season length, and non-growing season ET and precipitation accumulation. Some important assumptions and associated uncertainties with application of ET Demands are assuming detrended and future temperature dependent planting, greenup, and harvest dates for annual and perennial crops, respectively, generalized winter cover classes, and that precipitation is in liquid form. Bias correction of historical and future projections of reference ET based on agricultural station measured and METDATA estimated reference ratios are also an important consideration, and can be highly uncertain if no agricultural station data exist. All of these assumptions impact seasonal and annual crop ET, effective precipitation, and net irrigation water requirements.

The impact of increased CO_2 on reduced crop transpiration was assumed based on simple empirical functions between plant dependent (i.e. C3 or C4) crop stomatal conductance and transpiration sensitivities and CO_2 changes (Kruijt et al. 2008). However, because of plant dependency, adaptation, unknown non-linear near surface boundary layer feedbacks from reduced transpiration, increased leaf temperatures, and vapor pressure deficits, uncertainties of increased leaf area index, stomatal and aerodynamic resistances, and plant dependent stomatal sensitivities, estimating CO_2 induced changes on irrigation demands remains a difficult and uncertain task.

The spatial resolution of the application of ET Demands is considered local scale (i.e. due to the use of point Metnodes – single METDATA and MACA grid cells in each HUC8), and does not consider spatial variations in climate within each HUC8. Spatial variations in soil type and water holding properties within each HUC8 were averaged across crop land

areas, and are therefore representative of HUC8 scale for crop land areas only. Future applications of ET Demands will allow for spatially variable application and calibration.

REFERENCES

Abatzoglou, J.T., 2011. Development of gridded surface meteorological data for ecological applications and modelling. *International Journal of Climatology* 33 (1), 121–131.

Abatzoglou, J. T., and T. J. Brown. 2012. A comparison of statistical downscaling methods suited for wildfire applications. *International Journal of Climatology*, 32(5), 772-780.

Allen, R. G., F. N., Gichuki, C. Rosenzweig (1991). "CO_2 Induced Climatic Changes and Irrigation Water Requirements. *Journal of Water Resources Planning and Management*," Vol. 117, No. 2, pp. 157-178.

Allen, R.G. 1996. "Assessing Integrity of Weather Data for use in Reference Evapotranspiration estimation," *Journal of Irrigation and Drainage Engineering*, ASCE 122(2):97–106.

Allen, R.G., L.S. Pereira, D. Raes, and M. Smith. 1998. "Crop Evapotranspiration: Guidelines for Computing Crop Water Requirements," Irrigation and Drainage Paper 56, Food and Agriculture Organization of the United Nations, Rome, 300 p.

Allen, R.G., L.S. Pereira, M. Smith, D. Raes, and J.L. Wright. 2005a. "FAO-56 Dual Crop Coefficient Method for Estimating Evaporation from Soil and Application Extensions," *Journal of Irrigation and Drainage Engineering*, ASCE, 131(1):2–13.

Allen, R.G. and C.W. Robison. 2009. "Evapotranspiration and Consumptive Irrigation Water Requirements for Idaho," University of Idaho Report, 222 p. Available at http://www.kimberly.uidaho.edu/ETIdaho/.

ASCE-EWRI. 2005. The ASCE Standardized Reference Evapotranspiration Equation, Report 0-7844-0805-X, ASCE Task Committee on Standardization of Reference Evapotranspiration, Reston, Virginia., American Soc. Civil Engineers. Available at http://www.kimberly.uidaho.edu/water/asceewri/

Brower, A. 2008. ET Toolbox – Evapotranspiration Toolbox for the Middle Rio Grande, A Water Resources Decision Support Tool, Version 2.1. Bureau of Reclamation, Water and Environmental Resources Division, Technical Service Center, 159 p.

Bureau of Reclamation (Reclamation). 2011. West-wide Climate Risk Assessments: Bias-Corrected and Spatially Downscaled Surface Water Projections, Technical Service Center, Denver, Colorado, March 2011.

Christensen, N.S., A.W. Wood, D.P. Lettenmaier, and R.N. Palmer. 2004. "Effects of Climate Change on the Hydrology and Water Resources of the Colorado River Basin," *Climatic Change* Vol. 62, Issue 1–3, 337–363.

Christensen, N.S. and D.P. Lettenmaier. 2007. "A multimodel ensemble approach to assessment of climate change impacts on the hydrology and water resources of the Colorado River basin," *Hydrology and Earth System Sciences*, 11:1417–1434.

Daly, C., Neilson, R.P., Phillips, D.L., 1994. "A statistical-topographic model for mapping climatological precipitation over mountainous terrain," *Journal of Applied Meteorology* 33 (2), 140–158.

deTar, W.R. 2004. "Using a Subsurface Drip Irrigation System to Measure Crop Water Use," *Irrigation Science* 23(3):111-122.

Hidalgo, H, Dettinger MD, Cayan DR, 2008. Downscaling with constructed analogues – Daily precipitation and temperature fields over the United States: California Energy Commission PIER Final Project Report CEC-500-2007-123; p. 48.

Hill, R.W., B. Barker, and C.S. Lewis. 2011. Crop and Wetland Consumptive Use and Open Water Surface Evaporation for Utah, Utah Agricultural Experiment Station Research Report 213, 138 p. Available at http://uaes.usu.edu/files/uploads/Publications/Research%20Reports/Surface%20Evaporation.pdf.

Howell, T.A., J.L. Steiner, A.D. Schneider, S.R. Evett, and J.A. Tolk. 1997. "Seasonal and Maximum Daily Evapotranspiration of Irrigated Winter Wheat, Sorghum, and Corn-Southern High Plains," *Transactions of the American Society of Agricultural Engineers*, 40(3):623–634.

Huntington, J.L. and R. Allen. 2010. Evapotranspiration and Net Irrigation Water Requirements for Nevada, Nevada State Engineer's Office Publication, 266 p.

Huntington, J.L., Gangopadhyay, S., Spears, M., Allen, R. King, D., Morton, C., Harrison, A., McEvoy, D., and A. Joros, (2015). West-Wide Climate Risk Assessments: Irrigation Demand and Reservoir Evaporation Projections. Bureau of Reclamation, Technical memorandum No. 68-68210-2014-01, 196p., 841 app, http://www.usbr.gov/watersmart/wcra/

Islam, Adlul, Lajpat R. Ahuja, Luis A.Garcia, Liwang Ma, Anapalli S. Saseendran, and Thomas J. Trout. 2012. Modeling the impacts of climate change on irrigated corn production in the Central Great Plains, *Agricultural Water Management*, 110, issue C, p. 94–108.

Jacobs, C. M. J. and H. A. R. De Bruin (1992). "The Sensitivity of Regional Transpiration to Land-Surface Characteristics - Significance of Feedback." *Journal of Climate* 5(7): 683-698.

Jacobs, C. M. J. and H. A. R. De Bruin (1997). "Predicting regional transpiration at elevated atmospheric CO2: influence of the PBL-vegetation interacton." *Journal of applied meteorology* 36: 1663-1675.

Jensen, M.E. 1998: Coefficients for Vegetative Evapotranspiration and Open Water Evaporation for the Lower Colorado River Accounting System. Report prepared for the Bureau of Reclamation, Boulder City, Nevada.

Kimball, B.A. and B.S. Idso. 1983. Increasing atmospheric CO2: Effects on crop yield, water use, and climate. *Agricultural Water Management* 7(1):55–72.

Kruijt B., J.P.M. Witte, C.M.J. Jacobs, T. Kroon. 2008. Effects of rising atmospheric CO_2 on evapotranspiration and soil moisture: A practical approach for the Netherlands, *Journal of Hydrology*, 349(3-4):257–267.

Manabe, S. and R.T. Wetherald. 1987. Large-scale changes of soil wetness induced by an increase in atmospheric carbon dioxide. *Journal of the Atmospheric Sciences* 45(5):1211–1235.

Marek, T., P. Colaizzi, T.A. Howell, D. Dusek, and D. Porter. 2006. "Estimating Seasonal Crop ET Using Calendar and Heat Unit Based Crop Coefficients in the Texas High Plains Evapotranspiration Network," ASABE Paper No: 062206, 2006 ASABE Annual International Meeting, Portland, Oregon, July 9–12, 2006, 11 p.

Maurer, E.P., L. Brekke, T. Pruitt, and P.B. Duffy. 2007. "Fine-resolution climate projections enhance regional climate change impact studies," Eos Trans. AGU 88(47):504.

Maurer, E.P., H.G. Hidalgo, T. Das, M.D. Dettinger, and D.R. Cayan. 2010. "The utility of daily large-scale climate data in the assessment of climate change impacts on daily streamflow in California," *Hydrology and Earth System Sciences* 14:1125–1138, DOI: 10.5194/hess-14-1125-2010.

Mitchell, K.E., Lohmann, D., Houser, P.R., Wood, E.F., Schaake, J.C., Robock, A., ... Bailey, A.A., 2004. The multi-institution North American Land Data Assimilation System (NLDAS): Utilizing multiple GCIP products and partners in a continental distributed hydrological modeling system. *Journal of Geophysical Research - Atmospheres* 109, D7 (1984–2012).

Payne, J.T., A.W. Wood, A.F. Hamlet, R.N. Palmer, and D.P. Lettenmaier. 2004. "Mitigating the effects of climate change on the water resources of the Columbia River basin," *Climatic Change* 62(1–3):233–256.

Rosenberg, N.J. 1981. The increasing CO2 concentration in the atmosphere and its implication on agricultural productivity. I: Effects on photosynthesis, transpiration and water use efficiency. *Climatic Change* 3(3):265–279.

Sammis, T.W., C.L. Mapel, D.G. Lugg, R.R. Lansford, and J.T. McGuckin. 1985. "Evapotranspiration Crop Coefficients Predicted Using Growing Degree Days," *Transactions American Society of Agricultural Engineers* 28(3):773–780.

Slack, D.C., E.D. Martin, A.E. Sheta, F.A. Fox, Jr., L.J. Clark, and R.O. Ashley. 1996. "Crop Coefficients Normalized for Climatic Variability with Growing-degree-days," Proc., International Conf., Evapotranspiration and Irrigation Scheduling, San Antonio, Texas, C.R. Camp, E.J. Sadler, and R. E. Yoder (eds.). American Society of Agricultural Engineers, St. Joseph, Michigan, pp. 892–898.

Snyder, R.L., D. Spano, C. Cesaraccio, and P. Duce. 1999. "Determining Degree-day Thresholds From Field Observations," *International Journal of Biometeorology* 42:177–182.

USDA-NRCS. 1991. "State Soil Geographic (STATSGO) Data Base Data use information," United States Department of Agriculture Natural resources Conservation Service, National Soil Survey Center, Miscellaneous Publication number 1492.

United States Department of Agriculture (USDA). 2010. Field Crops - Usual Planting and Harvesting Daves. October 2010, 50 p. Available at http://usda01.library.cornell.edu/usda/current/planting/planting-10-29-2010.pdf

Wood, A.W., L.R. Leung, V. Sridhar, and D.P. Lettenmaier. 2004. "Hydrologic implications of dynamical and statistical approaches to downscaling climate model outputs," *Climatic Change* 15:189–216.

Wright, J.L. 1982. "New evapotranspiration crop coefficients," *Journal of Irrigation and Drainage Engineering* 108(1):57–74.

Wright, J.L. 2001. "Growing Degree Day Functions for Use With Evapotranspiration Crop Coefficients," CD-ROM, American Society of Agronomy, Agronomy Abstracts.

Van Rheenen, N.T., A.W. Wood, R.N. Palmer, D.P. Lettenmaier. 2004. "Potential implications of PCM climate change scenarios for Sacramento-San Joaquin River Basin hydrology and water resources," *Climatic Change* 62:257–281.

APPENDIX

Digital appendices are organized by basin and contain HUC8 (i.e. ET Cell and Metnode) properties, statistics for MACA baseline and future ET Demands simulation results illustrated as spatial plots within the results section, and baseline and future time series plots for all variables and Metnodes. Digital appendices can be found at www.dri.edu/water-use/cat.